CLONING AND CHARACTERIZATION OF *rcs5*, SPOT BLOTCH RESISTANCE GENE AND PATHOGEN INDUCED *NEC3* GENE INVOLVED IN PROGRAMMED CELL DEATH IN BARLEY

A Dissertation
Submitted to the Graduate Faculty
of the
North Dakota State University
of Agriculture and Applied Science

By

Gazala Ameen

In Partial Fulfillment of the Requirements
for the Degree of
DOCTOR OF PHILOSOPHY

Major Department:
Plant Pathology

July 2019

Fargo, North Dakota

North Dakota State University
Graduate School

Title

Cloning and characterization of *rcs5*, spot blotch resistance gene and pathogen induced *Nec3* gene involved in programmed cell death in barley

By

Gazala Ameen

The Supervisory Committee certifies that this ***disquisition*** complies with North Dakota State University's regulations and meets the accepted standards for the degree of

DOCTOR OF PHILOSOPHY

SUPERVISORY COMMITTEE:

Dr. Robert S. Brueggeman
Chair

Dr. Shaobin Zhong

Dr. William Underwood

Dr. Richard D. Horsley

Approved:

07/26/2019
Date

Dr. Jack Rasmussen
Department Chair

ABSTRACT

Upon sensing pathogens, plants initiating defense responses typically resulting in programmed cell death (PCD). PCD effectively subdues biotrophic pathogens but is hijacked by necrotrophs that colonize the resulting dead tissues. We showed that barley wall associated kinase (WAK) genes, underlying the *rcs5* QTL, are manipulated by the necrotrophic fungal pathogen *Bipolaris sorokiniana* to cause spot blotch disease. The *rcs5* genetic interval was delimited to ~0.23 cM, representing an ~234 kb genomic region containing four WAK genes, designated *HvWak2*, *Sbs1*, *Sbs2*, and *HvWak5*. Post-transcriptional gene silencing of *Sbs1&2* in the susceptible barley cultivars Steptoe and Harrington resulted in resistance, suggesting a dominant susceptibility function. *Sbs1&2* expression is undetectable in barley prior to pathogen challenge; however, specific upregulation of *Sbs1&2* occurred in the susceptible lines post inoculation. Promotor sequence polymorphisms were identified in the allele analysis of *Sbs1&2* from eight resistant and two susceptible barley lines, which supported the possible role of promotor regulation by virulent isolates contributing to susceptibility. Apoplastic wash fluids from virulent isolates induced *Sbs1*expression, suggesting regulation by an apoplastic-secreted effector. Thus, the *Sbs1&2* genes are the first susceptibility/resistance genes that confer resistance against spot blotch, a disease that threatens barley and wheat production worldwide. The *nec3* mutants of barley are hyper-susceptible to many necrotrophs and show distinctive cream to orange necrotic lesions that are induced by infection, representing aberrant PCD. The γ-irradiation induced necrotic mutant, *nec3*-γ1 (Bowman) was confirmed as a *nec3* mutant by allelism tests. The F_2 progeny of a cross of *nec*3 x Quest inoculated with *B. sorokiniana* segregated as a single recessive gene fitting a 3 WT: 1 mutant ratio. The homozygous F_2 mutant progeny were genotyped with four SSR and 25 SNP markers at *nec3* locus on chromosome 6H, a

physical region spanning ~ 16.96 Mb containing 91 high and low confidence annotated genes. Exome capture sequencing of *nec3* mutants failed to identify a candidate gene, however, RNAseq analysis identified two candidates in the *nec3* region with >three-fold downregulation. We hypothesize that the underlying aberrant PCD mechanism in the *nec3* barley mutant facilitates extreme susceptibility to multiple adapted fungal pathogens of barley.

ACKNOWLEDGEMENTS

This dissertation and the highest degree awarded with it, is a contribution of several people. Be it a scientific queries, experimental help or words of encouragement in the tough times, these people had helped me reach to completion. The first on the list is my academic advisor, Dr. Robert Saxon Brueggeman, who provided me with the platform, where I can perform some cutting-edge hypothesis driven research. His continuous encouragement, support, and guidance shaped my scientific enthusiasm into a well-organized scientific approach. There were many failures and moment of hopelessness during this endeavor, yet his selfless time and encouragement were sometimes all that kept me going.

My labmates, past and present created an amicable environment in the lab, during formal and informal meetings, which nurtured creative thinking and cooperation. The research presented in this dissertation is either based on some critical work of other researchers or some have contributed in the research itself. The *rcs5* and *Nec3* projects were initiated in Dr. Andris Klienhofs lab at WSU and Dr. Brueggeman and Dr. Thomas Drader from Dr. Kleinhofs lab lead both projects before me. The *Nec3* mapping was conducted by our former labmates Lauren Bittara and Dr. Jonathon Richards. The current lab member, who also happens to be my husband, Dr. Shyam Solanki has contributed to both manuscripts with the countless thoughtful discussions, constructive criticisms, and immense support. I would also like to thank my Ph.D. supervisory committee, Dr. Shaobin Zhong, Dr. William Underwood and Dr. Richard Horsley for their constructive suggestions and support during my PhD.

Last but not the least thanks to my family and forever friends, Shyam, Kriti, Leah, Kishore, Shalu and Sudarshna.

DEDICATION

In the memory of my beloved *dada*, Haneef Sheikh, who served as a high school mathematics teacher and inspired me with his generosity of spirit.

TABLE OF CONTENTS

LIST OF TABLES

LIST OF FIGURES

CHAPTER 1. LITERATURE REVIEW

The Host: Barley

Introduction

Barley (*Hordeum vulgare* L. subsp. *vulgare*) is one of the founder crops of old world agriculture and is currently grown worldwide and ranks fourth among cereals in production. It was historically used as a staple food for humans but currently the largest share of its use is as feed for livestock and for alcohol production from malted barley (1–3). Malting represents the high value use of barley which only accounts for 9-22 % of crop production (4). Barley was cultivated on 47 million ha which produced 147 million tonnes worldwide in the year 2017 (4). Apart from being an economically important crop, barley is a model species for cereal genomics, mainly because it is a self- pollinated, diploid grass species (5).

Barley has two sub-populations based on the spike morphology, six- row types that have three fertile spikelets at each node and the two- row types with one central fertile spikelet and has sterile lateral spikelets at each node on the spike. Barley was domesticated about 10,000 years ago from its wild progenitor *H. vulgare* subsp. *spontaneum*, which is a two-row type with brittle rachis (6). There are five genetic loci that independently converts the two-row to six-row types, namely *vrs1* (*vulgare row-type spike 1*), *vrs2*, *vrs3*, *vrs4* and *vrs5* (7,8). The five mutants produce varying degrees of the six-row phenotype and a single recessive gene *vrs1* on the chromosome 2H is known to predominantly control the development of the six-row types of barley. Based on the growth habits barley is classified into three types; spring, winter and facultative types. The spring types are predominantly sown in the spring and harvested in the summer, winter barley needs vernalization; hence it is sown in late fall and are harvested the

following summer. The facultative types are the cold-tolerant barley with no vernalization requirement for flowering; therefore, they can be grown as spring or winter types.

Origin and Speciation

Barley like wheat and rye belongs to the *triticaceae* tribe of the family Poaceae (Gramineae). Barley belongs to the genus *Hordeum* and has 33 wild species, out of which 24 are perennial grasses and the rest are annuals (9). The genus *Hordeum* is widespread and is found at different altitudes, climates and ecological zones of the world (9,10). The archaeological remains found at various sites in the Fertile Crescent had remnants of emmer wheat and barley, traceable to before 8000 BC. Both cultivated barley (*Hordeum vulgare* L. subsp. *vulgare*) and its wild progenitor *H. vulgare* subsp. *spontaneum* are diploid (2n=14), self-pollinating but completely interfertile and forms the primary gene pool of barley. Other than the wild progenitor of barley, the closest relative of cultivated barley is the wild relative *H. bulbosum*, which is an obligate out-crossing (self- incompatible) species and is capable of producing fertile progenies with some difficulty, when crossed with the domesticated *H. vulgare* ssp. *vulgare* and forms the secondary gene pool of barley. However, the fertility of these hybrids is strongly reduced or the *H. bulbosum* chromosomes are completely eliminated at a early stage of development and may result in haploid plants (5,11). Wide- hybridization among barley and other *Hordeum* species have been less successful as they produce sterile hybrids and belong to the tertiary gene pool of barley.

One of the distinct features of wild barley are its brittle rachis due to thin cell walls at the rachis nodes which is governed by two tightly linked, complementary and dominant genes *BTR1* (Brittle Rachis 1) and *BTR2* (Brittle Rachis 2) located on chromosome 3H (12). Domesticated barley has deletions in either *BTR1* or *BTR2* that abolish the disarticulation of the spike at

maturity and converted the rachis to non-brittle types, making it an easier to harvest and is considered the major domestication trait (13). The mutations in *Btr1* and *Btr2* were two independent events arguably promoting the concept of two domestication events of cultivated barley in the middle east (14).

Genome Complexity

The *Hordeum* genus has various ploidy levels, from diploid to hexaploids and has combinations of four basic genomes referred as H, I, Xa and Xu (8). The wild barley*, H. spontaneum* is an annual, diploid and referred as the I genome. *H. vulgare* is an annual, diploid but similar to *H. bulbosum* it can be diploid or tetraploid without any head morphology distinction between the two ploidy classes*. H. bulbosum* also has the close genetic relationship to *H. vulgare* as it has a high level of shared synteny in contrast to the other *Hordeum* species and both are denoted by the H genome. *H. bulbosum* belongs to the secondary gene pool but is the only *Hordeum* species besides *H. spontaneum* that allows for homeologous chromosome pairing and recombination when crossed with cultivated barley (15).

The size of the barley genome is ~ 5.1 Gb, which is 14 times larger than the rice (*Oryza sativa* L.) genome and 45 times larger than the *Arabidopsis* (*Arabidopsis thaliana* L.) genome which is largely due to repetitive elements that make up 80% of the barley genome. However, the barley genome is three times smaller than the hexaploid wheat genome and contains the seven chromosomes in synteny that makes it a good moderate genome size plant species. The latest whole genome assembly of a US spring type, six-rowed cultivar Morex was sequenced using Illumina paired end and mate-pair technology and is assembled from 4.5 terabases of raw data (16,17). The N50 value increased from 79 Kb to 1.9 Mb consisting of 6,347 super scaffolds. The current assembly represents ~95% (4.79 Gb) of the genomic content. Mapping of the

transcriptome and reference protein sequences from other plant species identified 83,105 putative gene loci with 39,734 high-confidence and 41,949 low-confidence genes, 19,908 long non-coding RNAs and 792 microRNA (16). The reference genome of barley represents the best assembled genome in cereals and is a great resource for not just barley researchers but also for researchers working on more complex, polyploid sequenced cereals belonging to the *triticaceae* tribe, including wheat.

Barley as a Model Crop

With the threat of growing population and the impact of climate change, crop yields have stagnated and it is only going to be worse in the near future. Barley is unique in its suitability to a wide environmental range and different end users, who are spanning from low economies of the developing world to the higher economies of the developed world. It has therefore emerged as an excellent model for investigating the impacts of various climate change scenarios, like drought tolerance. Among the *Hordeum* genus, *H. bulbosum* has higher cold tolerance, shared synteny to barley, can hybridize with barley to produce fertile offsprings, and is a perennial with good regrowth ability; thus, it is an excellent genetic resource for the introgression of abiotic and biotic resistance in barley. Although the archaeological remains of barley date back to ~10,000 years ago, the recent sequencing and reconstruction of the genome from an ~6000 year old barley seed excavated from Israel marks it as the most ancient genome sequenced to date (13). In the future, genome resequencing using single molecule, long read sequencing and genomic linkage analysis with suitable statistical analysis will provide a better understanding and power to identify important genetic variation in barley.

The Pathogen: *Bipolaris Sorokiniana*

Introduction

Bipolaris sorokiniana (Sacc.) Shoem. is a ascomycete fungus belonging to family Pleosporaceae in the order Pleosporales in the class Dothideomycetes. Shoemaker proposed the name '*Bipolaris*' to the *Helminthosporium* species that produces fusoid, straight or curved conidia with 3-10 septation that germinate to produce one germtube from each end. The teleomorphic (sexual stage) is *Cochliobolus sativus*, which rarely occurs in nature (18). The sexual fruiting body is a pseudothecia with erect beaks carrying clavate asci. The ascospores are hyaline, filamentous, with 4-10 septae and spirally flexed within asci.

Host Range

Bipolaris sorokiniana is one of the most destructive pathogens of both wheat and barley. It can also infect wild emmer (*Triticum diccoides*), triticale (xTriticosecale), oats (*Avena sativa*), rye (*Secale cereale*), *Brassica campestris*, maize (*Zea mays*), sorghum (*Sorghum bicolor*), soybean (*Glycine max*) and many grasses including switch grass (*Panicum virgatum*) and *Brachypodium distachyon* (18).

Virulence Factors

In the upper Midwest regions of the US, four pathotypes were designated based on their virulence pattern on the three barley differential lines, ND5883, Bowman and NDB112. Isolates having low virulence on all three are Pathotype 0, whereas isolates having high virulence on the ND5883 and low virulence on other two differential are pathotype 1 and high virulence on Bowman and low virulence on the other two differentials are pathotype 2 (19). Recently, an isolate was identified as having high virulence on all three differentials and was denoted as Pathotype 3 (20).

The genome of *B. sorokiniana* Pathotype 2 (ND90Pr) is 34.42 Mb (21,22) represented by 157 scaffolds. Comparing the two genomes of Pathotype 0 (ND93-1) and Pathotype 2 (ND90Pr) revealed 60,448 SNPs, indicating higher similarity between the two pathotype isolates. The high virulence of pathotype 2 isolate ND90Pr was mapped in a biparental population created by crossing ND90Pr and ND93-1 to a *VHv1* locus (19,22). The *VHv1* locus had 43 predicted genes out of which two genes encoded for secondary metabolites belonging to nonribosomal peptide synthetases (NRPSs) and were unique to the pathotype 2 isolate. Deletion of one of the two genes (115356) effectively reduces virulence on barley cultivar Bowman; thus, representing one of the virulence genes of *B. sorokiniana* (21).

The Genus *Bipolaris*

The genus *Bipolaris* includes historically important species such as *B. oryzae* (*C. miyabeanus*) that causes the brown spot disease of rice and caused the infamous bengal famine (epidemic in 1942-43); *B. maydis* (*C. heterostrophus*) that causes Southern corn leaf blight (epidemic in 1970); *B. victoriae* (*C. victoriae*) that causes the Victoria blight in oats (epidemic in 1940), and *B. zeicola* (*C. carbonum*) that causes the northern corn leaf spot. The unique feature of the *Bipolaris* genus is that they produce host selective toxins (HST) as the virulence factors to cause disease in their respective hosts. Based on the whole genome assembly, among the *Bipolaris* species, *B. sorokiniana* is closely related to *B. maydis* (21). All the *Bipolaris* species have been estimated to have diverged and speciated less than 20 million years ago; thus, they have gained a lot of research attention due to the historically important plant diseases they cause. Some of the plant diseases are described below:

1. *B. Zeicola* race 1 produces the HST known as HC-toxin in maize. In fact the first R gene cloned in the plant host was the dominant resistant gene *Hm1* from Maize (23). *Hm1* encodes

an enzyme NADPH HC-toxin reductase that detoxifies the HC-toxin. The HC-toxin is chemically an cyclic tetrapeptide that is detoxified by the Hm1 by reducing the critical carbonyl group of the HST (23). The expression of *Hm1* directly corresponds with the resistance level in the host plant maize.

2. In the year 1942/43, brown spot of rice caused the infamous Bengal famine. The epidemic led to huge yield losses of the only staple food in the region and the death of two to three million people due to starvation (24,25). Till date no HST has been reported from the pathogen *B. oryzae* and no resistance genes have been cloned from the host rice against brown spot disease (26).
3. Before 1970 race 0 of *B. maydis* was predominant and was of minor economic importance. However, in 1970, the race T of *B. maydis* became predominant and caused a major epidemic of Southern corn leaf blight (27). The maize carrying the texas male sterile cytoplasm (Tcms) which was largely favored by growers because of its non-requirement of detasselling to prevent self-crossing for production of hybrid seeds, carried the corresponding host susceptibility gene *T-urf13*. The resultant monoculture of the Tcms maize led to the Southern corn leaf blight epidemic in the US (28).
4. In the 1940's, a monoculture of oats carrying the *Pc-2* gene predominated due to the resistance it provided against crown rust of oat (caused by *Puccinia coronata*) (29). *B. victoriae* producing HST victorin, a chlorinated cyclic pentapeptide, was able to cause Victoria blight on the oat genotypes carrying the dominant *Vb* allele. The *Vb* gene and *Pc-2* have never been genetically separated and either are the same gene or are tightly linked genetically (30). The susceptibility of *Arabidopsis* to the victorin containing *B. victoriae* isolates led to the cloning of a susceptibility gene *LOV1*, which encodes a coil-coiled

nucleotide binding site leucine rich repeat (CC-NBS-LRR) protein (31). The physiology of the Victoria blight resistance has callose deposition at the site of fungal penetration, respiratory burst, lipid peroxidation, ethylene production, extracellular alkalinization, phytoalexin synthesis, potassium ion efflux and apoptotic- like cell death (32), which were thought to be hallmarks of resistance to biotrophic fungi. This suggests that the same underlying mechanism that provides resistance to the biotrophic pathogen *P. coronata* is favoring the necrotrophic pathogen *B. victoriae*. Thus, victorin subverts the function of an *R*-gene to induce susceptibility by intentionally inducing Programmed Cell Death (PCD) (31,33).

The Disease: Spot Blotch of Barley

Introduction

Spot blotch disease is caused by *Bipolaris sorokiniana* and is one of the most common and economically devastating diseases of barley (34). The spot blotch disease is prevalent worldwide, covering all five continents, wherever wheat and barley are cultivated, including the upper Midwest region of the US and the Canadian Prairie (35,36). The spot blotch disease is one of the economically devastating diseases of barley and pose threat to the bread basket of South America and Asia and is reported to be the number one disease in the Indian sub-continent (37).

Distribution and Importance

The first report of spot blotch disease in the US was in Ames, Iowa in 1890 (38). Yield losses of about 30% have been reported under favorable conditions and the disease also impacts the malting quality of barley (39). It was reported that this disease was sampled in every field of Manitoba, Canada in the year 2002 (40). Spot blotch in the northern New South Wales and Queensland, Australia has been reported to cause more than 30% yield losses, which accounts

for an annual loss of $1 to $2 million in years when environmental conditions are conducive for disease epidemic development (41).

Symptoms and Disease Cycle

The characteristic symptom of spot blotch is the brown necrotic lesions on the leaves with or without chlorosis depending on the pathotype of pathogen and host genotype (34,42,43). *B. sorokiniana* can also cause common root rot of wheat and barley. The pathogen can also infect the spikes and render the seeds shriveled with black discoloration known as black point or kernel blight in wheat and barley. In 1999, the disease severity scale was developed by Fetch and Steffenson ranging from 1 to 9 based on the relative size of the necrotic lesions and the chlorotic margins on the barley seedlings. The 1 to 9 rating scale was further summarized as 1-3 as resistant, 4-5 as moderately resistant, 6-7 as moderately susceptible and 8-9 as susceptible (43).

B. sorokiniana is a polycyclic plant pathogen and tends to infect the older leaves first and progress towards the upper leaves (44,45). Long duration of leaf wetness (>12 h) with higher relative humidity and temperatures between 18 to 32˚C, favors the conidia germination and infection (46). The disease cycle begins when the asexual spores (conidia) land on the surface of the barley leaf and germinate from both ends of the spore and directly penetrate the cuticle of the leaves via appressoria (47,48). The apparently biotrophic phase is confined to the first penetrated epidermal cell of the host and later invades the neighboring cells by multiple branching of the infection hyphae which is marked as the switch to its necrotrophic phase (48). The necrotrophic phase is associated with the cell-death (49). The necrotic and/ or chlorotic lesions appear on the leaves and the pathogen produces multiple secondary asexual cycles giving rise to multiple infection cycles by conidia. *B. sorokiniana* can survive as a saprophyte along with the other pathogenic fungi of wheat and barley that overwinters as mycelia or conidia on the dead crop

residues or infected seeds (50). This saprophytic stage of different species of plant pathogenic fungi during which they share the same host has provided the opportunity for horizontal gene transfer of virulence factors. A good example is the *ToxA* effector that has been reported to be present in *Parastagonospora nodorum*, *Pyrenophora tritici repentis* and recently transferred to the *B. sorokiniana* genome (51,52). With the onset of the next growing season, the overwintering mycelia or conidia germinate to produce the asexual spores as a source of primary inoculum and the disease cycle continues (53).

Disease Management

Spot blotch can be managed by cultural practices through the destruction of the previous year crop residues which serves as a primary source of inoculum (54). The destruction of crop residues can be achieved by burying, burning or removal of the residues. Crop rotation with a non-host crop or with a fallow period can also decrease the primary inoculum in the field (34). Two or more year rotations with Flax (*Linum usitatissimum*) has been reported to decrease viable inoculum of *B. sorokiniana* in the soil (55). Other strategies include seed treatments by systemic fungicides like Carboxin, Metconazole, Difenconazole, Mefenoxam, Ipconazole, Metalaxyl, Pyraclostrobin and Imidicloprid or spraying of fungicides for the control of the leaf spot with copper based fungicides, Mancozeb, Azoxystrobin, Pyraclostrobin and the triazoles like Metconazole, Cyproconazole, Tebuconazole and Propiconazole (56). Biological control by a saprophytic ascomycete *Chaetomium globosum* has also been reported to control this disease (57). However, the most economic and environmentally friendly way to manage this disease is by breeding for host resistance.

Resistance to Spot Blotch

Introduction

The most economical and environmentally feasible strategy to manage any plant disease is by deployment of cultivars with host resistance. Resistance to spot blotch of barley has been deployed against pathotype 1 of *B. sorokiniana* and has remained effective for more than 50 years, and remains so till today (58,59). The pathotype 1 of *B. sorokiniana* is predominant in the upper Midwest region of the US (60). This durable resistance was selected from the barley line NDB112 and has been widely utilized in breeding programs, resulting in several resistant cultivars, like Morex, Dickson and Robust. The barley line NDB112 was selected from the cross CI 7117-77 X Kindred at North Dakota State University (39). The seedling resistance in the cultivar Morex was conferred by a single gene, namely *resistance to Cochliobolus sativus* 5 (*Rcs5*) (now referred to as *rcs5*), which also provides varying levels of adult plant resistance (58,61).

Bi- Parental Mapping

The early studies to map spot blotch resistance were conducted in a double-haploid population from a cross between the the resistant cultivar Morex and the susceptible cultivar Steptoe, where all the seedling resistance was provided by a 3.3 cM region of the short arm of barley chromosome 7H (58). Several other bi-parental populations also supported the finding that the 7H locus provides all the seedling resistance to spot blotch (61,62). There were minor QTLs reported on 1H and 3H along with the major QTL on 7H in another double-haploid population of Morex by Dicktoo (61).

Genome Wide Association Mapping

A genome-wide association study on a large breeding panel identified three quantitative loci behind the Midwest six-row durable spot blotch resistance. The three QTL identified were *Rcs-qtl-1H-11_10764*, *Rcs-qtl-3H-11_10565* and *Rcs-qtl-7H-11_20162* (59). The largest allelic effect was conferred by the *Rcs-qtl-7H-11_20162* across different populations, which corresponds to *Rcs5* (59).

Importance of *Rcs5*

Rcs5 has remained responsible for the majority of seedling and some adult plant resistance in both current six-row and two-row barley cultivars (58,59,61). *Rcs5* was mapped in an NDB112 derived resistant cultivar Morex by susceptible cultivar Steptoe double haploid population to short arm of chromosome 7H (1), 2.0 cM proximal to the marker ABC167A and 4.2 cM distal to ABG380 (58). The *Rcs5* region was further saturated with additional markers utilizing *Brachypodium* and rice synteny which further delimited *Rcs5* to a 2.8cM region between the markers BF627133 and BG414713 corresponding to a seven BAC contig physical region spanning an ~2 Mb genomic region (63,64).

Plant Immunity

Introduction

Plants encounter diverse microbes, pathogenic and non-pathogenic, that they need to defend against. They do resist most of the microbes and thus disease is the exception in most host microbe interactions (65). Unlike animals plants do not have an adaptive or acquired immunity, in which receptors (antibody) for pathogen derived molecule (antigen) are acquired (66). Moreover, a circulatory system with the receptors is also absent in plants and therefore each

cell of plants needs to sense the non-self molecules and trigger efficient host defense which is considered as plant innate immunity (67).

Plants have a sophisticated innate immunity system. Early active plant defenses are initiated by the perception of pathogen attack by host cell membrane bound receptors. These membrane bound receptors known as Pattern recognition receptors (PRRs) perceive the damage associated molecular patterns (DAMPs) or 'altered self' or the microbe/pathogen associated molecular patterns (MAMPs/ PAMPs) which represent 'non-self molecules' which are conserved microbial signatures. Recognition of MAMPs/PAMPs triggers reactive oxygen species (ROS) burst, ion fluxes, altered levels of plant hormones, expression of defense-related genes, activation of mitogen activated protein kinases (MAPK) and in many instances, results in a low amplitude localized programmed cell-death (PCD). The downstream signal-transduction events culminate in pathogen growth arrest and ultimately provides plant defense. Thus, any obstruction provided by a pathogen derived molecule or effectors in the signal transduction or a missing/non-functional host component in the resistance pathway is able to halt plant defense and ultimately results in host susceptibility. The plant pathogens have evolved a set of virulence effectors that are able to disarm components of the host immune responses by modifying or degrading host proteins for a compatible reaction. The repertoire of virulence effectors carried by pathogen genotypes are the determinant of its host range (68,69). In response to the typically cytoplasmic secreted virulence effectors, plants evolved a second tier of cytoplasmic localized receptors which mostly belong to the conserved protein family of nucleotide-binding, leucine-rich repeat receptors (NLR) proteins (70). Direct or indirect recognition of virulence effectors by the NLRs generally result in a strong PCD response, designated as the hypersensitive response (HR) (71).

The lifestyle of plant pathogen adds another layer of complexity in the understanding of plant defense against microbes. Plant pathogens that require living host tissue to subsist and often form specialized feeding structures like haustoria to acquire host-derived nutrients and complete their lifecycle in the living host are known as biotrophs. The plant pathogens that induce host cell death and derive nutrients from the dead host tissue to complete their lifecycle are known as necrotrophs. The hemi-biotrophs are the third class of plant pathogens that have an initial biotrophic phase of variable length and a later necrotrophic phase depending on the stage of their lifecycle and the environment that they are colonizing. During the host-pathogen interaction, the host immunity responses that results in localized PCD would contain and arrest the growth of biotrophic or a hemi-biotrophic pathogens in their biotrophic phase by restricting them from living cells. On the other hand the necrotrophs seems to hijack the host defenses, purposefully eliciting PCD pathways with temporal and spatial specificity (72,73). One of the classical examples of resistance to a biotrophic fungus, incurring susceptibility to a necrotrophs is the oat Victoria blight and crown rust diseases. As discussed before the resistance to *P. coronata* provided by the *Pc-2* gene confers susceptibility to the necrotrophic pathogen *B. victoriae* producing the HST victorin (31,33).

As the outcome of this dissertation is the cloning and characterization of the major spot blotch resistance gene *rcs5* in barley, which we report to be a membrane bound receptor, the following sections will provide details of the strategies of known membrane bound receptors in pathogen recognition, signal-transduction, transcriptional reprogramming and activation of host defenses.

The DAMPs/PAMPs Recognition by PRRs, Signaling and Defense Mechanism

Plants are sessile organism that are constantly exposed to microbes. To defend themselves from potential plant pathogenic microbes, they rely on both preformed and innate immunity responses. The preformed immunity acts as a physical barrier like cuticle and cell wall. However, the active surveillance of innate immunity is provided by the pattern recognition receptors or PRRs. The PRRs are cell membrane bound receptors with general architecture of an extracellular region, a transmembrane and absence or presence of a cytoplasmic kinase domain denoted as Receptor like Proteins (RLPs) or Receptor Like Kinases (RLKs). The extracellular domains of RLPs or RLKs recognize the conserved Microbe Associated Molecular Pattern (MAMPs) or secreted effectors during pathogen attack. The perception of elicitors triggers a dynamic association/dissociation of co-receptors and transphosphorylation triggers the downstream signaling via Mitogen Activated Protein Kinases or MAPKs to induce defense responses that include callose appositions, reactive oxygen species (ROS) production, calcium influx and in some instances a hypersensitive responses or cell death.

PRRs with Leucine Rich Repeats Ectodomain

The membrane bound receptors fall into several classes; the most abundant in plant system is the RLKs or RLPs that contain extracellular Leucine Rich Repeats (LRRs). LRRs are found in eukaryotes and viruses and consists of 2 to 45 motifs of 20 to 30 amino acids that folds into a horseshoe or arch shape. The LRR arch provides a structural framework for ligand binding. The most widespread across the higher plant RLKa are the flagellin sensitive 2 (FLS2) which perceive the bacterial 22-amino-acid flagellin fragment (flg22) (74–76). The bacterial flagellin is a polymer and gets glycosylated by a β-galactosidase 1 (BGAL1) which releases the flagellin elicitor to be further degraded by plant proteases into the 22-amino-acid fragments

which binds with the FLS2 receptor (77). The bacterial *Pseudomonas syringae* infected plants revealed a BGAL1 suppressed by a heat-stable, small bacterial suppressor (77). The flg22 binding with the FLS2 recruits a LRR-RK co-receptor brassinosteroid insensitive 1-associated kinase 1(BAK1) and forms a ligand-dependent complex with FLS2 and leads to the quick phosphorylation of both (75). The FLS2-BAK1 phosphorylation triggers phosphorylation of the cytoplasmic receptor Botrytis induced kinase 1 (BIK1) and other PBS-Like (PBL) proteins, which dissociates from the complex and through MAPKs signaling induce transcriptional reprogramming of the defense related genes. BIK1 directly phosphorylates the NADPH oxidase RbohD to induce ROS production (78). The RbohD in turn induces callose deposition via Powdery Mildew Resistance 4 (PMR4) which encodes a callose synthase (79). The cytoplasmic phosphorylation cascades initiates a Ca2+ burst, activation of Ca2+ dependent protein kinases (CDPKs), ion movement, hormone signaling and transcriptional changes of thousands of genes (80). Thereafter, the ligand activated FLS2-BAK1 complex is internalized via a trans golgi-network into endosomes/vesicles where they get degraded (76,81). The degradation that occurs post endocytosis of the activated PRRs is possibly to downregulate the induction capacity which keeps the host defense in check. The other layer of downregulation of activated PRRs are via phosphatases that dephosphorylate the kinase phosphorylation. For instance, kinase associated protein phosphatase (KAPP) in general negatively regulates the AtFLS2 kinase signaling (82).

Interestingly, BAK1 which is also known as somatic embryogenesis receptor kinase 3 (SERK3), forms ligand-dependent complexes with several PRRs like elongation factor-TU receptor (EFR), FLS2 (plant immunity) and also brassinosteroid insensitive 1 (BRI1), which is also an LRR-RLK receptor that perceives the plant growth hormone brassinosteroids (BRs). Another LRR-RLK is the *Arabidopsis* RLP23 which recognizes the conserved 20 amino acid of

the necrosis and ethylene inducing peptide-1 like protein (nlp20), produced by several prokaryotes (bacteria) and eukaryotes (oomycetes and Fungi) (83). RLP23 forms a non-ligand activated complex with LRR-RLK Suppressor of BIR1-1 (SOBIR1) and ligand induced tripartite complex with BAK1 to induce immunity (83). The ectopic expression of RLP23 in potato enabled it to have enhanced immunity against *Sclerotinia sclerotiorum* and *Phytophthora infestans* (83). Moreover, SOBIR1 is involved in normal floral organ shedding, tolerance to high auxin and high salt concentrations in *Arabidopsis* (84). Thus, the RLK receptor BAK1 and SOBIR1 functions as a shared signaling node connecting plant immunity and development.

PRRs with LysM Ectodomain

Another class of PRRs has the LysM ectodomain like the carbohydrate PAMPs recognizing RLK CERK1 (85). The CERK1 receptor recognizes many carbohydrate PAMPs of pathogens, including the fungal cell wall component chitin, peptidoglycan and bacterial lipopolysaccharides (LPS), bacterial cell wall component, as a first tier of host defense (86,87). During chitin perception in rice, OsCERK1, interacts with another plasma membrane bound PRR, the Chitin Elicitor Binding Protein (CEBiP), a LysM-RLP in a chitin oligomer dependent manner to elicit defense responses (88). Both OsCERK1 and CEBiP are required for the chitin dependent defense signaling in rice (86,88–90). However, in *Arabidopsis* AtCEBiP is dispensable for AtCERK1 perceived chitin signaling. Although chitin oligomer perception differs among plant species, the peptidoglycan perception is similar in rice and *Arabidopsis*. AtCERK1 and OsCERK1 interacts with the LysM RLPs LYP4, LYP6 and LYM1 and LYM3 in *Arabidopsis* and rice, respectively (86,87). Thus, a single PRR can be conserved among plants, and retain their function yet can have some variation in the perception mechanisms of the same elicitor. Also, a single PRR can recognize several elicitors to provide efficient defense signaling.

PRRs with Lectin Ectodomain

The third class of PRRs have a lectin ectodomain such as the *Arabidosis* RLK DORN1 which recognizes the exogenous eATP released from wounded *Arabidopsis*, which at a lower concentration induces stomatal opening and at higher concentrations induces stomatal closure (91). The cytosolic ATP is the source of energy for all multicellular organism and the extracellular ATP released during wounding by herbivores or pathogen attack acts as a DAMP in multicellular organism (92). DORN1 interacts with the cell wall through the RGD domain in the extracellular lectin domain (93,94). In *Arabidopsis*, during *Phytophthora infestans* infection, *in planta* effector induced-O (IPI-O) is released, which interacts with DORN1 and weakens the plasma-membrane cell-wall connection, to promote infection (93). In the absence of the effector, the eATP DAMP is released during pathogen attack which induces a calcium influx in a dose dependent manner and elicit defense responses via MAPK signaling (95).

PRRs with EGF-like Ectodomain

The fourth class of LRRs is the EGF-like ectodomain including the *Arabidopsis* oligogalacturonoids (OG) that are recognized by the wall-associated kinases (WAK) 1 and 2 (96). The WAKs are a conserved large family of plant proteins that have expanded via evolutionary forces and are often found in clusters across crop species (97). The WAKs have apoplast localized epidermal growth factor (EGF) repeats and galacturonic acid binding (GUB) domains and a cytoplasmic receptor kinase (96). The GUB domains physically binds with pectin in the cell wall. In *Arabidopsis*, WAK1 and WAK2 antisense experiment provided clues to their role in cell expansion by binding to pectin (96,98). However, in vitro studies reported that the WAK1 or 2 receptors bind to fragmented pectin OGs with higher affinity, suggesting activation of their functional switch between development and defense (99). Through, the use of a domain

swap approach between EFR and WAK1, it was demonstrated that a fusion of the WAK ectodomain with the EFR TM and intracellular kinase domain was able to perceive OGs and induce typical EFR-mediated responses, such as ethylene production and defense gene expression via MAPK signaling (100). The WAK1 interacts with the *Arabidopsis* Glycine-Rich Protein (GRP3) and this complex interacts with intracellular Kinase Associated Protein Phosphatase (KAPP) (101,102). KAPP interacts with several RLKs, including SERK1 and FLS2, negatively regulating the downstream signaling of such receptors. In *Arabidopsis*, mutants of both GRP3 and KAPP enhanced the resistance to *Botrytis cinerea*, *Psedomonas syringae* and *Pectobacterium caratovorum* in plants induced with OGs, flg22 and overexpressing WAK1, indicating a negative role of the GRP3 and KAPP in the WAK signaling (102).

WAKs in Plant Immunity

The first WAK reported to function in plant immunity was the *Arabidopsis* AtWAK1, providing resistance against *Botrytis cinerea*. The ectodomain of AtWAK1 binds to the Oligogalacturonides (OGs) released from the breakdown of cell wall pectins during the infection process. Another WAK protein in *Arabidopsis Resistance to Fusarium oxysporum* (RFO1) provides resistance to several *forma specialis* of *F. oxysporum* (103), possibly recognizing a conserved MAMP. ZmWAK-RLK1 and ZmWAK confer quantitative resistance to northern corn leaf blight caused by *Exserohilum turcicum* and head smut caused by *Sporisorium reilianum* resistance in maize (104). However, the pathogen elicitor being recognized by the ZmWAK proteins is still unknown. The wheat *Stb6* gene provides resistance to *Septoria tritici* blotch disease caused by *Zymoseptoria tritici* by indirect recognition of the *AvrStb6* effector carrying isolates. However, the wheat WAK, Snn1 directly interacts with the cognate effector SnTox1 *in vitro*, inducing susceptibility to the necrotrophic pathogen *Parastagonospora nodorum* (105).

The rice *Xa4* confers race-specific durable resistance against *Xanthomonas oryzae* pv. *oryzae* by strengthening the cell wall by cellulose synthesis and suppressing cell wall loosening even in the absence of the pathogen. Thus, WAKs recognize diverse elicitors that are either of fungal/bacterial origin or plant origin.

Discussion and Prospects of Membrane Bound Receptors

Engineering of PRRs have revealed the conserved function of the cytoplasmic domains of RLKs, like the chimera with the BRI1 ectodomain fused to the cytoplasmic kinase domain of AtWAK2 revealed that perception of Brassinosteroid hormone as well as the maintenance of cellular homeostasis was intact which is a function of BRI1 and AtWAK2, respectively. Similarly, swapping the ectodomain of EFR with AtWAK1 and vice-versa kept the ectodomains recognition and activated the cytoplasmic kinase signaling (100). Moreover, the recognition of the cognate ligand elf18 by the chimeric receptor with the ectodomain of EFR and cytoplasmic WAK1 activated the same plant defense against fungal and bacterial pathogens (100). Several other combinations have demonstrated that PRRs can be successfully engineered to increase the magnitude of resistance and also increase the spectrum of pathogen recognition in plants.

Lesion Mimic Mutants and Their Role in Defense Response

During an incompatible host-pathogen interaction, HR is observed as a rapid localized cell death response at the site of infection, which provides resistance against biotrophic or hemi-biotrophic pathogens in their biotrophic phase. This HR based resistance is commonly observed when a pathogen Avr (avirulence) effector is recognized by the host R (resistance) protein. There have been several lesion mimic mutants (LMMs) isolated in many crops, which mimic the HR phenotype and produce spontaneous necrotic lesions on plants due to mis-regulated PCD responses. There are two kinds of LMMs, the initiation LMMs, with inappropriately induce PCD

that form necrotic lesions, whereas the propagation LMMs cannot stop it, once PCD is initiated (106). The constitutive activation of PCD in the LMMs suggests outcome of genes regulating cell death in plants. As cell death is the result of the abiotic and biotic stresses as well as different developmental PCD pathways, many LMMs have impaired one or many of such stress related pathways. Thus, all LMMs have impaired PCD, but few LMMs have mis-regulated host defense response. The characterization of the defense related LMMs would provide us valuable information about the conserved genes underlying defense related PCD in plants (106).

Development of LMMs by Mutagenesis

Mutagenesis has been a valuable tool to produce mutants in cereal crops for close to 100 years (Stadler 1928). There have been multiple LMMs isolated in various crops, including barley, by exposure to both chemical and physical mutagens (106–108). Among the radiation-based methods of mutagenesis, γ-ray and fast neutron are used more often than X-ray bombardment. Among these, γ-ray bombardment causes point mutations to small deletions whereas the fast neutron bombardment causes translocations, chromosome losses, and a range of 1 base pair to even several mega base deletions (109,110). Chemical mutagenesis via sodium azide and ethylmethanesulfanate (EMS) tend to produce frequent deletions and point mutations. Compared to chemical mutagens, radiation cause damage on a larger scale and therefore severely reduces viability of plants (111). However, if the aim is to have gene/s deleted, radiation mutagenesis is a better tool than chemical mutagenesis in plants. The mutagens generate chimeric or heterozygous mutant alleles in the M_1 generation and are therefore selfed and screened at the M_2 generation for any loss of function. Regardless of the mutational procedure utilized, the point of developing mutants is to identify traits of interest so as to utilize

reverse/forward genetics approaches to characterize the mutated gene and its effect on the phenotypes of the plant.

Lesion Mimic Mutants in Barley Pertaining to Plant Immunity

In barley, although several LMMs have been described (112), only two LMM genes have been cloned, *nec1* and *mlo*. The *Hvnec1* gene encodes a cyclic-gated ion channel protein (CNGC4) (112,113) and is a homolog of the previously cloned *Arabidopsis HLM1* gene (113,114). The mutants in both genes had increased pathogen-related (PR) protein expression, salicylic acid accumulation and produces spontaneous necrotic lesions and leaf tip necrosis with increased susceptibility to certain pathogens (114). The CNGC4 proteins are involved in regulating the intracellular ion fluxes like Ca^{2+} and thus function in the homeostasis, development, plant defense and PCD (115). The barley mutant *nec1* has a frameshift mutation of the CNGC4 and constitutive over expression of PR-1 (116).

The loss of function of gene *Mildew Locus O* (Mlo) confers recessive broad-spectrum resistance to the ascomycete fungal pathogen *Erysiphe graminis* f. sp. *hordei,* the cause of barley powdery mildew. The *mlo* race non-specific resistance was deployed in Northern Europe as a source of durable powdery mildew resistance in barley in late 1970s to early 1980s (117–119). However, due to its LMM spontaneous necrotic phenotype it incurs an ~4% yield penalty on varieties even in absence of powdery mildew disease, thus making it economically effective only under high disease pressure (120). The barley *Mlo* gene encodes a ROP like G-protein which is a plasma membrane integral protein that has a apoplastic amino end, seven transmembrane domains and a cytoplasmic carboxy tail which binds to calmodulin to provide complete susceptibility during powdery mildew infection (119,121). Interestingly, the *mlo* resistance is functional even before the cell wall appositions and spontaneous necrotic lesion phenotype

appear in barley plant, suggesting that the absence of the *Mlo* gene primes the defense responses and is similar to the *Arabidopsis* lesion simulating disease 1 (*lsd1*) mutant where resistance precedes the spontaneous cell death lesions (122,123). The *Mlo* gene, a negative regulator of PCD, is conserved and found in other species like wheat, pea, *Arabidopsis,* apple, cucumber, grapevine, melon, pepper, rose and tomato where the absence or silencing of this gene provides powdery mildew resistance (119). The *mlo* mutants which provide resistance against powdery mildew also provide resistance against the root rot causing pathogen *Phytophthora palmivora*, but remain susceptible to *Magneporthe oryzae, Ramularia collo-cygni* and culture filtrates of *B. sorokiniana* (124,125). The Mlo protein dual function in regulating cell death and induced in defense response suggests that the underlying downstream signaling pathways in both phenomena do integrate and are possibly conserved. In animals PCD is irreversibly triggered by the cytochrome *c* release from mitochondria by the pores formed by the BAX proteins (126). Interestingly, overexpression of the Barley homologue of BAX inhibitor 1 (*BI-1*) does induce susceptibility in the *mlo* resistant plants (127).

nec3

The Necrotic Leaf Spot 3 (*nec3*) mutants are propagation mutants as the gene is likely to regulate PCD initiated by pathogen perception. The *nec3* mutants were previously described as runaway PCD mutants with large orange tan necrotic lesions (112,128,129) and the mutations was mapped to the short arm of chromosome 6H of barely. The gamma irradiated mutant was generated in cv Bowman to mutate the gene/s conferring dominant susceptibility to *B. sorokiniana* pathotype two. The other barley fast neutron mutant FN362 (*nec3.l*; GSHO 3605) and FN363 (*nec3.m*; GSHO 3606) were isolated from the cv Steptoe at the IAEA Seibersdorf facility at Austria. The *nec3.d* (GSHO 2065) in cv Proctor and *nec3.e* (GSHO 2066) in cv Villa

were obtained from Dr. J. Francowiack. Allelism test of the mutants revealed that FN362 and FN363 are allelic to the previously described *nec3d* (GSHO 2065) and *nec3e* (GSHO 2066) mutant alleles (112,130).

Previous Affymetrix transcriptome analysis of the *nec3* mutant did not yield the mutant gene but provided some evidence as to what genes are over or under expressed when compared to the wild type (129). The Affymetrix data suggested similarities between abiotic stresses and *nec3* phenotype, however the *nec3* mutants tissue used for transcript analysis were not from pathogen or biotic stress challenged plants. It was determined in our study that pathogen challenge is essential because unlike true LMMs *nec3* mutants expresses a pathogen induced PCD phenotype. The transcriptome of the *nec3* mutants analyzed had differential expression of several abiotic and abiotic stress related genes and cell-wall modifying genes including several enzymes, including expansin and extensin proteins, providing clues that there could be a cell-wall modification triggering the PCD during pathogen attack. In order to identify *nec3*, our research group developed a mapping population to localize the gene and performed RNAseq to identify candidate genes (130,131). Four independent *nec3* mutants (FN362, FN363, nec3.d, and nec3.e) were shown to be allelic to gamma1, and like gamma1, only exhibit the runaway PCD phenotype upon specific pathogen challenge (130). Genetic analysis of F_2 progeny generated by crossing gamma1 and the cultivar Quest indicated that this recessive mutation mapped to a region delimited to approximately 5.8 cM at the centromeric region of barley chromosome 6H between the flanking markers GBM1053 and GBM1423, and co-segregates with the marker GBM1212 (130). This region corresponds to the previous low-resolution mapping of the *nec3* gene.

Literature Cited

1. Newton AC, Flavell AJ, George TS, Leat P, Mullholland B, Ramsay L, et al. Crops that feed the world 4. Barley: a resilient crop? Strengths and weaknesses in the context of food security. Food Sec. 2011 Jun;3(2):141–178.
2. Dawson IK, Russell J, Powell W, Steffenson B, Thomas WTB, Waugh R. Barley: a translational model for adaptation to climate change. New Phytol. 2015 May;206(3):913–931.
3. Schmid K, Kilian B, Russell J. Barley domestication, adaptation and population genomics. In: Stein N, Muehlbauer GJ, editors. The Barley Genome. Cham: Springer International Publishing; 2018. p. 317–336.
4. FAOSTAT. FAOSTAT Statistics Division of Food and Agriculture Organization of the United Nations [Internet]. 2019. Available from: http://www.fao.org/faostat/en/#data/QC/visualize
5. Stein N, Muehlbauer GJ, editors. The Barley Genome. Cham: Springer International Publishing; 2018.
6. Badr A, Müller K, Schäfer-Pregl R, El Rabey H, Effgen S, Ibrahim HH, et al. On the origin and domestication history of Barley (Hordeum vulgare). Mol Biol Evol. 2000 Apr;17(4):499–510.
7. Komatsuda T, Pourkheirandish M, He C, Azhaguvel P, Kanamori H, Perovic D, et al. Six-rowed barley originated from a mutation in a homeodomain-leucine zipper I-class homeobox gene. Proc Natl Acad Sci USA. 2007 Jan 23;104(4):1424–1429.

8. Sakuma S, Salomon B, Komatsuda T. The domestication syndrome genes responsible for the major changes in plant form in the Triticeae crops. Plant Cell Physiol. 2011 May;52(5):738–749.

9. Blattner FR. Progress in phylogenetic analysis and a new infrageneric classification of the barley genus Hordeum (Poaceae: Triticeae). Breed Sci. 2009;59(5):471–480.

10. Westerbergh A, Lerceteau-Köhler E, Sameri M, Bedada G, Lundquist P-O. Towards the development of perennial barley for cold temperate climates—evaluation of wild barley relatives as genetic resources. Sustainability. 2018 Jun 12;10(6):1969.

11. Wendler N. The genomes of the secondary and tertiary gene pools of barley. In: Stein N, Muehlbauer GJ, editors. The Barley Genome. Cham: Springer International Publishing; 2018. p. 337–344.

12. Pourkheirandish M, Kanamori H, Wu J, Sakuma S, Blattner FR, Komatsuda T. Elucidation of the origin of "agriocrithon" based on domestication genes questions the hypothesis that Tibet is one of the centers of barley domestication. Plant J. 2018 May;94(3):525–534.

13. Mascher M, Schuenemann VJ, Davidovich U, Marom N, Himmelbach A, Hübner S, et al. Genomic analysis of 6,000-year-old cultivated grain illuminates the domestication history of barley. Nat Genet. 2016 Jul 18;48(9):1089–1093.

14. Pourkheirandish M, Hensel G, Kilian B, Senthil N, Chen G, Sameri M, et al. Evolution of the grain dispersal system in barley. Cell. 2015 Jul 30;162(3):527–539.

15. Ruge-Wehling B, Wehling P. The Secondary Gene Pool of Barley (Hordeum bulbosum): Gene Introgression and Homoeologous Recombination. In: Kumlehn J, Stein N, editors.

Biotechnological approaches to barley improvement. Berlin, Heidelberg: Springer Berlin Heidelberg; 2014. p. 331–343.

16. Mascher M, Gundlach H, Himmelbach A, Beier S, Twardziok SO, Wicker T, et al. A chromosome conformation capture ordered sequence of the barley genome. Nature. 2017 Apr 26;544(7651):427–433.

17. Mascher M, Muehlbauer GJ, Rokhsar DS, Chapman J, Schmutz J, Barry K, et al. Anchoring and ordering NGS contig assemblies by population sequencing (POPSEQ). Plant J. 2013 Nov;76(4):718–727.

18. Tinline RD. Cochliobolus sativus, a pathogen of wide host range. Genetics of plant pathogenic fungi. Elsevier; 1988. p. 113–122.

19. Valjavec-Gratian M, Steffenson BJ. Pathotypes of Cochliobolus sativus on Barley in North Dakota. Plant Dis. 1997 Nov;81(11):1275–1278.

20. Zhong S, Ali S, Leng Y, Wang R, Garvin DF. Brachypodium distachyon-Cochliobolus sativus Pathosystem is a New Model for Studying Plant-Fungal Interactions in Cereal Crops. Phytopathology. 2015 Apr;105(4):482–489.

21. Condon BJ, Leng Y, Wu D, Bushley KE, Ohm RA, Otillar R, et al. Comparative genome structure, secondary metabolite, and effector coding capacity across Cochliobolus pathogens. PLoS Genet. 2013 Jan 24;9(1):e1003233.

22. Zhong S, Steffenson BJ, Martinez JP, Ciuffetti LM. A molecular genetic map and electrophoretic karyotype of the plant pathogenic fungus Cochliobolus sativus. Mol Plant Microbe Interact. 2002 May;15(5):481–492.

23. Johal GS, Briggs SP. Reductase activity encoded by the *HM1* disease resistance gene in maize. Science. 1992 Nov 6;258(5084):985–987.

24. Padmanabhan SY. The great bengal famine. Annu Rev Phytopathol. 1973 Sep;11(1):11–24.

25. Collingham L. Taste of War: World War II and the Battle for Food. Penguin; 2012.

26. Barnwal MK, Kotasthane A, Magculia N, Mukherjee PK, Savary S, Sharma AK, et al. A review on crop losses, epidemiology and disease management of rice brown spot to identify research priorities and knowledge gaps. Eur J Plant Pathol. 2013 Jul;136(3):443–457.

27. Tatum LA. The southern corn leaf blight epidemic. Science. 1971 Mar 19;171(3976):1113–1116.

28. Miller RJ, Koeppe DE. Southern corn leaf blight: susceptible and resistant mitochondria. Science. 1971 Jul 2;173(3991):67–69.

29. Mayama S, Matsuura Y, Iida H, Tani T. The role of avenalumin in the resistance of oat to crown rust, Puccinia coronata f. sp. avenae. Physiological Plant Pathology. 1982 Mar;20(2):189–199.

30. Luke HH, Wheeler HE, Wallace AT. Victoria-type resistance to crown rust separated from susceptibility to Helminthosporium blight in Oats. Phytopathology. 1960;

31. Lorang JM, Sweat TA, Wolpert TJ. Plant disease susceptibility conferred by a "resistance" gene. Proc Natl Acad Sci USA. 2007 Sep 11;104(37):14861–14866.

32. Wolpert TJ, Lorang JM. Victoria Blight, defense turned upside down. Physiol Mol Plant Pathol. 2016 Jul;95:8–13.

33. Wolpert TJ, Navarre DA, Moore DL, Macko V. Identification of the 100-kD victorin binding protein from oats. Plant Cell. 1994 Aug;6(8):1145–1155.

34. DE Mathre. Compendium of barley diseases. Compendium of barley diseases [Internet]. 1982 [cited 2018 Feb 20];(633). Available from: http://www.sidalc.net/cgi-bin/wxis.exe/?IsisScript=UACHBC.xis&method=post&formato=2&cantidad=1&expresion=mfn=072782

35. Gupta PK, Chand R, Vasistha NK, Pandey SP, Kumar U, Mishra VK, et al. Spot blotch disease of wheat: the current status of research on genetics and breeding. Plant Pathol. 2017 Nov 21;67(3):508–531.

36. Acharya, Dutta K, Pradhan AK, Prakash. Bipolaris sorokiniana ' (Sacc.) Shoem.: The most destructive wheat fungal pathogen in the warmer areas. Australian Journal of Crop Science. 2011;

37. Savary S, Willocquet L, Pethybridge SJ, Esker P, McRoberts N, Nelson A. The global burden of pathogens and pests on major food crops. Nat Ecol Evol. 2019 Mar;3(3):430–439.

38. Pammel LH, King CM, Bakke AL. Two barley blights, with comparison of species of Helminthosporium upon cereals. Iowa Agricultural Experimental Station. 1910;116:178–190.

39. Wilcoxson RD. Development of barley resistant to spot blotch and genetics of resistance. Plant Dis. 1990;74(3):207.

40. Tekauz A, Gilbert J, Mueller E, Stulzer M, Beyene M, Ghazvini H, et al. Canadian Plant Disease Survey. Canadian plant disease survey. 2003;83:60–61.

41. Murray GM, Brennan JP. Estimating disease losses to the Australian barley industry. Austral Plant Pathol. 2010;39(1):85.

42. Fetch TG, Steffenson BJ. Rating Scales for Assessing Infection Responses of Barley Infected with*Cochliobolus sativus*. Plant Dis. 1999 Mar;83(3):213–217.

43. Fetch TG, Steffenson BJ. Identification of Cochliobolus sativus isolates expressing differential virulence on two-row barley genotypes from North Dakota. Canadian Journal of Plant Pathology. 1994 Sep;16(3):202–206.

44. Brandle JE, Namwila JCP, Little R. Effect of plant architecture on levels of Helminthosporium sativum infection on spring wheat grown in Zambia. Crop Prot. 1987 Jun;6(3):153–156.

45. Raemaekers RH. Helminthosporium sativum: disease complex on wheat and sources of resistance in Zambia. 1988.

46. Duveiller E. Controlling Foliar Blights of Wheat in the Rice-Wheat Systems of Asia. Plant Dis. 2004 May;88(5):552–556.

47. Braun EJ, Howard RJ. Adhesion of fungal spores and germlings to host plant surfaces. Protoplasma. 1994 Mar;181(1-4):202–212.

48. Kumar J, Schafer P, Huckelhoven R, Langen G, Baltruschat H, Stein E, et al. Bipolaris sorokiniana, a cereal pathogen of global concern: cytological and molecular approaches towards better control. Mol Plant Pathol. 2002 Jul;3(4):185–195.

49. Santén K, Marttila S, Liljeroth E, Bryngelsson T. Immunocytochemical localization of the pathogenesis-related PR-1 protein in barley leaves after infection by Bipolaris sorokiniana. Physiol Mol Plant Pathol. 2005 Jan;66(1-2):45–54.

50. Kiesling RL. The diseases of barley. Barley [Internet]. 1985 [cited 2018 Feb 20];269–312. Available from: https://dl.sciencesocieties.org/publications/books/abstracts/agronomymonogra/barley/269

51. Friesen TL, Holmes DJ, Bowden RL, Faris JD. ToxA Is Present in the U.S. Bipolaris sorokiniana Population and Is a Significant Virulence Factor on Wheat Harboring Tsn1. Plant Dis. 2018 Dec;102(12):2446–2452.

52. McDonald MC, Ahren D, Simpfendorfer S, Milgate A, Solomon PS. The discovery of the virulence gene ToxA in the wheat and barley pathogen Bipolaris sorokiniana. Mol Plant Pathol. 2018;19(2):432–439.

53. Duczek LJ. Comparison of the common root rot reaction of barley lines and cultivars in northwestern Alberta and central Saskatchewan. Canadian Journal of Plant Pathology. 1984 Mar;6(1):81–89.

54. Duczek LJ, Sutherland KA, Reed SL, Bailey KL, Lafond GP. Survival of leaf spot pathogens on crop residues of wheat and barley in Saskatchewan. Canadian Journal of Plant Pathology. 1999 Jun;21(2):165–173.

55. Conner RL, Duczek LJ, Kozub GC, Kuzyk AD. Influence of crop rotation on common root rot of wheat and barley. Canadian Journal of Plant Pathology. 1996 Sep;18(3):247–254.

56. Friskop A, Markell SG, Khan M. 2019 North Dakota Field Crop Plant Disease Management Guide — Publications [Internet]. 2019 [cited 2019 Jun 1]. Available from: https://www.ag.ndsu.edu/publications/crops/2018-north-dakota-field-crp-plant-disease-management-guide

57. Moya P, Pedemonte D, Amengual S, Franco MEE, Sisterna MN. Antagonism and modes of action of Chaetomium globosum species group, potential biocontrol agent of barley foliar diseases. Bol Soc Argent Bot. 2016 Dec 30;51(4):569.

58. Steffenson BJ, Hayes PM, Kleinhofs A. Genetics of seedling and adult plant resistance to net blotch (Pyrenophora teres f. teres) and spot blotch (Cochliobolus sativus) in barley. Theor Appl Genet. 1996 Apr;92(5):552–558.

59. Zhou H, Steffenson B. Genome-wide association mapping reveals genetic architecture of durable spot blotch resistance in US barley breeding germplasm. Mol Breeding. 2013 Jun;32(1):139–154.

60. Ghazvini H, Tekauz A. Host-Pathogen Interactions Among Barley Genotypes and Bipolaris sorokiniana Isolates. Plant Dis. 2008 Feb;92(2):225–233.

61. Bilgic H, Steffenson BJ, Hayes PM. Comprehensive genetic analyses reveal differential expression of spot blotch resistance in four populations of barley. Theor Appl Genet. 2005 Nov 15;111(7):1238–1250.

62. Bovill J, Lehmensiek A, Sutherland MW, Platz GJ, Usher T, Franckowiak J, et al. Mapping spot blotch resistance genes in four barley populations. Mol Breeding. 2010 Dec;26(4):653–666.

63. Drader T, Johnson K, Brueggeman R, Kudrna D, Kleinhofs A. Genetic and physical mapping of a high recombination region on chromosome 7H(1) in barley. Theor Appl Genet. 2009 Feb;118(4):811–820.

64. Drader T, Kleinhofs A. A synteny map and disease resistance gene comparison between barley and the model monocot Brachypodium distachyon. Genome. 2010 May;53(5):406–417.

65. Staskawicz BJ. Genetics of plant-pathogen interactions specifying plant disease resistance. Plant Physiol. 2001 Jan;125(1):73–76.

66. Duxbury Z, Ma Y, Furzer OJ, Huh SU, Cevik V, Jones JDG, et al. Pathogen perception by NLRs in plants and animals: Parallel worlds. Bioessays. 2016 Jun 24;38(8):769–781.

67. Bacete L, Mélida H, Miedes E, Molina A. Plant cell wall-mediated immunity: cell wall changes trigger disease resistance responses. Plant J. 2018 Feb 2;93(4):614–636.

68. Schulze-Lefert P, Panstruga R. A molecular evolutionary concept connecting nonhost resistance, pathogen host range, and pathogen speciation. Trends Plant Sci. 2011 Mar;16(3):117–125.

69. Krattinger SG, Keller B. Molecular genetics and evolution of disease resistance in cereals. New Phytol. 2016 Oct;212(2):320–332.

70. Dodds PN, Rathjen JP. Plant immunity: towards an integrated view of plant-pathogen interactions. Nat Rev Genet. 2010 Aug;11(8):539–548.

71. Boyes DC, Nam J, Dangl JL. The Arabidopsis thaliana RPM1 disease resistance gene product is a peripheral plasma membrane protein that is degraded coincident with the hypersensitive response. Proc Natl Acad Sci USA. 1998 Dec 22;95(26):15849–15854.

72. Glazebrook J. Contrasting mechanisms of defense against biotrophic and necrotrophic pathogens. Annu Rev Phytopathol. 2005;43:205–227.

73. Mengiste T. Plant immunity to necrotrophs. Annu Rev Phytopathol. 2012 Jun 15;50:267–294.

74. Boller T, Felix G. A renaissance of elicitors: perception of microbe-associated molecular patterns and danger signals by pattern-recognition receptors. Annu Rev Plant Biol. 2009;60:379–406.

75. Chinchilla D, Zipfel C, Robatzek S, Kemmerling B, Nürnberger T, Jones JDG, et al. A flagellin-induced complex of the receptor FLS2 and BAK1 initiates plant defence. Nature. 2007 Jul 26;448(7152):497–500.

76. Zipfel C, Robatzek S, Navarro L, Oakeley EJ, Jones JDG, Felix G, et al. Bacterial disease resistance in Arabidopsis through flagellin perception. Nature. 2004 Apr 15;428(6984):764–767.

77. Buscaill P, Chandrasekar B, Sanguankiattichai N, Kourelis J, Kaschani F, Thomas EL, et al. Glycosidase and glycan polymorphism control hydrolytic release of immunogenic flagellin peptides. Science. 2019 Apr 12;364(6436).

78. Li L, Li M, Yu L, Zhou Z, Liang X, Liu Z, et al. The FLS2-associated kinase BIK1 directly phosphorylates the NADPH oxidase RbohD to control plant immunity. Cell Host Microbe. 2014 Mar 12;15(3):329–338.

79. Luna E, Pastor V, Robert J, Flors V, Mauch-Mani B, Ton J. Callose deposition: a multifaceted plant defense response. Mol Plant Microbe Interact. 2011 Feb;24(2):183–193.

80. Couto D, Zipfel C. Regulation of pattern recognition receptor signalling in plants. Nat Rev Immunol. 2016 Aug 1;16(9):537–552.

81. Robatzek S, Chinchilla D, Boller T. Ligand-induced endocytosis of the pattern recognition receptor FLS2 in Arabidopsis. Genes Dev. 2006 Mar 1;20(5):537–542.

82. Gómez-Gómez L, Bauer Z, Boller T. Both the extracellular leucine-rich repeat domain and the kinase activity of FSL2 are required for flagellin binding and signaling in Arabidopsis. Plant Cell. 2001 May;13(5):1155–1163.

83. Albert I, Böhm H, Albert M, Feiler CE, Imkampe J, Wallmeroth N, et al. An RLP23-SOBIR1-BAK1 complex mediates NLP-triggered immunity. Nat Plants. 2015 Oct 5;1:15140.

84. Liebrand TWH, van den Burg HA, Joosten MHAJ. Two for all: receptor-associated kinases SOBIR1 and BAK1. Trends Plant Sci. 2014 Feb;19(2):123–132.

85. Monaghan J, Zipfel C. Plant pattern recognition receptor complexes at the plasma membrane. Curr Opin Plant Biol. 2012 Aug;15(4):349–357.

86. Miya A, Albert P, Shinya T, Desaki Y, Ichimura K, Shirasu K, et al. CERK1, a LysM receptor kinase, is essential for chitin elicitor signaling in Arabidopsis. Proc Natl Acad Sci USA. 2007 Dec 4;104(49):19613–19618.

87. Desaki Y, Kouzai Y, Ninomiya Y, Iwase R, Shimizu Y, Seko K, et al. OsCERK1 plays a crucial role in the lipopolysaccharide-induced immune response of rice. New Phytol. 2018 Feb;217(3):1042–1049.

88. Kaku H, Nishizawa Y, Ishii-Minami N, Akimoto-Tomiyama C, Dohmae N, Takio K, et al. Plant cells recognize chitin fragments for defense signaling through a plasma membrane receptor. Proc Natl Acad Sci USA. 2006 Jul 18;103(29):11086–11091.

89. Wan J, Zhang X-C, Neece D, Ramonell KM, Clough S, Kim S-Y, et al. A LysM receptor-like kinase plays a critical role in chitin signaling and fungal resistance in Arabidopsis. Plant Cell. 2008 Feb 8;20(2):471–481.

90. Liu T, Liu Z, Song C, Hu Y, Han Z, She J, et al. Chitin-induced dimerization activates a plant immune receptor. Science. 2012 Jun 1;336(6085):1160–1164.

91. Hao L-H, Wang W-X, Chen C, Wang Y-F, Liu T, Li X, et al. Extracellular ATP promotes stomatal opening of Arabidopsis thaliana through heterotrimeric G protein α subunit and reactive oxygen species. Mol Plant. 2012 Jul;5(4):852–864.

92. Khakh BS, Burnstock G. The double life of ATP. Sci Am. 2009 Dec;301(6):, 92.

93. Bouwmeester K, de Sain M, Weide R, Gouget A, Klamer S, Canut H, et al. The lectin receptor kinase LecRK-I.9 is a novel *Phytophthora* resistance component and a potential host target for a RXLR effector. PLoS Pathog. 2011 Mar;7(3):e1001327.

94. Choi J, Tanaka K, Liang Y, Cao Y, Lee SY, Stacey G. Extracellular ATP, a danger signal, is recognized by DORN1 in Arabidopsis. Biochem J. 2014 Nov 1;463(3):429–437.

95. Tanaka K, Choi J, Cao Y, Stacey G. Extracellular ATP acts as a damage-associated molecular pattern (DAMP) signal in plants. Front Plant Sci. 2014 Sep 3;5:446.

96. Kohorn BD, Kobayashi M, Johansen S, Friedman HP, Fischer A, Byers N. Wall-associated kinase 1 (WAK1) is crosslinked in endomembranes, and transport to the cell surface requires correct cell-wall synthesis. J Cell Sci. 2006 Jun 1;119(Pt 11):2282–2290.

97. Zhang S, Chen C, Li L, Meng L, Singh J, Jiang N, et al. Evolutionary expansion, gene structure, and expression of the rice wall-associated kinase gene family. Plant Physiol. 2005 Nov;139(3):1107–1124.

98. Kohorn BD, Johansen S, Shishido A, Todorova T, Martinez R, Defeo E, et al. Pectin activation of MAP kinase and gene expression is WAK2 dependent. Plant J. 2009 Dec;60(6):974–982.

99. Kohorn BD, Kohorn SL. The cell wall-associated kinases, WAKs, as pectin receptors. Front Plant Sci. 2012 May 8;3:88.

100. Brutus A, Sicilia F, Macone A, Cervone F, De Lorenzo G. A domain swap approach reveals a role of the plant wall-associated kinase 1 (WAK1) as a receptor of oligogalacturonides. Proc Natl Acad Sci USA. 2010 May 18;107(20):9452–9457.

101. Park AR, Cho SK, Yun UJ, Jin MY, Lee SH, Sachetto-Martins G, et al. Interaction of the Arabidopsis receptor protein kinase Wak1 with a glycine-rich protein, AtGRP-3. J Biol Chem. 2001 Jul 13;276(28):26688–26693.

102. Gramegna G, Modesti V, Savatin DV, Sicilia F, Cervone F, De Lorenzo G. GRP-3 and KAPP, encoding interactors of WAK1, negatively affect defense responses induced by oligogalacturonides and local response to wounding. J Exp Bot. 2016 Mar;67(6):1715–1729.

103. Diener AC, Ausubel FM. *RESISTANCE TO FUSARIUM OXYSPORUM 1*, a dominant Arabidopsis disease-resistance gene, is not race specific. Genetics. 2005 Sep;171(1):305–321.

104. Hurni S, Scheuermann D, Krattinger SG, Kessel B, Wicker T, Herren G, et al. The maize disease resistance gene Htn1 against northern corn leaf blight encodes a wall-associated receptor-like kinase. Proc Natl Acad Sci USA. 2015 Jul 14;112(28):8780–8785.

105. Shi G, Zhang Z, Friesen TL, Raats D, Fahima T, Brueggeman RS, et al. The hijacking of a receptor kinase-driven pathway by a wheat fungal pathogen leads to disease. Sci Adv. 2016 Oct 26;2(10):e1600822.

106. Lorrain S, Vailleau F, Balagué C, Roby D. Lesion mimic mutants: keys for deciphering cell death and defense pathways in plants? Trends Plant Sci. 2003 Jun;8(6):263–271.

107. Druka A, Franckowiak J, Lundqvist U, Bonar N, Alexander J, Houston K, et al. Genetic dissection of barley morphology and development. Plant Physiol. 2011 Feb;155(2):617–627.

108. Penmetsa RV, Cook DR. Production and characterization of diverse developmental mutants of Medicago truncatula. Plant Physiol. 2000 Aug;123(4):1387–1398.

109. Li X, Song Y, Century K, Straight S, Ronald P, Dong X, et al. A fast neutron deletion mutagenesis-based reverse genetics system for plants. Plant J. 2001 Aug;27(3):235–242.

110. Koornneef M, Dellaert LW, van der Veen JH. EMS- and radiation-induced mutation frequencies at individual loci in Arabidopsis thaliana (L.) Heynh. Mutat Res. 1982 Mar;93(1):109–123.

111. Tadele Z. Mutagenesis and TILLING to dissect gene function in plants. Curr Genomics. 2016 Dec;17(6):499–508.

112. Rostoks N, Schmierer D, Kudrna D, Kleinhofs A. Barley putative hypersensitive induced reaction genes: genetic mapping, sequence analyses and differential expression in disease lesion mimic mutants. Theor Appl Genet. 2003 Oct;107(6):1094–1101.

113. Rostoks N, Schmierer D, Mudie S, Drader T, Brueggeman R, Caldwell DG, et al. Barley necrotic locus nec1 encodes the cyclic nucleotide-gated ion channel 4 homologous to the Arabidopsis HLM1. Mol Genet Genomics. 2006 Feb;275(2):159–168.

114. Balagué C, Lin B, Alcon C, Flottes G, Malmström S, Köhler C, et al. HLM1, an essential signaling component in the hypersensitive response, is a member of the cyclic nucleotide-gated channel ion channel family. Plant Cell. 2003 Feb;15(2):365–379.

115. Ma W, Berkowitz GA. Ca2+ conduction by plant cyclic nucleotide gated channels and associated signaling components in pathogen defense signal transduction cascades. New Phytologist. 2011 May 1;

116. Keisa A, Kanberga-Silina K, Nakurte I, Kunga L, Rostoks N. Differential disease resistance response in the barley necrotic mutant nec1. BMC Plant Biol. 2011 Apr 15;11:66.

117. Jorgensen IH. Discovery, characterization and exploitation of Mlo powdery mildew resistance in barley. Euphytica. 1992;63(1-2):141–152.

118. Lyngkjær MF, Carver TL. Conditioning of cellular defence responses to powdery mildew in cereal leaves by prior attack. Mol Plant Pathol. 2000 Jan 1;1(1):41–49.

119. Kusch S, Panstruga R. *mlo*-based resistance: an apparently universal "weapon" to defeat powdery mildew disease. Mol Plant Microbe Interact. 2017 Mar 30;30(3):179–189.

120. Kjaer B, Jensen HP, Jensen J, Jorgensen JH. Associations between three ml-o powdery mildew resistance genes and agronomic traits in barley. Euphytica. 1990 Apr;46(3):185–193.

121. Kim MC, Panstruga R, Elliott C, Müller J, Devoto A, Yoon HW, et al. Calmodulin interacts with MLO protein to regulate defence against mildew in barley. Nature. 2002 Mar 28;416(6879):447–451.

122. Wolter M, Hollricher K, Salamini F, Schulze-Lefert P. The mlo resistance alleles to powdery mildew infection in barley trigger a developmentally controlled defence mimic phenotype. Mol Gen Genet. 1993 May;239(1-2):122–128.

123. Büschges R, Hollricher K, Panstruga R, Simons G, Wolter M, Frijters A, et al. The barley *Mlo* gene: a novel control element of plant pathogen resistance. Cell. 1997 Mar 7;88(5):695–705.

124. Le Fevre R, O'Boyle B, Moscou MJ, Schornack S. Colonization of Barley by the Broad-Host Hemibiotrophic Pathogen Phytophthora palmivora Uncovers a Leaf Development-Dependent Involvement of Mlo. Mol Plant Microbe Interact. 2016 May 2;29(5):385–395.

125. McGrann GRD, Steed A, Burt C, Nicholson P, Brown JKM. Differential effects of lesion mimic mutants in barley on disease development by facultative pathogens. J Exp Bot. 2015 Jun;66(11):3417–3428.

126. Eskes R, Antonsson B, Osen-Sand A, Montessuit S, Richter C, Sadoul R, et al. Bax-induced cytochrome C release from mitochondria is independent of the permeability transition pore but highly dependent on Mg2+ ions. J Cell Biol. 1998 Oct 5;143(1):217–224.

127. Hückelhoven R, Dechert C, Kogel K-H. Overexpression of barley BAX inhibitor 1 induces breakdown of mlo-mediated penetration resistance to Blumeria graminis. Proc Natl Acad Sci USA. 2003 Apr 29;100(9):5555–5560.

128. Lundqvist U, Franckowiak JD, Konishi T. New and revised descriptions of barley genes. Barley genetics newsletter. 1997;

129. Keisa A, Brueggeman R, Drader T, Kleinhofs A, Rostoks N. Transcriptome analysis of the barley nec3 mutant reveals a potential link with abiotic stress response related signaling pathways. Environ Exp Bot. 2010;8:1–16.

130. Sager-Bittara LP. Characterization of Programmed Cell Death Responses Involved in Disease Resistance/Susceptibility Responses in Barley. thesis. 2015;

131. Ameen G, Bittara L, Richards J, Solanki S, Friesen T, Brueggeman R. The Nec3 gene is a putative negative regulator of pathogen induced programmed cell death in barley. Amer Phytopathological Soc; 2018.

CHAPTER 2. *rcs5*- MEDIATED SPOT BLOTCH RESISTANCE IN BARLEY IS CONFERRED BY WALL-ASSOCIATED KINASES THAT RESIST PATHOGEN MANIPULATION

Abstract

Plant biotrophic pathogen disease resistances rely on immunity receptor-mediated programmed cell death (PCD) responses, but specialized necrotrophic/hemi-biotrophic pathogens hijack these mechanisms to colonize the resulting dead tissue in their necrotrophic phase. Thus, immunity receptors can become necrotrophic pathogen dominant susceptibility targets but resistance mechanisms that resist necrotroph manipulation are recessive resistance genes. The barley *rcs5* QTL imparts recessive resistance against the disease spot blotch caused by the hemi-biotrophic fungal pathogen *Bipolaris sorokiniana*. The *rcs5* genetic interval was delimited to ~0.23 cM, representing an ~234 kb genomic region containing four wall-associated kinase (WAK) genes, designated *HvWak2, Sbs1, Sbs2* (susceptibility to *Bipolaris sorokiniana* 1&2), and *HvWak5*. Post-transcriptional gene silencing of *Sbs1&2* in susceptible barley cultivars resulted in resistance showing dominant susceptibility function. Allele analysis of *Sbs1&2* from resistant and susceptible barley cultivars identified sequence polymorphisms associated with phenotypes in their primary coding sequence and promoter regions, suggesting differential transcriptional regulation may contribute to susceptibility. Transcript analysis of *Sbs1&2* showed nearly undetectable expression in resistant and susceptible cultivars prior to pathogen challenge; however, upregulation of both genes occurred specifically in susceptible cultivars post-inoculation with a virulent isolate. Apoplastic wash fluids collected from barley infected with a virulent isolate induced *Sbs1*, suggesting regulation by an apoplastic-secreted effector. Thus, *Sbs1*&2 function as *B. sorokiniana* susceptibility targets and non-functional alleles or alleles that

resist induction by the pathogen mediate *rcs5*-recessive resistance. The *sbs1&2* alleles underlying the *rcs5* QTL that the pathogen is unable to manipulate are the first resistance genes identified against spot blotch.

Significance Statement

The *rcs5* locus in barley confers a high level of seedling resistance and a moderate level of adult plant resistance to spot blotch. It is part of a complex that has provided durable spot blotch resistance in many North American barley cultivars (cv) for more than 50 years. Genetic characterization and positional cloning of *rcs5* identified the dominant susceptibility genes, *Sbs1* and *Sbs2* (susceptibility to *Bipolaris sorokiniana* 1 and 2) as wall-associated kinases. These genes are hijacked by the hemibiotrophic pathogen in its necrotrophic phase to induce programmed cell death, facilitating disease development. We report the first spot blotch resistance/susceptibility genes cloned that function via alleles that cannot be specifically induced and hijacked by virulent isolates of the pathogen.

Introduction

Barley ranks fourth among cereals with respect to area under production in the world (1). Although barley is not a staple food crop, it possesses unique malting characteristics that are valued for the production of beer and spirits; multi-billion dollar industries across the world. Recent studies predicted that climate change presents a threat to barley production due to higher temperatures and water deficiencies (2). Although, climate change results in drought stricken regions, others experience excess precipitation (3) and combined with elevated temperatures will provide environments more conducive to the development of fungal disease epidemics. Thus, climate change will exacerbate disease problems in areas experiencing excess precipitation,

which was not addressed in the recent predictions of future barley shortages suggesting it could be worse than predicted (2).

One of the major diseases attacking barley is spot blotch, which is caused by the hemi-biotrophic/ necrotrophic ascomycete pathogen *Bipolaris sorokiniana* (teleomorph: *Cochliobolus sativus*). Spot blotch attacks both barley and wheat, causing necrotic, elongated lesions on the leaves, sheath, and stem. In addition to the foliar spot blotch disease, *B. sorokiniana* also causes black point on the kernels (4) and common root rot (5). Spot blotch is distributed worldwide causing yield losses exceeding 30% in barley (6) and ~25% in wheat (7) as well as lower grain quality (8). Disease resistance is the best and most sustainable strategy of managing spot blotch, thus understanding and managing resistance sources is critical.

In the Upper Midwestern United States, spot blotch in barley has been effectively managed for more than 50 years through the deployment of resistant six-rowed cultivars (9–11). This seedling resistance in the cultivar (cv) Morex was conferred predominately by the *Rcs5* gene (now referred to as *rcs5*) (11), which also imparts varying levels of adult plant resistance (9,11). An association genetics study on a large breeding panel provided a comprehensive assessment of the genetic architecture of this durable spot blotch resistance, identifying three quantitative trait loci (QTL): *Rcs-qtl-1H-11_10764*, *Rcs-qtl-3H-11_10565* and *Rcs-qtl-7H-11_20162*. Of these QTL, *Rcs-qtl-7H-11_20162* conferred the largest allelic effect across different populations (10) with several genetic studies positioning *rcs5* within the interval of this chromosome 7H QTL (9–11). Thus, the gene/s underlying the *rcs5* QTL is an important target for cloning and functional characterization, which was the objective of this study.

Millions of years of host-parasite interactions evolved diverse multi-layered plant immunity mechanisms with enough commonality in spatial and temporal pathogen detection that

they have been placed, somewhat arbitrarily, into dichotomous levels. The first level of early-induced resistance responses typically rely on perception of conserved pathogen or more appropriately microbe associated molecular patterns (PAMPs or MAMPs) by transmembrane cell-surface immunity receptors. These receptors were designated pattern recognition receptors (PRRs) with either receptor-like kinase (RLK) or receptor-like protein (RLP) domain structure (12). The RLKs and RLPs have extracellular "receptor" domains and a single transmembrane domain, but RLKs also have an intracellular serine / threonine protein kinase (PK) signalling domain (12). The RLPs interact with RLKs or intracellular PKs to form receptor complexes that recognize extracellular MAMPs, which elicits cytoplasmic PAMP/MAMP-triggered immunity (PTI) signalling (13). The PTI signalling result in transcriptional reprogramming, synthesis and trafficking of defense metabolites, callose deposition, H_2O_2 burst, and in some instances a low amplitude PCD response (13,14).

The best characterized PTI resistance against fungi involves the perception of the major fungal MAMP, chitin, by the rice and *Arabidopsis* PRR complexes that contain homo- and heteroduplexes of RLKs and RLPs with chitin binding LysM ectodomains (15). The rice RLK/RLP heterocomplex containing OsCERK1 and OsCEBiP provides broad non-host resistance to fungal pathogens (16). The Arabidopsis AtCERK1 can act alone to bind chitin to elicit fungal defenses but may also form signalling complexes with other chitin binding RLKs like AtLYK5 (17). CERK1 orthologs in other species also play a role as a co-receptors in complexes that recognize divers MAMPs (17). The rice OsSERK1 RLK also functions in increase resistance to the blast fungus and overexpression of OsSERK1 results in PCD manifested as a disease lesion mimic mutant (18). Our *in silico* protein-protein interaction

analysis reported here suggest that barley CERK1 and SERK1 orthalogs may also be a co-receptor or play a role in *Rcs5*-mediated susceptibility.

The pressure imposed by the PTI non-host resistance mechanisms resulted in the adaptation of pathogen specificity by evolving secreted effectors that suppress PTI signalling, resulting in effector triggered susceptibility (19). The second layer of the plant innate immunity system evolved to recognize pathogen effectors directly or indirectly--typically by cytosolic nucleotide binding-leucine rich repeat (NLR) resistance (R) protein receptors (19). Effector perception by NLRs activates effector triggered immunity (ETI) responses (19), typically characterized by a higher amplitude PCD called the hypersensitive response (HR) (20) that are detrimental to the biotrophic pathogen's feeding structures (i.e. haustoria) that rely on living host cells to extract nutrient.

Research on necrotrophic pathosystems revealed that they produce small secreted necrotrophic effector (NE) proteins to induce immunity responses that result in PCD so the pathogens can colonize, feed, and complete their life cycles on the dead tissue effectively hijacking the plants immune system to cause disease (21). The identification of the host NE-target proteins showed that some fall into the NLR class of resistance (R-) genes, which elicit ETI-mediated HR responses (21,22). Characterization of the *Parastagonospora nodorum* NE SnToxA and its cognate susceptibility target *Tsn1* in wheat, determined that this NLR once triggered by SnToxA activated ETI-like HR responses (21). Thus, necrotrophic specialists elicit responses that evolved to provide immunity against biotrophs to facilitate colonization and further disease development via necrotrophic effector triggered susceptibility (NETS) (23).

The wall-associated kinases (WAKs) are plant RLKs with conserved protein domain architecture including a predicted N-terminal extracellular cell wall binding region with a wall-

associated cysteine-rich galacturonan-binding (GUB-WAK), an Epidermal Growth Factor-Calcium binding domain (EGF_Ca^{2+}) followed by a transmembrane domain (TM) and a C-terminal intracellular localized serine/threonine protein kinase (PK) signalling domain. The WAK proteins function in cell elongation and development, sensing abiotic stresses, and provide resistance to biotrophic pathogens (24,25). This broad functionality is due to their ability to perceive stresses at the cell-wall/plasma membrane interface which includes degradation induced by pathogen cell wall degrading enzymes (26,27).

Damage associated molecular patterns (DAMPs) are plant extracellular matrix components that are inappropriately released from compromised plant cell walls as a result of pathogen-induced degradation or damage. These oligo-galacturonide (OG) cell wall subunits can be detected as "compromised self" by the WAKs (13). The WAK extracellular "receptor" domains bind long polymers of cross-linked pectin in the cell wall as well as soluble OG pectin fragments that are inappropriately released from the cell wall during pathogen ingress. This detection of OG DAMPs by the Arabidopsis WAK1 receptor elicits PTI-like defense signalling (28,29). Both PAMP and DAMP recognition by PRRs activate intracellular defense signalling via the MAPK pathways (30,31).

The WAK class of RLKs have been implicated as dominant resistance genes that follow Flor's gene-for-gene model (32) against biotrophic fungal pathogens. The maize genes *ZmWAK* and *Htn1* encode WAK proteins that confer resistance to *Sporisorium reilianum,* the causal agent of the disease head smut (33,34), and the hemibiotrophic pathogen *Exserohilum turcicum,* the causal agent of the disease northern corn leaf blight (35). A third WAK R-gene, designated *Stb6*, from wheat confers resistance to *Zymoseptoria tritici* isolates carrying the corresponding avirulence gene *AvrStb6* (36).

The wheat WAK gene *Snn1* has been shown to be targeted by the necrotrophic fungal pathogen *Parastagonospora nodorum* in an inverse gene-for-gene manner (37). The *Snn1* protein functions as a dominant susceptibility factor and its cognate NE, designated SnTox1, was identified and shown to directly interact with the *Snn1* WAK receptor (37). Wheat varieties carrying *Snn1* recognize *P. nodorum* isolates that produce SnTox1 eliciting PCD, which facilitates colonization and completion of its lifecycle on the resulting dead tissue. The SnTox1/Snn1 direct interaction suggests that *P. nodorum* evolved to activate *Snn1*-mediated signalling by interacting with its extracellular domain rather than the expected perception of DAMPs or OGs.

Here, we report the cloning and characterization of the *rcs5* gene/s and show that *rcs5* has a recessive resistance nature or more appropriately represents dominant susceptibility conferred by two tightly linked wall-associated kinase (WAK) proteins designated *Sbs1* and *Sbs2*. The *Sbs1* and *Sbs*2 proteins function as susceptibility targets and are specifically up regulated by virulent isolates to induce PCD facilitating disease development in the susceptible barley cultivars. Thus, *Sbs1* and *Sbs2* alleles that are either non-functional or resist induction by the pathogen provide *rcs5*-mediated resistance when present in the homozygous state.

Results

rcs5 Recessive Resistance/Dominant Susceptibility

Fifteen Morex (resistant) x Steptoe (susceptible) F_1 progeny were phenotyped using the rating scale developed by Fetch and Steffenson (38) and all the F_1 individuals assayed demonstrated an intermediate reaction of moderate resistance to moderate susceptibility to *B. sorokiniana* isolate ND85F. The F_1s exhibited infection types (ITs) ranging from 4.5 to 5.5 with an average of 5. The evaluation of 120 Morex x Steptoe F_2 progeny resulted in 4 resistant (scores

of 1 - 3), 25 moderately resistant (scores of 3.1 - 5), 24 moderately susceptible (scores of 5.1-7) and 67 susceptible progeny (scores of 7.1 - 9). Using a cut-off score of 5 and lower as resistant and 5.1 and higher as susceptible, the progeny fit a segregation ratio of 1 resistant: 3 susceptible ($\chi^2 = 0.444$) at p-value 0.8330 (Supp. File. 1; Supp. Fig. 1) showing *rcs5* recessive resistance.

rcs5 Genetic Mapping

To resolve the *rcs5* region 1,536 Steptoe x Morex F_2 progeny, representing 3,072 recombinant gametes, were genotyped using the cMWG773 CAPS and BF627428 markers identifying twenty-five recombinant individuals within the previously delimited ~ 2.8 cM *rcs5* interval (39). The twenty-five critical recombinant lines were allowed to self and $F_{2:3}$ individuals were genotyped and progeny selected that contained homozygous recombinant gametes. These immortal critical recombinants were further saturated using SNP markers within the region identifying seven recombinants that delimit *rcs5*. The high-resolution mapping showed markers Sbs1 STS, Sbs2 SNP, 790 SNP, ctg_1606998_STS, 800 SNP, and BF_256735 co-segregating with *rcs5* and the SNP markers BF257002 and HvWak1 SNP delimited the gene distally and 11_20162 delimited the gene proximally (Fig. 2.1A).

rcs5 Physical Mapping, Sequencing and Gene Prediction

The *rcs5* flanking markers HvWak1_SNP and 11_20162 delimited *rcs5* to an ~0.23 cM genetic interval (Fig. 1.1A) that was present within a single BAC contig represented by three overlapping resistant cv Morex bacterial artificial chromosome (BAC) clones (Fig. 1.1B) (40). The sequence annotation of the three overlapping BAC clones (506G19, 427D04 and 555P07) identified five-candidate genes predicted to encode four wall-associated-kinases (WAKs); HvWak2, *Sbs1*, *Sbs2*, and HvWak5 (Fig. 2.1B), and a predicted non-functional truncated leucine rich-repeat (LRR) gene. Comparison of the BAC contig assembled by restriction mapping and

sequencing versus the barley genome sequence (41) showed the same gene content within the *rcs5* region, yet had a different gene order (Fig. 2.1B). A major concern was that the discrepancies in the gene ordering between the BAC contig and genome assembly resulted in different numbers of candidate genes within the delimited region. However, due to the known accuracy of the BAC restriction mapping and the BAC contig gene order having perfect correlation with the high-resolution genetic mapping, more confidence was placed in the BAC contig assembly (Fig.2.1B). Contrary to the physical map generated by the whole genome assembly, which delimited *rcs5* to a single candidate gene (*Sbs1*), the BAC contig assembly showed that the *rcs5* candidate genes were actually delimited to the four WAK genes, *HvWak2, Sbs1, Sbs2*, and *HvWak5* (Fig. 2.1B).

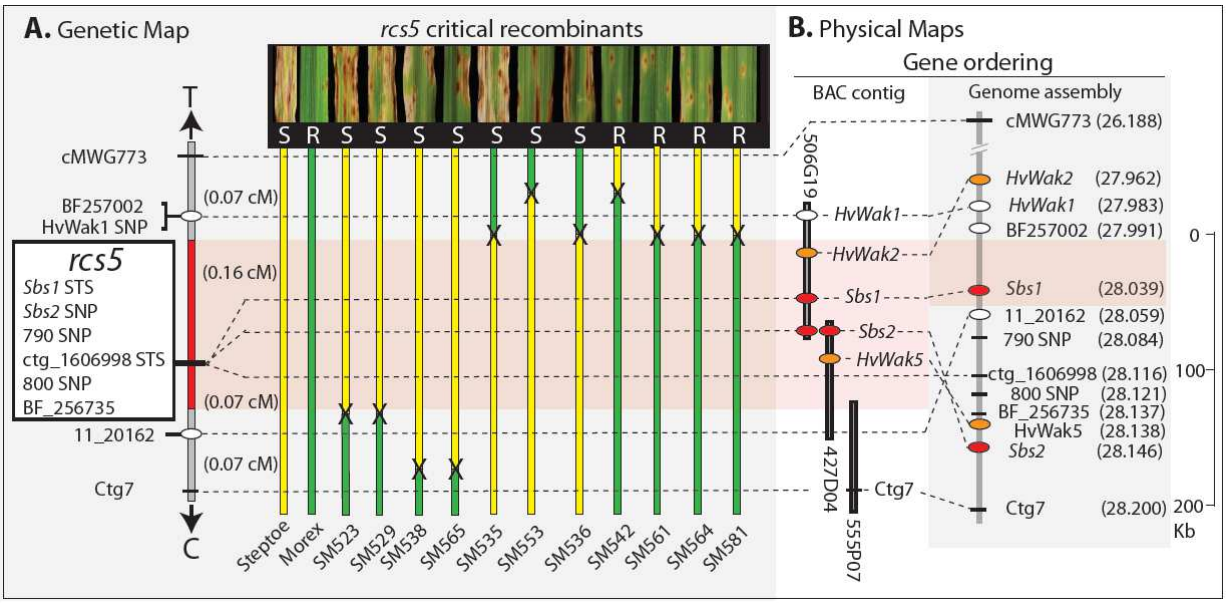

Figure 2.1. High-resolution genetic and physical mapping of the *rcs5* interval. **A)** The vertical gray and red bar on the left depicts the high-resolution genetic map with the molecular markers labeled on the left. The white ovals indicate positions of the *rcs5* proximal and distal flanking markers and the white box contains *rcs5* cosegregating markers. The red bar shows the delimited *rcs5* region with approximate cM distances shown to the right. The arrows indicate the direction of telomere (T) and centromere (C). The yellow vertical bars represent cultivar (cv) Steptoe genotypes, whereas the green bars represent cv Morex genotypes with the black Xs representing the crossover points in the critical recombinants. The vertical dashed lines show the position of each genetic marker. The phenotypic reactions of the recombinants and parents are shown above (S = susceptible and R = resistant). The parents and recombinant nomenclatures are provided below. **B)** Two physical maps are provided with the one on the left produced by cv Morex bacterial artificial chromosome (BAC) contig restriction mapping and sequencing and the one on the right mined from the cv Morex barley genome assembly. Vertical gray bars with black outlines represent the three cv Morex BACs representing the *rcs5* minimum-tilling path with BAC nomenclature provided. The black horizontal bars represent approximate positions of molecular markers and the colored ovals represent candidate genes. The red ovals are validated *rcs5* wall associated kinase (WAK) genes and orange ovals are WAK genes eliminated as *rcs5* candidates. The red shading depicts the delimited *rcs5* regions. For the genome physical map the vertical gray bar represents the genome sequence assembly with Mb positions provided for each gene and marker in parentheses with scale in kilobases provided on the right.

<u>*Rcs5* Candidate Gene Characterization</u>

The four candidate *rcs5* genes delimited by high-resolution mapping have conserved WAK protein domain architecture. Phylogenetic analysis using the predicted nucleotide sequences of the five WAK genes clustered at the *rcs5* region from the resistant cv Morex and

susceptible cv Steptoe showed that they belong to three different clades, with *HvWak1* and *HvWak2* in subclade I, *Sbs1* alone in subclade II, and *Sbs2* and *HvWak5* closely related in subclade III (Supp. File. 1 (Supp. Fig. 2)).

The *HvWak2* gene is encoded by 2,689 bases of gDNA in both the susceptible cv Steptoe and resistant cv Morex, with the annotated gene designated HORVU7Hr1G020660 in the barley whole genome assembly. The intron/exon structure supported by qPCR and RNAseq data contains three exons and two introns. The 2,181 nucleotide *HvWak2* mRNA is predicted to encode a 726 amino-acid (aa) protein, ~79.86 kDa with the typical WAK protein architecture containing the predicted GUB, EGF_Ca, TM and PK domains. There were no non-synonymous nucleotide polymorphisms between the cv Steptoe and cv Morex alleles; thus, *HvWak2* was not a strong *rcs5* candidate.

The resistant cv Morex *Sbs1* allele is transcribed from 1,069 bases of gDNA predicted to contain two exons and one intron producing an 870 nucleotide mRNA (Supp. File. 1 (Supp Fig 3A)) predicted to encode a 289 aa protein, ~31.79 kDa, with the GUB and TM domains, and a truncated PK domain (Supp. File. 1 (Supp Fig 3B)). The predicted cv Morex *Sbs1* mRNA was supported by RNAseq and cDNA sequencing (Supp. File. 1 (Supp Fig. 3B)). Amplicons from gDNA of the 5' region of the cv Steptoe *Sbs1* allele were sequenced and showed that the cv Morex resistant allele contained a 635 bp deletion in exon1 adjacent to but not containing the exon1-intron1 splice junction, eliminating the EGF_Ca binding domain (Supp. File. 1 (Supp Fig. 3B)). The cv Morex *Sbs1* allele also had a two-nucleotide deletion in the second exon of the predicted mRNA at positions 845-846 that caused a frameshift in the coding region and was predicted to produce a truncated PK domain due to presence of an early stop codon. The cv Steptoe *Sbs1* allele was transcribed from 2,462 bases of gDNA that was predicted to produce a

2,052 nucleotide mRNA supported by qPCR and RNAseq data. The annotated mRNA is predicted to encode a 683 aa WAK protein, ~75.13 kDa, with the typical GUB, EGF_Ca, TM and PK domains (Supp. File. 1 (Supp Fig. 3B)). The primary sequence polymorphisms between the resistant and susceptible *Sbs1* alleles suggested that it was a strong *rcs5* candidate gene.

Sbs2 is transcribed from 2,702 bases of gDNA containing four exons and three introns, producing a 2,160 base mRNA (Supp. File. 1 (Supp Fig. 3A)) predicted to encode a 719 aa protein, ~79.09 kDa with a predicted signal peptide (SP) and all the typical GUB, EGF_Ca, TM and PK WAK domains (Supp. File. 1 (Supp Fig. 3B)). The predicted Morex allele also encodes a 719 aa protein that is polymorphic at the N-terminal coding region as compared to the cv Steptoe allele with 28 synonymous SNPs and 16 non-synonymous SNPs suggesting that it was also a strong candidate *rcs5* gene (Supp. File. 1 (Supp Fig. 3B)).

The *HvWak5* gene is transcribed from 2,134 bases of genomic sequence and contains three exons and two introns, producing a 1,731 nucleotide mRNA predicted to encode a 576 aa protein, ~63.36 kDa. The predicted protein contains the typical EGF_Ca, TM and PK WAK domains, but is missing the GUB domain. The predicted HvWak5 protein has identical primary aa sequence for both cv Morex and cv Steptoe alleles suggesting that it was not a strong *rcs5* candidate.

The predicted LRR gene within the delimited *rcs5* region has a stop codon 780 bp from the predicted start methionine, which resulted in a 260 aa protein containing only LRR repeats. Expression analysis via qPCR of the predicted LRR was conducted for cv Morex and cv Steptoe inoculated with *B. sorokiniana* isolate ND85F from infected leaf tissues collected at 0, 12, 24, 36, 48 and 72 hours post inoculation (hpi). The analysis showed no expression before inoculation or at any time-point during the infection process. RNAseq analysis also showed no transcripts

present in the cvs Harrington and Steptoe inoculated with isolate ND85F at 72 hpi, which validated our expression analysis results. The data suggested that the LRR is a pseudogene in both resistant and susceptible cvs eliminating it as an *rcs5* candidate.

RNAseq Validation of Predicted Gene Structures

HvWak2, *Sbs1* and *HvWak5* were predicted as high confidence genes, with the HORVU7Hr1G020660, HORVU7Hr1G020740 and HORVU7Hr1G020810 gene nomenclatures, respectively, in the recently released cv Morex genome sequence (41). However, the HORVU7Hr1G020740 gene prediction is not a full-length transcript for *Sbs1*, and *Sbs2* was not predicted as a high or low confidence gene. All four-candidate gene annotations were validated with RNAseq data from the non-inoculated susceptible cv Harrington and both cvs Steptoe and Harrington at 72 hpi with *B. sorokiniana* isolate ND85F. *HvWak2* was expressed pre- and post-inoculation, whereas *Sbs1*, *Sbs2* and *HvWak5* were only expressed at 72 hpi in the susceptible cvs Steptoe and Harrington, corroborating the qPCR transcript analysis described below.

Validation of *rcs5* Candidate Genes by Virus Induced Gene Silencing

The *Barley Stripe Mosaic Virus*-virus induced gene silencing (BSMV-VIGS) system (42) was utilized for post-transcriptional gene silencing of the four candidate WAK genes in the resistance cv Morex and the two susceptible cvs Steptoe and Harrington. Controls inoculated with only empty BSMV constructs, FES, or *B. sorokiniana* alone were used, along with the four-candidate gene specific BSMV silencing constructs. The silencing of the candidate genes in the resistant cv Morex did not alter disease phenotypes. The seedlings remained resistant across all the treatments with average infection types not significantly different than the BSMV empty virus and non-virus FES controls, with a mean disease severity of 3 on the 1-9 scale (38) (Fig. 2.2A and D). The susceptible cvs Steptoe and Harrington both remained susceptible when infected with the empty vector control, pSL38.1 and the BSMV:*HvWak2* and BSMV:*HvWak5*

silencing constructs, showing average disease scores of 6.6, 7.0 ,6.0 and 6.4, 6.1, 6.2, respectively. The disease scores were not significantly different between the *HvWak2* and *HvWak5* silencing construct and the empty virus control treatments on the susceptible cvs Steptoe and Harrington (Fig. 2.2B-D).

The BSMV:*Sbs1* and BSMV:*Sbs2* treated cvs Steptoe and Harrington seedlings had significantly lower spot blotch disease scores than the BSMV empty control, and the BSMV:*HvWak2* and BSMV:*HvWak5* experimental constructs. The BSMV:*Sbs1* treatment had mean disease scores of 5.3 for cv Steptoe and 4.75 for cv Harrington, and BSMV:*Sbs2* had mean disease scores of 4.8 for cv Steptoe and 4.4 for cv Harrington for 20 replicates (Fig. 2.2D). The shift from compatibility (susceptibility) towards incompatibility (resistance) in the susceptible cvs for both BSMV:*Sbs1* and BSMV:*Sbs2* silenced plants resulted in infection types as low as 2.75. This demonstrated that silencing either of the two closely linked *Sbs1* or *Sbs2* dominant susceptibility genes resulted in a significant increase of resistance in both of the susceptible cvs (Fig. 2.2B-D).

Quantitative PCR (qPCR) analysis was conducted to assess the specific silencing of the targeted genes based on their transcripts levels at the time points when the highest levels of gene expression were observed during *B. sorokiniana* infection. Three biological replicates of each BSMV:*Sbs1*, BSMV:*Sbs2* and BSMV:*HvWak5* treatment and the empty BSMV control were used to validate specific silencing of the targeted candidate genes. The BSMV:*Sbs1* treated seedlings had more than 85% lower *Sbs1* transcripts than were observed in comparison with the BSMV control treatments (Supp. File. 1 (Supp Fig 4A)). Similarly, the BSMV:*Sbs2* treated seedlings had more than 71% lower *Sbs2* transcript levels than were observed in comparison with the BSMV control (Supp. File. 1 (Supp Fig 4B)). The BSMV:*HvWak5* treatment resulted in

~ 72% lower transcript levels of *HvWak5* in comparison with the BSMV control (Supp. File.1 (Supp Fig. 4C)).

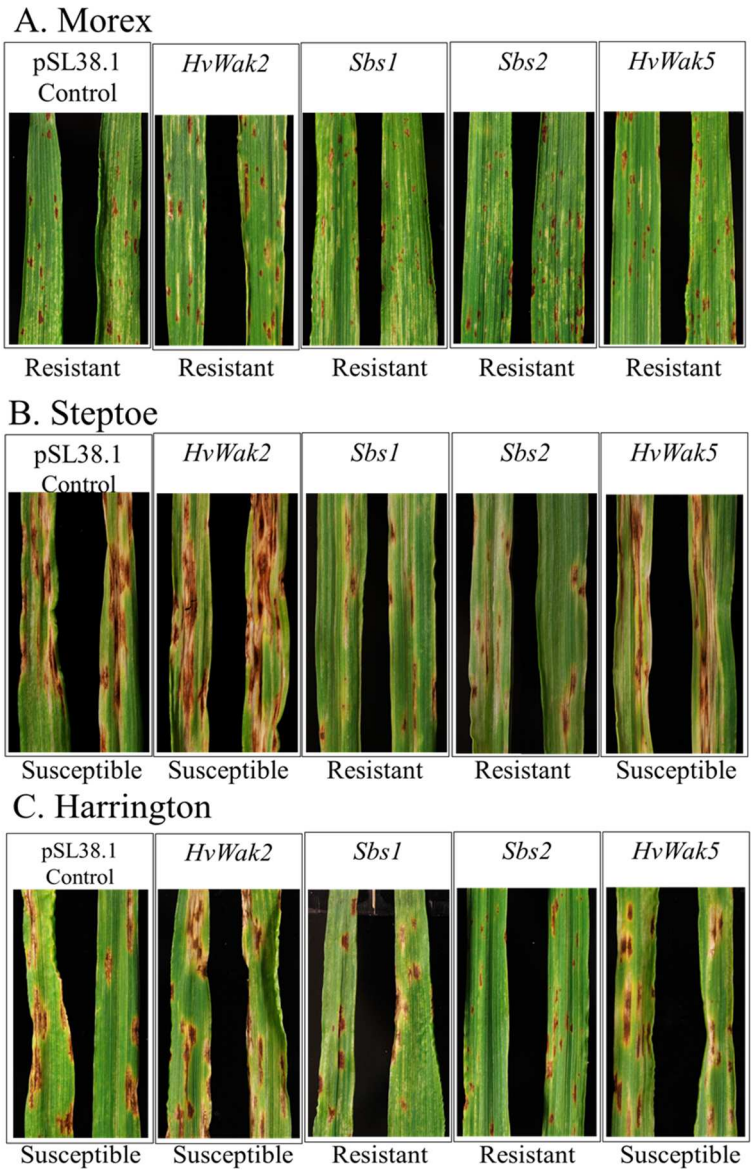

Figure 2.2. Utilization of BSMV-VIGS for the validation of the *HvWak2, Sbs1, Sbs2 and HvWak5* as *rcs5*. For the functional validation of *HvWak2, Sbs1, Sbs2* and *HvWak5* as a dominant susceptibility gene for spot blotch disease, resistant barley cultivar (cv) Morex **A)**, and susceptible barley cvs Steptoe **B)** and Harrington **C)** analyzed after BSMV-VIGS-mediated post transcriptional gene silencing of the *HvWak2, Sbs1, Sbs2* and *HvWak5* genes, and the empty BSMV-VIGS control (pSL38.1). Pictures show typical reactions for each construct with general reactions labeled below. **D)** Graphs show disease phenotyping data using a 0-9 disease rating scale (y-axis). The x-axis shows the cvs Steptoe (blue), Harrington (green) and Morex (red). For each genotype n=20 plants. The average disease rating values were calculated with standard error of mean ±1.

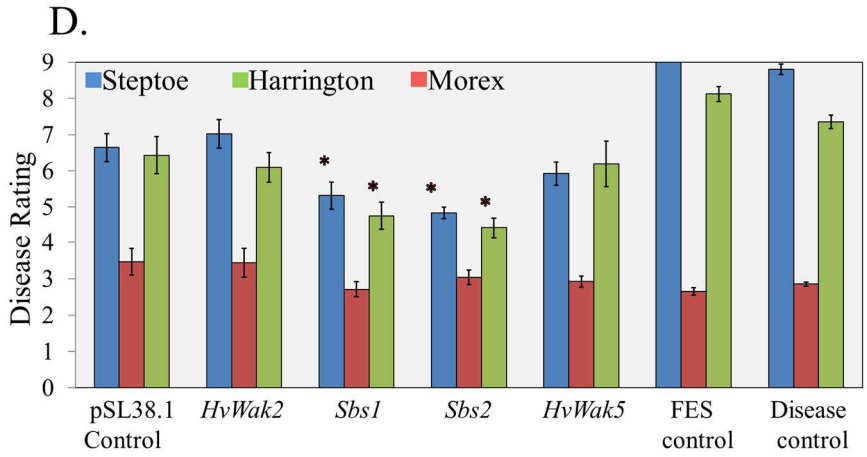

Figure 2.2. Utilization of BSMV-VIGS for the validation of the *HvWak2, Sbs1, Sbs2 and HvWak5* as *rcs5* (continued). For the functional validation of *HvWak2, Sbs1, Sbs2* and *HvWak5* as a dominant susceptibility gene for spot blotch disease, resistant barley cultivar (cv) Morex **A)**, and susceptible barley cvs Steptoe **B)** and Harrington **C)** analyzed after BSMV-VIGS-mediated post transcriptional gene silencing of the *HvWak2, Sbs1, Sbs2* and *HvWak5* genes, and the empty BSMV-VIGS control (pSL38.1). Pictures show typical reactions for each construct with general reactions labeled below. **D)** Graphs show disease phenotyping data using a 0-9 disease rating scale (y-axis). The x-axis shows the cvs Steptoe (blue), Harrington (green) and Morex (red). For each genotype n=20 plants. The average disease rating values were calculated with standard error of mean ±1.

Allele Analysis of *Sbs1* and *Sbs2*

For the *Sbs1* and *Sbs2* allele analysis, PCR primers were designed that produce a 4,242 bp amplicon containing the full length predicted *Sbs1* gene and 1,380 bp of the promoter region (Supp. File. 2) and a 4,711 bp (based on the cv Morex allele) *Sbs2* amplicon that contained the full length predicted gene and 2,009 bp of the promoter region (Supp. File.5). The amplicons were sequenced from two susceptible and eight resistant cvs on an Ion Torrent PGM instrument to ~ 4,000 X coverage of each genotype specific *Sbs1* and *Sbs2* amplicon. Sequence comparisons showed allelic variation of both the *Sbs1* and *Sbs2* genes within the predicted coding and promoter regions that correlated with *rcs5*-mediated resistance or more accurately, *Rcs5*-mediated dominant susceptibility.

Based on the *Sbs1* allele comparative analysis, the resistant cvs were classified in resistant group-1 (RG1) including the cvs Morex, NDB112, Robust, Tradition and Pinnacle and resistant group-2 (RG2) including the cvs Bowman, ND Genesis and TR306 (Supp. File 4 and 7). The two susceptible genotypes were placed into the susceptible group (SG), which included the cvs Steptoe and Harrington. Within the *Sbs1* coding region RG2 shared higher amino acid (aa) sequence identity with the SG (99.4%) than with RG1 (74%) (Supp. File. 4). Most of the divergence between RG1 and RG2 was contributed by deletions present in RG1 that eliminated the EGF-Ca domain (Supp. File. 7) and truncated the PK domain (Supp. File. 1 (Supp. Fig. 2A)). Sequence polymorphisms also included other synonymous and non-synonymous base substitutions (Supp. File. 2-4). The SG and RG2 *Sbs1* alleles encode the full length 683 aa proteins, whereas the RG1 alleles encode the much smaller 289 aa predicted nonfunctional protein (Supp. File. 4). The Protein Variation Effect Analyzer (PROVEAN) software predicted that the aa deletions from 150-289 and truncated PK in the RG1 allele are deleterious mutation that would result in non-functional proteins; (PROVEAN scores of -420.8 with significant PROVEAN score cutoff was -2.5) (43). Despite the deletions that result in a predicted non-functional protein in RG1 *Sbs1* alleles, it appeared that the presence of these deletions were not solely determinant of a nonfunctional susceptibility gene because they were not present in the RG2 alleles.

There were multiple SNPs and small INDELS identified in the 1,380 bp of the 5' untranslated region (UTR) and promoter regions sequenced from the *Sbs1* alleles showing a high level of diversity (Supp. File. 2). This suggested that the differences between RG2 and SG *Sbs1* gene expression could also determine if alleles function in dominant susceptibility/ recessive resistance. However, the comparative analysis across the predicted promoter regions sequenced

only identified a single polymorphic base substitution (G50A based on the nucleotide sequence provided) that perfectly correlated with the resistance –vs- susceptible alleles (Supp. File. 2).

The *Sbs2* allele analysis of the ten barley genotypes revealed the same phylogenetic grouping (RG1, RG2 and SG) as that of *Sbs1* (Supp. File. 4 and 7). Contrary to *Sbs1*, comparison of the *Sbs2* alleles showed that at the primary aa level RG1 and RG2 alleles were more similar to one another (99%), with RG1 and RG2 alleles having greater divergence compared to SG, 97.7% and 98.4% aa identity, respectively (Supp. File. 7). Interestingly, the RG2 *Sbs2* allele appeared to be a recombinant allele with the promoter region and 5' CDS region translating to the first 64 amino acids having high similarity to RG1 and amino acids 167 to 701 having high similarity with the SG (Supp. File. 7).

The predicted protein alignments of *Sbs2* alleles identified 18 aa substitutions among the ten barley genotypes analyzed (Supp. File. 7) with nine (A16F, I20A, V27T S32T, S35G, M38R R46K, K60N Q64R D227E) that could putatively contribute to resistance as they were common between RG1 and RG2 and different as compared to the SG allele (Supp. File. 7). Additionally, RG1 and RG2 compared one to another had aa substitutions T127K, Y167F, E369Q, I444T, C697R and P701S (Supp. File. 7). There was also a unique D536N aa substitution in the kinase domain of the RG2 as compared to RG1 and SG, which was predicted to be deleterious for the function of the *Sbs2* protein according to PROVEAN with a score of -4.6 (cutoff of -2.5) (Supp. File. 7).

Multiple SNPs and small indels were present in the 2009 bp sequence upstream of the *Sbs2* coding region, representing the *Sbs2* 5'UTR and promoter region. The predicted promoter region of the RG2 alleles had a C1483G, G1504A and insertion of C at 1535 compared to RG1 and SG. The SG had A1510G, T1525C, a deletion from 1527-1539 and CC1541TT compared

with both RG1 and RG2 (Supp. File. 5). Thus, we speculated that differential transcriptional regulation due to promoter region polymorphism/s in the RG1 and RG2 alleles compared with the SG could contribute to the inability of the pathogen to induce RG1 *Sbs2* and RG2 *Sbs1* and *Sbs2*, a hypothesis that was tested via expression analysis.

Expression Analysis of *HvWak2*, *Sbs1*, *Sbs2*, *HvWak5*, and *HvMapk3*

The polymorphisms in the promoter regions of RG1 and RG2 vs SG *Sbs1* and *Sbs2* alleles could result in differential expression across the infection process, suggesting that the ability of the pathogen to induce expression of the WAKs could also be a determinant of resistance vs susceptibility. The qPCR analyses (Supp. File 9) determined that *HvWak2* was constitutively expressed in both the susceptible cv Steptoe and the resistant cv Morex across the infection time course analyzed. However, in the susceptible cv Steptoe, *Sbs1* was induced five-fold at 36 hpi and remained more than two-fold upregulated at the later time-points, while in the resistant cv Morex *Sbs1* showed very low to no expression and was not induced post inoculation (Fig. 2.3A). Similarly, *Sbs2* was specifically upregulated six and seven-fold in susceptible cv Steptoe at 12 and 72 hpi, respectively, and had very low to no expression in resistant cv Morex. Thus, the susceptible alleles of *Sbs1* and *Sbs2* were induced by the pathogen and the resistant alleles were not (Fig. 2.3B). The *HvWak5* gene was specifically upregulated ~190-fold at 24 hpi in the susceptible cv Steptoe and the expression level steadily increased across the later time-points to over 1000-fold at 72 hpi (Supp. File. 8 (Supp. Fig. 7A)). However, since *HvWak5* expression was nearly undetectable before inoculation the induced expression levels as determined by the Cq values were relatively similar to that of *Sbs1* and *Sbs2*.

WAK receptors are known to initiate Mitogen-activated protein kinases (MAPK) signalling pathways, activating host defence responses (44), so *HvMapk3* transcript expression

was analysed by qPCR through the 0 to 72 hpi time course and it was found that the susceptible cv Steptoe showed approximately two-fold upregulation at 36 hpi and the transcripts remained upregulated at the later time-points during the infection process (Supp. File. 8 (Supp. Fig. 7B)). However, *HvMapk3* expression was not induced in the resistant cv Morex at any time.

To validate the expression hypothesis, we analyzed *Sbs1* and *Sbs2* expression levels via qPCR in the inoculated and non-inoculated RG2 cv Bowman at 0, 12, 24, 36, 48 and 72 hpi and performed RNAseq at 72 hpi. The qPCR analysis showed very low to zero expression of both candidate *rcs5* genes at time point zero and no differential upregulation of either transcript in the non-inoculated versus inoculated resistant RG2 cv Bowman during the infection process (Fig. 2.3A and B).

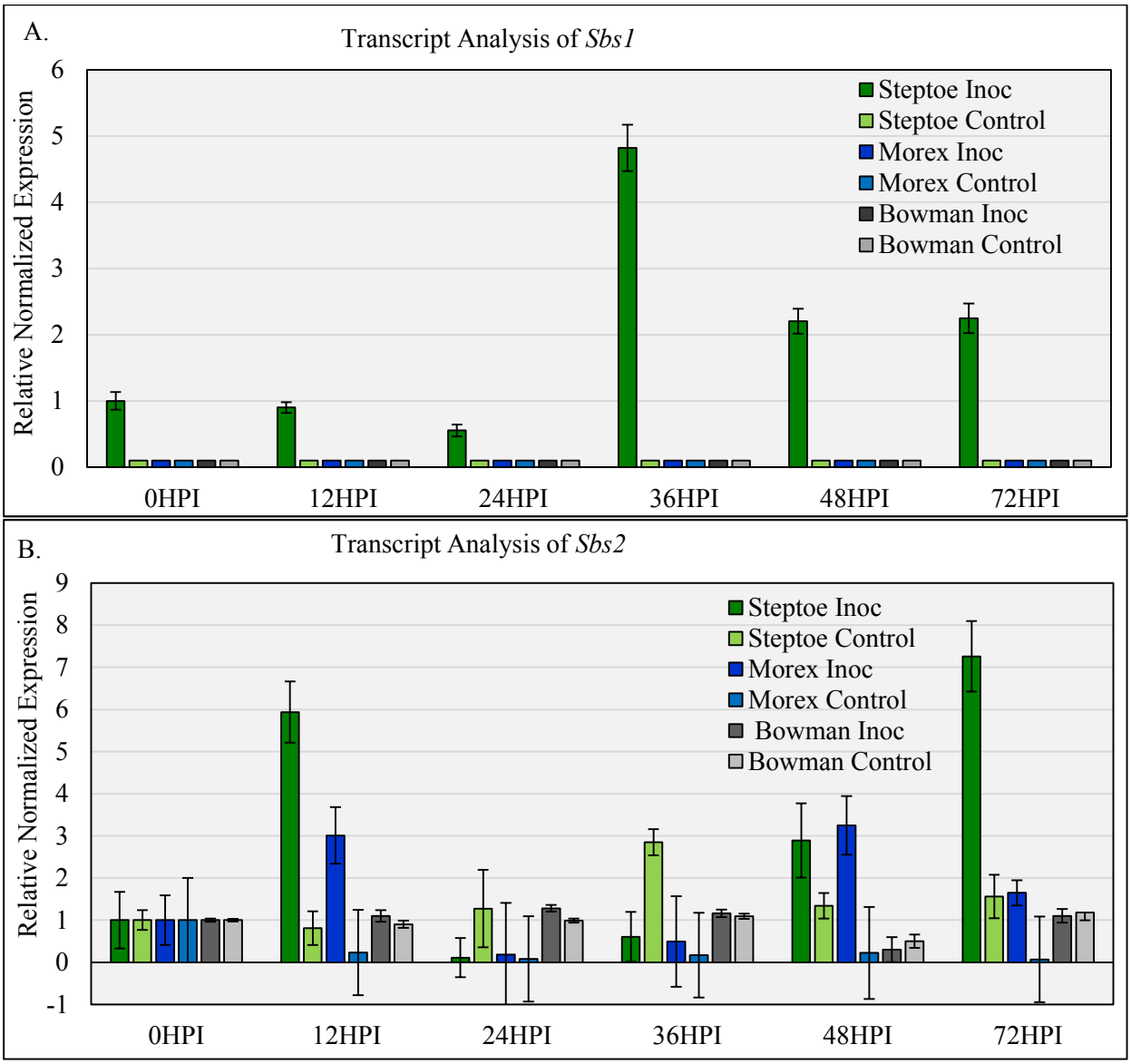

Figure 2.3. Time course qRT-PCR expression analysis of the **3A)** *Sbs1* and **3B)** *Sbs2* genes during the infection process with *Bipolaris sorokiniana* isolate ND85F in the barley cultivars (cvs) Steptoe, Morex, and Bowman. Pathogen inoculated susceptible cv Steptoe and resistant cvs Morex and Bowman and tween20 controls were analyzed for *Sbs1* and *Sbs2* expression. *HvSnoR14* expression was used to normalize the transcript data at each time point (X-axis). Error bars depict SEM±1(n=3). The time point 0 HPI was used as control sample for relative expression analysis (Y-axis).

Transcriptional Responses of *Sbs1* and *Sbs2* Post Intercellular Wash Fluid Infiltration

Based on the post-inoculation transcript data generated for *Sbs1* and *Sbs2*, it was hypothesized that, *B. sorokiniana* triggers the upregulation of the susceptibility genes possibly by

a fungal elicitor that is secreted into the apoplast of the host. The intercellular wash fluids (IWFs) collected at 12, 36 and 72 hpi, from cv Steptoe inoculated with the virulent *B. sorokiniana* isolate ND85F induced *Sbs1* ~20 fold at 72 hours post- infiltration (Supp. File. 8 (Supp. Fig. 8A)). A similar result was also observed for a second independent replication of the experiment, showing *Sbs1* induction, but in the second replication *Sbs1* upregulation was also observed at 12 and 36 hours post-infiltration as well as at 72 hours post infiltration with the IWFs (Supp. File. 8 (Supp. Fig. 8B)). In both replications of the infiltration experiments, the *B. sorokiniana* avirulent isolate BS035 IWF did not induce expression of either *Sbs1* or *Sbs2* (Supp. File. 8 (Supp. Fig. 8A and B)).

To test if the effector that putatively induces *Sbs1* in the IWFs collected from susceptible plants inoculated with the *rcs5* virulent isolate is a protein, the IWFs were treated with pronase prior to infiltration along with a non-pronase treated control. The experiment resulted in no change in upregulation of the *Sbs1* gene, providing evidence of a non-proteinaceous elicitor of the *Sbs1* susceptibility gene (Supp. File. 8 (Supp. Fig. 8C)).

DAB (3,3′-Diaminobenzidine) Staining

Plants produce reactive oxygen species (ROS), including H_2O_2, which precludes PCD/ HR to defend themselves against biotrophic pathogens, however, this defense strategy is exploited by the necrotrophs that purposefully induce the host's immunity mechanisms to tailor an environment that is conducive to their lifestyle of colonizing dead tissues (45). In the barley-*B. sorokiniana* Pathotype 1 (avirulent on *rcs5*) interaction, we observed leaves at 0, 6, 12, 18, 24, 30, 36 and 48 hpi on the resistant barley cv Morex (*rcs5*+) and the susceptible cv Steptoe (*Rcs5*-). Early and pronounced DAB staining associated with all the *B. sorokiniana* penetration sites as early as 18 hpi were apparent in the inoculated susceptible cv Steptoe. The DAB staining was not

observed in the resistant cv Morex at the early time-points showing that the early ROS detection correlated with the timing of *Sbs2* upregulation during infection of the susceptible cv Steptoe (Supp. File. 8 (Supp. Fig. 9)). During the later time-points (24-48 hpi) the DAB staining associated with penetration and colonization in the susceptible cv Steptoe, rapidly increased in the neighboring cells including the underlying mesophyll cells. However, in resistant cv Morex, the DAB staining was not observed until 24 hpi but appeared to have a higher intensity and remained limited to just a few cells adjacent to the penetration site with little expansion at the later time-points (Supp. File. 8 (Supp. Fig. 9)).

Transcriptome Analysis Post *Bipolaris sorokiniana* Infection

RNAseq analysis at 72 hpi identified a total of 3,221 differentially expressed genes **(**DEGs) with greater than a threefold change (1,488 upregulated and 1,733 downregulated) in the susceptible cv Harrington in comparison with non-inoculated controls (Supp. File 10). For the resistant cv Bowman, which carries RG2 alleles of *Sbs1* and *Sbs2*, 1,532 DEGs (923 upregulated and 609 downregulated) were identified (Supp. File 11). Comparison of the upregulated gene list from cv Harrington and cv Bowman, showed that 634 genes were common, 845 Harrington-specific and 270 Bowman-specific DEGs. A comparison of the downregulated genes between the susceptible and resistant genotypes showed 376 common DEGs, with 1,357 cv Harrington-specific and 233 cv Bowman-specific DEGs (Supp. File. 8 (Supp. Fig. 10)).

The gene ontology (GO) enrichment analysis showed that *Sbs1* and *Sbs2* fall into the biotic stress related category and consistent with the qPCR data were upregulated specifically in the susceptible cv Harrington and not upregulated in cv Bowman (RG2) in response to *B. sorokiniana* infection (Supp. File. 8 (Supp. Fig. 10A)). The GO analysis showed significant upregulation of the redox category of genes in cv Harrington suggesting that the upregulation of

the genes responsible for the oxidative burst by the reactive oxygen species (ROS) an early PTI and ETI response (14) may be mediated through the WAK gene signaling pathways (Supp. File 12).

Interestingly, nine genes that were upregulated in the susceptible cv Harrington and downregulated in the resistant cv Bowman at 72 hpi (Supp. File. 10 and 11) fell into the nitrogen compound/ steroid/ lipid metabolic and amino acid catabolic process and cell growth and morphogenesis classes using the GO biological process classification (PANTHER) (46). Using protein-protein interactions from the STRING database analysing 500 of the DEGs in the susceptible cv Harrington interaction (the top 250 upregulated and downregulated genes) at 72 hpi compared with the non-inoculated control resulted in an interaction network with 893 edges and 361 nodes connecting the differentially regulated genes. Interestingly, all the *Arabidopsis* WAK homologs from the *rcs5* QTL had edges that connected to an *Arabidopsis* chloroplastic gene AKHSDH2 (AT4G19710.2) homologous to the barley HORVU5Hr1G053950.13 gene, effectively representing an interaction hub protein (Supp. File. 8 (Supp. Fig. 11A)) with aspartokinase/homoserine dehydrogenase activity that catalyzes the synthesis of essential amino acids.

The analysis using STRING data was unable to take into account 'non differentially regulated genes' that may be important for connecting the DEGs and making a more reliable interaction network. To mitigate this problem, we developed a Protein-Protein Interaction Network (PPIN) pipeline (submitted in https://github.com/Gazala-Ameen/PPIN). The PPIN analysis with the same 500 barley DEGs in the spot blotch susceptible cv Harrington (top 250 upregulated and downregulated genes) at 72 hpi compared with the non-inoculated control resulted in 361 unique Arabidopsis homolog IDs, which were used for network analysis along

with the Arabidopsis homologs of the barley WAK genes that underlie the *rcs5* QTL. Using our PPIN analysis codes with *AtWak3* as an interaction focal point on the same dataset, we generated a functional protein network of 31,125 possible interaction edges (Supp. File. 8 (Supp. Fig. 11B); Supp. File 13).

Discussion

High-resolution mapping delimited the *rcs5* spot blotch resistance QTL to an ~234 kb physical region of barley chromosome 7H. Four *rcs5* candidate WAK genes were identified within the region. Allele sequencing and VIGS confirmed two of the genes, *Sbs1* and *Sbs2*, as spot blotch dominant susceptibility genes in the susceptible cultivars. Allele analysis and transcript analysis across the infection process and apoplast wash fluid infiltration showed that susceptible alleles of *Sbs1* and *Sbs2* are induced by the hemibiotrophic pathogen then hijacked to promote PCD in an inverse gene-for-gene manner to colonize and complete its life cycle on the resulting dead tissues.

Alleles of host susceptibility target genes with polymorphisms that result in loss of interaction with pathogen virulence effectors or NEs in the case of necrotrophic specialists result in inverse gene-for-gene interactions genetically characterized as recessive resistance genes (22,47). Thus, the recessive allele conferring resistance must be present in the homozygous state to eliminate dominant susceptibility. Host populations pressured by pathogens containing these virulence effectors evolve to eliminate the dominant susceptibility targets through gene mutation that block manipulation by the pathogen. Some of these recessive resistances have been successfully deployed in the field including the rice *xa25* and *xa13* genes that are effective against bacterial blight, *eIF4G* effective against the rice tungro spherical virus, *mlo*-based

resistance against powdery mildew in barley, and *tsn1* and *snn1* in wheat that are effective against *P. nodorum* (21,37,48–51).

Interestingly, *xa13*-mediated resistance is determined by polymorphism in the OsSweet11 gene promoter region that block *Xanthomonas oryzae* transcriptional activator-like (TAL) effector PthXo1 binding. It was hypothesized that PthXo1 evolved to induce OsSWEET11 upregulation to facilitate nutrient acquisition, thus, is a dominant susceptibility target (52). This induced transcription is similar to the *rcs5* locus as the virulent isolate of *B. sorokiniana* appears to upregulate the dominant susceptibility genes *Sbs1* and *Sbs2*.

The polymorphisms resulting in a putative nonfunctional Sbs1 protein in the resistant cv Morex and differences in expression of *Sbs1* and *Sbs2* between the cv Morex RG1 allele and the cvs Steptoe and Harrington SG alleles suggested that the pathogen induces the expression of the WAK susceptibility targets then hijack the receptors to facilitate colonization and disease development. Thus, the *rcs5*-mediated recessive resistance is conferred by the *Sbs1* and *Sbs2* alleles that have diverged and are no longer functional susceptibility proteins or are driven by regulatory elements that the pathogen can't induce. The RG2 class of resistant genotypes have *Sbs1* alleles that closely resembled the SG alleles at the primary aa sequence representing natural allelic variation to test the expression hypothesis. The RG2 also contain recombinant-like *Sbs2* alleles that have a promoter region and N-terminal coding region similar to RG1 but a C-terminal coding region more closely related to SG, providing natural allelic variation that is very similar to a promoter swap assay that could be used to test the induction hypothesis. The allele analysis and observations that the RG2 *Sbs1* and *Sbs2* allele are not induced by the virulent isolate of *B. sorokiniana* supports the hypothesis that the pathogen evolved to induce the WAK genes to become virulent. Thus, *Sbs1* and *Sbs2* susceptible alleles have regulatory elements that the

pathogen can manipulate and alleles of either one of the *Sbs* genes that block induction or are non-functional results in impaired colonization and disease suppression.

We posit that the Sbs1 and Sbs2 proteins are hijacked to induce increased levels of PCD as was shown by the DAB staining across the infection cycle (Supp. File. 8 (Supp. Fig. 9)). Therefore, it was an attractive hypothesis that *B. sorokiniana* isolates virulent on *rcs5* secrete effectors in the apoplast that induce *Sbs1* and *Sbs2.* Intercellular wash fluids (IWFs) from virulent and avirulent isolates were used to infiltrate the susceptible cv Steptoe. Interestingly, the IWF from the *Rcs5* virulent *B. sorokiniana* isolate ND85F induced significant upregulation of *Sbs1* post infiltration at all the time points tested, suggesting that it upregulates the dominant susceptibility genes via an apoplastic secreted effector (Supp. File. 8 (Supp. Fig. 8A and B)). The avirulent isolate IWFs did not induce *Sbs1* or *Sbs2* suggesting that they do not contain the effector. To test if the effector/s that induced *Sbs1* was proteinaceous, the IWFs were treated with pronase prior to infiltration, which still resulted in upregulation of the *Sbs1* gene, providing preliminary evidence of a non-proteinaceous *B. sorokiniana* elicitor (Supp. File. 8 (Supp. Fig. 8C)). A previously reported strain specific secondary metabolite (synthesized by nonribosomal peptide synthetases) was shown to be a virulence factor in the *B. sorokiniana* pathotype 2 isolate ND90-Pr, which is in line with our observation that at least one of the pathotype 1 *rcs5* specific virulence effectors may be non-proteinaceous (53,54).

The *Sbs2* gene was not induced by the IWFs, suggesting that a second effector was not captured or a different concentration of the same effector is required for *Sbs2* induction. The diverse *Sbs1* and *Sbs2* promoter regions, differential timing of upregulation, and differential IWF induction indicates distinct effectors or mechanisms are eliciting the expression of the two *rcs5* susceptibility genes. Also, the necrosis or cell death phenotype was not observed after infiltration

with the IWFs, suggesting that the apoplastic localized elicitor that upregulates *Sbs1* does not induce PCD. The PCD response appears to be pathogen dependent suggesting a second elicitor or effector may induce ROS and subsequent PCD responses such as the continuous production of OG DAMPs by pathogen cell wall degrading enzymes (Fig. 2.4). This could be an essential event for triggering the PCD through the upregulated WAK genes considering that it been shown in other pathosystems that WAK RLKs act as biotrophic resistance genes-eliciting PCD responses after OG perception (29).

A quantitative mass-spectrometric-based phosphoproteomic analysis identified rapidly induced cellular events in Arabidopsis using OG and Flg22 induction *in planta* identifying seven overlapping induced phosphorylation sites indicating similarity between these two signalling pathways activated by two very distinct DAMP and PAMP recognition RLKs (55). FLS2 recognition of the bacterial flagellin epitope flg22, leads to ROS production and activation of defense related proteins through MAPK signalling (56). We report specific upregulation of *HvMAPK3* in the susceptible cultivars during the infection process in the barley-*B. sorokiniana* pathosystem suggesting that both LRR-PK and WAK RLKs have conserved downstream MAPK defense signalling pathway. Interestingly the RLK CERK1 identified as an interactor with the WAKs using PPIN analysis suggests a role in this conserved signalling pathway, as it is a co receptor that acts in the identification of diverse effectors/PAMPs and subsequent conserved signalling pathways that result in PCD responses.

The upregulation of *Sbs1* and *Sbs2* may amplify the initiation of MAPK signalling, inducing ROS production, activation of defense related proteins and ultimately PCD, similar to defense responses against biotrophic pathogens. Overexpression of *Arabidopsis AtWak1* causes increased OG responses such as ROS production and callose deposition, effectively subduing the

growth of biotrophic pathogens (57), but due to the lifecycle of necrotrophs this response facilitates disease development. Overexpression of OsWAK25 in rice resulted in increased susceptibility to the necrotrophic fungal pathogens *Bipolaris oryzae* (*Cochliobolus miyabeanus)* and *Rhizoctonia solani* (58). Interestingly over expression of OsWAK25 in rice also exhibited necrotic spots on leaves. These results are in line with *Sbs1* and *Sbs2* expression data suggesting an increased susceptibility for *B. sorokiniana* upon induction of the WAK genes by the virulent isolate.

Perturbation of cell wall structure is monitored by several receptor proteins such as WAKs, Feronia, and RLP44 (59) that initiate specific responses including the accumulation of ROS. Here we report that the barley *Sbs1* and *Sbs2* genes were upregulated at 36 and 12 hpi, respectively, by a virulent isolate of *B. sorokiniana*, which facilitates further disease development in the pathogen's necrotrophic phase. ROS production is considered as a signal cue for activating cell death responses providing resistance against biotrophic pathogens but increasing the virulence of a necrotroph (60). DAB staining of the susceptible barley cv Steptoe that contains functional *Sbs1* and *Sbs2* alleles and the resistant cv Morex showed a different timeline of H_2O_2 production. Early H_2O_2 production at 18 HPI was identified in Steptoe corresponding with the early upregulation of the *Sbs2* gene, which we interpret as facilitating the establishment of the pathogen and the later upregulation of *Sbs1* and *Sbs2* correlates with the later expanded ROS production which facilitates further colonization and disease development in the susceptible genotypes. The ROS production identified by DAB in resistant cv Morex was delayed (24 hpi) and localized, representing a limited growth opportunity for the necrotrophic pathogen.

The GO enrichment analysis showed significant upregulation of the redox category of genes in the susceptible cv Harrington suggesting that it is in part the result of the WAK receptor-mediated signaling resulting in PCD considering that the wall localized peroxidases significantly upregulated are a major source of ROS during plant-pathogen interactions (61). In Arabidopsis, it has been shown that the OG hypersensitive mutants tend to have overexpression of peroxidases, which facilitates the constitutive production of ROS and WAKs are major OG receptors. Several studies have also shown that the peroxidase mutants have impaired ROS production and activation of defense responses post PAMP/DAMP treatment and overexpression of the peroxidases triggers the production of ROS (61,62). In the comparative transcriptome analysis, there was significant overexpression of peroxidases in the susceptible transcriptome; for example, the HORVU2Hr1G018510 peroxidase superfamily protein was upregulated 8262 folds in the susceptible cv Harrington and only 14-fold upregulated in the resistant cv Bowman (Supp. File 12). Thus, in the transcriptome of the spot blotch susceptible cultivar overexpression of the peroxidases were accompanied by higher ROS production. We hypothesize that the pathogen induces *Sbs1* and *Sbs2* enriches the cell periphery with more WAK receptors that recognize the degradation of the cell wall, possibly by detecting OGs, which triggers signalling pathways that induce the overexpression of peroxidases and ROS and ultimately PCD (63) that *B. sorokiniana* utilizes to facilitate further disease development (Fig 2.4).

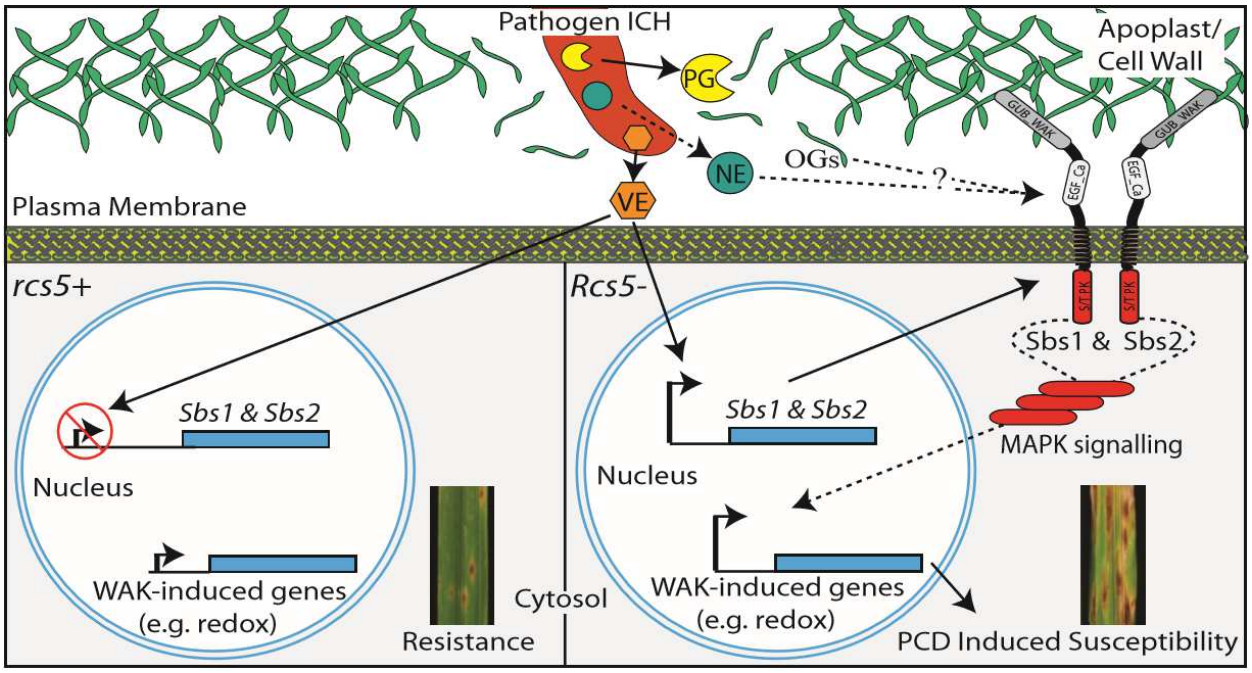

Figure 2.4. Proposed model of the spot blotch susceptibility due to the *Sbs1* and *Sbs2* wall-associated kinases (WAKs) as supported by the genetic, interaction, and signaling data presented for barley–*Bipolaris sorokiniana* pathosystem. The intracellular hyphae (Pathogen ICH) of *B. sorokiniana* enter the host, ~12 hours post inoculation (hpi) and secretes unknown virulence effector/s (VE) and cell-wall degrading enzymes, including Polygalacturonases (PG) into the apoplast. The bottom right box shows the induction of the WAK receptors (susceptibility genes) *Sbs1* and *Sbs2* that are involved in the identification of oligo-galacturonide (OG) damage associated molecular patterns (DAMP) elicitors released during the infection process or by an unknown necrotrophic effector (NE) that intern induce defense responses through MAPK signaling. The defense responses induce overexpression of redox related genes, which induce reactive oxygen species (ROS), programmed cell death (PCD), and favors the necrotrophic pathogen, which hijacks the host defense machinery to induce susceptibility. The bottom left box shows the presence of *sbs1* and *sbs2* alleles that do not function as susceptibility targets and resist pathogen induction results in spot blotch disease resistance mediated by the *rcs5* locus.

Comparative RNAseq analysis between cvs Bowman and Harrington infected with *B. sorokiniana* identified DEG's during the resistance and susceptibility responses. Nine genes were found to be upregulated in susceptible cv Harrington and downregulated in resistant cv Bowman, and of these nine genes *ASK3* and *DIR1* have been shown to be important in plant stress signalling. ASK3 is a cell membrane cytokine receptor (64), that functions as a histidine kinase relaying the stress signal to the downstream MAPK cascade (65). The DIR1 protein is part of a feedback regulatory loop consisting of G3P, DIR1 and AZI1 (66,67) that regulates systemic

acquired resistance (SAR) and is critical for glycerolipid biosynthesis (68). Thus, we speculate that the upregulation of these genes controlling plant immune signalling and amino acid catabolism are also playing a role in defense signalling that leads to PCD. Further, STRING protein interaction analysis between DEGs identified the possible hub protein ASKDSK2 that interacts with the *Arabidopsis Sbs1* and *Sbs2* WAK homologs. ASKDSK2 which encodes a bifunctional aspartokinase/homoserine dehydrogenase, catalyzes the synthesis of the essential amino acids threonine, isoleucine and methionine. DMR1, a homolog of HSK, which functions in the same pathway as ASKDSK2, is a downy mildew and *Fusarium* recessive resistance protein (69,70) indicating that this pathway plays an important role in disease resistance signaling. These data also corresponded with the cv Harrington upregulated genes being involved in aa catabolic processes via GO annotation and the fact that they interact with the WAK receptors suggest they may play an important role during the interaction that results in dominant susceptibility.

Interestingly, a KAPP (Kinase Associated Protein Phosphatase- AT5G19280) was also identified as an interaction hub having a direct predicted interaction with three of the upregulated genes, which are predicted to encode a putative S-locus protein kinase (AT1G61420), the chitin receptor kinase CERK1 (AT3G21630) and SERK1 (AT1G71830) which are involved in defense signalling events that result in ROS production and PCD. A downregulated protein kinase like protein (AT1G61590), the homolog of the Arabidopsis RIPK was also found to directly interact with KAAP. Further, a dense string of interactions were identified at the SERK1 node and shown as a group (Supp. File. 8 (Supp. Fig. 11B)). Interestingly, KAPP encodes for a protein phosphatase 2C 70 protein shown to be present in the cell membrane and is involved in the dephosphorylation of the *At*SERK1 receptor kinase (71). Thus, the PPIN helped to identify genes

that may be important in the resistance/susceptibility signalling pathway which are not differentially regulated and yet may represent important interaction hubs for future *rcs5* signalling pathway analyses.

We report that the *Rcs5* dominant susceptibility is conferred by alleles of two wall associated kinase genes, *Sbs1* and *Sbs2*, which are being induced by the necrotrophic pathogen to hijack their function, putatively inducing programmed cell death to facilitate disease development. The presence of the barley WAK *sbs1* and *sbs2* alleles that cannot be manipulated and induced by *Rcs5* virulent isolates of *B. sorokiniana* during the infection process result in the durable *rcs5*-mediated recessive resistance. This pathosystem also represents a novel mechanisms of dominant susceptibility/recessive resistance mediated by the coordinated pathogen induced regulation and function of the two WAK genes. Preliminary characterization of the putative pathogen effector/s lead to the conclusion that it may represent a non-proteinaceous effector, possibly a secondary metabolite that induce *Sbs1* expression and provides a pathogenicity advantage to *B. sorokiniana* isolates that carry it.

Materials and Methods

Barley Germplasm

The F_2 Progeny of Steptoe/Morex were used for genetic mapping of *Rcs5*. The spot blotch susceptible and resistant cvs used in this study are Steptoe, Harrington, Morex, NDB112, Robust, Tradition, Pinnacle, Bowman, ND Genesis, and TR306.

Spot-Blotch Inoculation and Phenotyping

The *B. sorokiniana* isolates used in the experiments were ND85F (pathotype 1, virulent on NDB112 and Bowman differential) and BS035 (pathotype 0, avirulent). The ND85F isolate has been used to screen barley genotypes for spot blotch resistance for over 20 years (10). The

BS035 isolate was isolated from *Hordeum jubatum* and determined to be pathotype 0 by screening on the barley differentials and other cultivars (2). Both isolates were grown on V8-PDA at 21°C under a 12-hour photoperiod. The conidial suspension of ~2,000 conidia/ml of distilled water with a 10µl/ 100ml of Tween-20 (Polysorbate 20) to facilitate distribution and adherence of conidia was prepared. Mock inoculations were carried out by same concentration of the Tween-20 in distilled water. Inoculated barley plants were kept in humidity chambers with 100% humidity for 24-hours and later kept in the growth chambers at 21°C with 16/8 h light/dark photoperiod until rating.

High Resolution Genetic Mapping

High-resolution genetic mapping was conducted utilizing the 1,536 Steptoe/Morex F_2 progeny (3,072 recombinant gametes), using the flanking markers BF627428 and cMWG773. This reduced the recombinants to 66, which were later screened with BF263248- BF627428 markers reducing the number to 25 recombinants. Finally, the SNP HvWak1- ctg 7 CAPS marker reduced the number of recombinants to 7 (Supp. File 9).

Transcriptional Expression

The cvs. Steptoe and Morex were inoculated with *B. sorokiniana* isolate ND85F along with seedlings inoculated with Tween-20 minus fungal spores as controls. Tissue was collected from three biological replicates of the infected seedlings and controls at 0 and 12, 24, 36, 48 and 72 hpi. The primers used were HvuSnoR14 -F1 and HvuSnoR14 -R1; WAK2Q-F1 and WAK2Q-R1; WAK3Q-F1 and WAK3Q-R1; WAK4Q-F1 and WAK4Q-R1 and W5-QF1 and W5-QR1 for *HvSnoR14, HvWak2*, *Sbs1*, *Sbs2*, and *HvWak5*, respectively (Supp. File 9). A 20 µl qPCR reaction was prepared using 0.8 µl of 100 nM of each gene specific forward and reverse primer, 4 µl of diluted cDNA template, 10 µl SsoAdvanced SYBR green supermix (BIO-RAD),

and 4.4 µl qPCR grade ultrapure water (Ambion, MA) in a hard-shell 96 well plate (BioRad, CA) and sealed with Microseal 'B' PCR plate seal (BioRad, CA). qPCR reactions were denatured for 30 sec at 95°C, followed by 45 cycles of denaturation at 95°C for 15 sec and annealing at primer at 58°C for 60 sec. Then a melt-curve was generated at temperatures from 65°C to 95°C with 0.5°C increment (2-5 sec per step). All representative cDNA fragments for each candidate gene and the control reference gene *HvSnoR14* were sequenced to ensure for targeted amplicon.

Virus Induced Gene Silencing

The post-transcriptional gene silencing was carried out utilizing *Barley Stripe Mosaic Virus*-Virus Induced Gene Silencing (*BSMV*-VIGS) following the methodology as described by (4). To design gene specific *BSMV*-VIGS constructs for each *rcs5* candidate gene, with minimal off target silencing, 150-200 bp fragments were identified from the predicted mRNA transcript of each gene that contained the highest unique nucleotide sequence (< 85% identity with other genes in the barley genome and avoiding regions that contain continuous stretches of 20 bp of similarity with the predicted cDNA of the wall-associated-kinases *HvWak2*, *Sbs1*, *Sbs2* and *HvWak5*. In the end, 181, 157, 156, and 165 bp specific sequences were identified for *HvWak2*, *Sbs1*, *Sbs2* and *HvWak5,* respectively. These amplicons were generated by PCR, using primers GA-WAK2KD-FP, GA-WAK2KD-RP and GA-WAK2KD-REV-FP, GA-WAK2KD-REV-RP for *HvWak2* GA-WAK3KD-FP, GA-WAK3KD-RP and GA-WAK3KD-REV-FP, GA-WAK3KD-REV-RP for *Sbs1* GA-WAK4KD2-FP,GA-WAK4KD2-RP and GA-WAK4KD2-REV-FP, GA-WAK4KD2-REV-RP for *Sbs2* GA-WAK5KD-FP, GA-WAK5KD-RP1 and GA-WAK5KD-REV-FP, GA-WAK5KD-REV-RP1 for *HvWak5* with Not1 and Pac1 sites in sense and anti-sense directions, from the cultivar Morex and Steptoe cDNA (Supp. File 9). The amplicons were then sequenced to confirm similarity in Morex and Steptoe. Once confirmed,

these cDNA fragments were cloned into the *BSMV* gamma genome based vector (pSL38.1) using NotI and PacI in both sense and anti-sense directions. RNA was synthesized using the mMessage mMachine T7 transcription kit (Ambion, MA), according to the manufacturer's guidelines for the alpha, beta and gamma genome of *BSMV* and gamma genome construct of each candidate gene. RNA of *BSMV* sense and antisense fragments were rub-inoculated onto 10-day-old seedlings of Morex, Steptoe and Harrington (20 replicates for each) with a carrier, FES (0.1M Glycine, 0.06M K_2HPO_4, 1% Bentonite w/v, 1% Celite w/v). *BSMV* only, FES only and *B. sorokiniana* only inoculations were also included as controls. After inoculation plants were kept in humidity chambers with 100% humidity for 24 h and later transferred to the growth chambers with 21°C temperature with 16/8 h light/dark photoperiod. After 14 days, when *BSMV* symptoms were systemic in the entire plant, *B. sorokiniana* isolate ND85F was inoculated as described above. After 6 and 10 dpi, the plants were evaluated as a double blind test for disease reaction on the 0-9 scale as described above. The disease severity rating were analysed and an LSD test applied at $\alpha = 0.05$ using SAS 9.4 (SAS Institute, Cary NC). The mean disease severity for the 20 replicates were calculated for each cultivar for all of the treatments and a t-test and one-way ANOVA was used to compare the group means at $\alpha = 0.05$. Tissue samples were collected from three biological replicates of each *BSMV*: Sbs1, *BSMV*: Sbs2 and *BSMV*: HvWak5 and the control empty *BSMV* treatments at 12, 36 and 72 hpi with *B. sorokiniana* for RNA extraction and RT-PCR was conducted using primers WAK2Q-F1and WAK2Q-R1; WAK3Q-F1 and WAK3Q-R1; WAK4Q-F1and WAK4Q-R1; W5-QF1 and W5-QR1 for *HvWak2*, *Sbs1*, *Sbs2* and *HvWak5,* respectively (Supp. File 9). For quantification of the transcripts post inoculation BSMV-VIGS, A 20 µl qPCR reaction was prepared using 0.8 µl of 100 nM of each gene specific forward and reverse primer, 4 µl of diluted cDNA template, 10 µl Sso Advanced supermix, and 4.4 µl qPCR

grade ultrapure water (Ambion®) in a hard-shell 96 well plate (BioRad) and sealed with Microseal 'B' PCR plate seal (BioRad). qPCR reactions was denaturation for 30 sec at 95°C, followed by 45 cycles of denaturation at 95°C for 15 sec and annealing at 58 °C for 60 sec. Then, a melt-curve was generated for temperatures from 65°C to 95°C with 0.5°C increment (2-5 sec per step). All the samples were normalized with the reference *SnoR14* transcript using primers HvuSnoR14 -F1 and HvuSnoR14 -R1and same qPCR conditions as described above.

Allele Analysis

Sbs1 and *Sbs2* allele analysis was performed on ten barley cvs (Morex, NDB112, Robust, Tradition, Pinnacle, Bowman, ND Genesis, TR306, Steptoe and Harrington) to identify polymorphisms that correlate with spot blotch resistance or susceptibility. DNA was isolated using the protocol described by Tsilo et al., 2010 (72). The *Sbs1* and *Sbs2* sequences available from the cv. Morex whole genome sequence assembly and cv. Bowman draft genome assembly (41) as well as the Steptoe sequence generated by Genome Walking, were utilized to design primers from conserved regions targeted to amplifying ~4.8kb genomic DNA covering the promoter and coding regions. The Allele analysis were carried out by amplifying the genomic fragments with primers Sbs1_F4 and Sbs1_PRO_R1 for *Sbs1* and Sbs2_F3 and Sbs2_R5 for *Sbs2* (Supp. File 9). The PCR reactions contained 2 µl (~20ng/ µl) of template gDNA, 200 µM dNTPs, 0.5 µM of each forward and reverse primer, 5 µl of 5X Q5 reaction buffer, 5 µl of 5X Q5 high GC enhancer, 0.02 unit/ µl final concentration of the Q5 high fidelity DNA polymerase and nuclease free water up to a 25 µl reaction volume. The PCR cycle parameters had an initial denaturation of 95°C for 5 min, followed by 35 cycles of 95°C for 60 sec, 60°C for 180 sec, and 72°C for 60 sec followed by a final extension of 72°C for 10 min. PCR products were visualized on a 1% agarose gel containing GelRed (Biotium, CA) and subsequently purified using E.Z.N.A.

Cycle Pure Kit (Omega Bio-Tek, Norcross, GA) following the manufacturer's standard protocol. The PCR amplicons were used to create barcoded Ion Torrent sequencing libraries using the NEBNext Fast DNA fragmentation and Library Prep Set for Ion Torrent following the manufacturer's standard protocol (Life Technologies, CA). Approximately 3 pg of the final multiplexed barcoded library was sequenced on the Ion Torrent PGM instrument utilizing the Ion PGM Template OT2 200 kit, Ion PGM Sequencing 200 Kit v2 and an Ion 314 Chip (Life Technologies), following the manufacturer's standard protocols. Barcoded libraries of each allele PCR fragment was sequenced resulting in a mean read length of 223 and an average of 240,000 reads per sample. The data analysis was conducted with CLC Genomics workbench 8.0.3 software (QIAGEN Bioinformatics, CA). Trimmed reads were aligned to a subset of reference file containing *Sbs1* (4347 bp) and *Sbs2* (4773 bp) genomic DNA sequence. 90-99 % read alignment was achieved for each genotype using our defined parameters of mismatch cost of 2, Insertion/ Deletion cost of 3, Insertion/ Deletion open cost of 6, Insertion/Deletion extend cost of 1, length fraction = 0.5 and similarity fraction = 0.8. Consensus sequence was extracted using aligned read to either *HvSbs1* or *HvSbs2* with minimum of 300 reads per base pair and PHRED quality score >30 for each base call. *HvSbs1* and *HvSbs2* consensus sequence was used for *in silico* analysis of promoter region on FGENESH (5).

RNAseq Experiment

Susceptible cv. Harrington and resistant cv. Bowman was used to perform the gene expression profile for spot blotch resistance and susceptibility (BioProject ID PRJNA522759). Leaf tissue of 3 biological replicates of cv Bowman and cv Harrington non-inoculated control and 72hpi with *B. sorokiniana* isolate ND85F were collected. An RNAseq library was constructed using TruSeq RNA library prep kit v2 (Illumina) and run on the Illumina NextSeq

500. The total reads obtained are summarized in Fig. 8C. Quality of reads were checked in FastQC v0.11.5 (6). The data analysis and comparisons were carried out in the CLC Genomics workbench 8.0.3 software (QIAGEN Bioinformatics, CA). The reads of the 12 samples were aligned using barley concatenated reference high confidence and low confidence gene list provided in the barley IBSC IPK 2016 database. Alignment was performed using mismatch cost 2, insertion and deletion cost 3, length and similarity fraction 0.9 and reads were aligned for both strand specificity and maximum number of hits for a read was set at 10. Expression was calculated using RPKM. Empirical analysis of DGE (EDGE) was performed to run "Exact test" for two group comparisons (7). fdr corrected $P< 0.05$ and EDGE $\geq$3 fold regulation values were used to get the differentially regulated genes between the non-inoculated and inoculated samples for both genotypes to create the final list of differentially regulated transcripts for spot blotch susceptibility and resistance. The final list was then compared between for the specific upregulated and downregulated genes during susceptibility and resistance.

Network Analysis

A protein-protein interaction network (PPIN) analysis with the top 250 up and downregulated genes (500 DEGs) identified in the susceptible barley cv. Harrington 72hpi with *B. sorokiniana* was carried out using data from STRING-db (8) and on a PPIN (protein-protein interaction network) analysis and visualization program developed on our own custom python script (9), based on NetworkX (14). Additionally, the Arabidopsis homolog of *Sbs1*, *Sbs2* and other candidate WAKs were included. Using our PPIN script (submitted in https://github.com/Gazala-Ameen/PPIN), candidate WAKs underlying the *Rcs5* QTL were denoted by yellow color, upregulated genes as red and downregulated genes as green. The protein-protein interaction network of *Arabidopsis thaliana* was created based on the interactions

database in String-DB v10.5, a curated database (8) combining interactions from different venues with their corresponding probabilities of occurrence (10). We then modeled identifying maximum reliability pathways connecting our up-regulated, down-regulated, and important genes as a Steiner Tree (11) problem on the largest connected component of the obtained PPIN. Our approach is novel as it allows for a selection of multiple genes to connect and identify their pathways and also include the genes which are not provided in the list but are important to connect and built a more reliable network. The Steiner Tree problem is NP-hard (12), and as such it would prove impossible to solve for the 24,265 vertices and 5,318,667 interactions of the largest connected component within the *Arabidopsis thaliana* proteome. Therefore, we solved it with the Kou approximation algorithm (13), using NetworkX (14) for graph processing and visualization purposes in our PPIN script.

DAB Staining

For visualization of ROS, five 3 cm leaf samples were collected from secondary leaves at 0, 6, 12, 18, 24, 30, 36 and 48 hpi from Morex and Steptoe and immediately transferred in 10 ml freshly prepared 1mg/ml DAB (Sigma Aldrich, MO) solution (pH 3.6) in 15 ml tubes. Samples were DAB stained for 6 hours on an orbital shaker (VWR) at room temperature at 120 rpm shaking. Later DAB solution was removed and samples were washed twice with anhydrous Farmer's fixative (3-ethanol:1- glacial acetic acid) and then cleared and fixed simultaneously in 30 ml Farmers' fixative (FF) for 12 hours transferring in 50 ml tubes. Farmer's fixative was changed once after 12 hours and samples were cleared for an additional 3 hours. Cleared samples were stored in fresh 45 ml Farmer's fixative solution in the 50 ml tube in dark until visualized under microscopy. To visualize the germination and growth of *B. sorokiniana* conidial spores and their association with DAB staining, we used wide-field florescence on a Zeiss Axio Imager

M2 epiflorescence upright microscope. Emission was 435-485, chromatic beam splitter was set at FT420 and excitation filter BP379-401 and Axio Visison rel. 4.8 software was used to visualize pathogen associated DAB (76).

Intercellular Wash Fluid Extraction and Infiltration

The cv Steptoe (200 plants) were inoculated with *B. sorokiniana* isolates ND85F and BS035 (~2000 spores/ml). One-third of the secondary leaves (~3 cm) were collected in 50 ml conical centrifuge tubes after 12, 36 and 72 hpi. The IWF extractions were conducted as described in Liu et al., 2015 (23), and the crude IWF extracted was ~3 ml/time-point/isolate. The IWF of each isolate (3 time-points) were mixed and infiltrated in the secondary leaves of cv Steptoe plants which were collected later for transcripts analysis. The infiltrated tissue were collected in liquid nitrogen at 12, 36 and 72 hours post-infiltration in three replicates for RNA extraction and subsequently qPCR assay to determine the targeted transcripts. This experiment was run twice. The Pronase treatment was applied to 5 ml of IWF of the ND85F and BS035 isolates, where the final concentration of Pronase was 1mg/ml and kept at room temperature for 4 hours along with the IWF without Pronase treatments and water-only treatments as control (16). These five treatments were then infiltrated into secondary leaves of Steptoe and infiltrated leaf tissues were collected at 72 hours post infiltration in three replicates in liquid nitrogen for subsequent transcript analysis. The primers used were HvuSnoR14 -F1 and HvuSnoR14 -R1; WAK3Q-F1 and WAK3Q-R1; WAK4Q-F1 and WAK4Q-R1 for *HvSnoR14, Sbs1*, *Sbs2* respectively at the same parameters described above for transcripts quantification (Supp. File 9).

Literature Cited

1. Fao WF. IFAD (2012) The state of food insecurity in the world 2012. Economic Growth is necessary but not Sufficient to Accelerate Reduction of Hunger and Malnutrition FAO, Rome, Italy. 2012;1–61.
2. Xie W, Xiong W, Pan J, Ali T, Cui Q, Guan D, et al. Decreases in global beer supply due to extreme drought and heat. Nat Plants. 2018 Nov;4(11):964–973.
3. Prein AF, Rasmussen RM, Ikeda K, Liu C, Clark MP, Holland GJ. The future intensification of hourly precipitation extremes. Nat Clim Chang. 2016 Dec 5;7(1):48–52.
4. Kiesling RL. The diseases of barley. Barley. 1985;269–312.
5. Kumar J, Schafer P, Huckelhoven R, Langen G, Baltruschat H, Stein E, et al. Bipolaris sorokiniana, a cereal pathogen of global concern: cytological and molecular approaches towards better control. Mol Plant Pathol. 2002 Jul;3(4):185–195.
6. Fetch TG, Steffenson BJ. Identification of Cochliobolus sativus isolates expressing differential virulence on two-row barley genotypes from North Dakota. Canadian Journal of Plant Pathology. 1994 Sep;16(3):202–206.
7. Dubin HJ, Ginkel M van. The status of wheat diseases and disease research in warmer areas. Wheat for the nontraditional warm areas: a proceedings of the International Conference July 29-August 3 1990 Foz do Iguaçu, Brazil. 1991;
8. Nutter FW, Pederson VD, Foster AE. Effect of Inoculations with Cochliobolus sativus at Specific Growth Stages on Grain Yield and Quality of Malting Barley 1. Crop Science. 1985;25(6):933–938.

9. Bilgic H, Steffenson BJ, Hayes PM. Comprehensive genetic analyses reveal differential expression of spot blotch resistance in four populations of barley. Theor Appl Genet. 2005 Nov 15;111(7):1238–1250.

10. Zhou H, Steffenson B. Genome-wide association mapping reveals genetic architecture of durable spot blotch resistance in US barley breeding germplasm. Mol Breeding. 2013 Jun;32(1):139–154.

11. Steffenson BJ, Hayes PM, Kleinhofs A. Genetics of seedling and adult plant resistance to net blotch (Pyrenophora teres f. teres) and spot blotch (Cochliobolus sativus) in barley. Theor Appl Genet. 1996 Apr;92(5):552–558.

12. Monaghan J, Zipfel C. Plant pattern recognition receptor complexes at the plasma membrane. Curr Opin Plant Biol. 2012 Aug;15(4):349–357.

13. Boller T, Felix G. A renaissance of elicitors: perception of microbe-associated molecular patterns and danger signals by pattern-recognition receptors. Annu Rev Plant Biol. 2009;60:379–406.

14. Torres MA. ROS in biotic interactions. Physiol Plant. 2010 Apr;138(4):414–429.

15. Desaki Y, Miyata K, Suzuki M, Shibuya N, Kaku H. Plant immunity and symbiosis signaling mediated by LysM receptors. Innate Immun. 2018;24(2):92–100.

16. Miya A, Albert P, Shinya T, Desaki Y, Ichimura K, Shirasu K, et al. CERK1, a LysM receptor kinase, is essential for chitin elicitor signaling in Arabidopsis. Proc Natl Acad Sci USA. 2007 Dec 4;104(49):19613–19618.

17. Cao Y, Liang Y, Tanaka K, Nguyen CT, Jedrzejczak RP, Joachimiak A, et al. The kinase LYK5 is a major chitin receptor in *Arabidopsis* and forms a chitin-induced complex with related kinase CERK1. Elife. 2014 Oct 23;3.

18. Hu H, Xiong L, Yang Y. Rice SERK1 gene positively regulates somatic embryogenesis of cultured cell and host defense response against fungal infection. Planta. 2005 Sep;222(1):107–117.

19. Jones JDG, Dangl JL. The plant immune system. Nature. 2006 Nov 16;444(7117):323–329.

20. Bonardi V, Dangl JL. How complex are intracellular immune receptor signaling complexes? Front Plant Sci. 2012 Oct 23;3:237.

21. Faris JD, Zhang Z, Lu H, Lu S, Reddy L, Cloutier S, et al. A unique wheat disease resistance-like gene governs effector-triggered susceptibility to necrotrophic pathogens. Proc Natl Acad Sci USA. 2010 Jul 27;107(30):13544–13549.

22. Lorang JM, Sweat TA, Wolpert TJ. Plant disease susceptibility conferred by a "resistance" gene. Proc Natl Acad Sci USA. 2007 Sep 11;104(37):14861–14866.

23. Liu Z, Holmes DJ, Faris JD, Chao S, Brueggeman RS, Edwards MC, et al. Necrotrophic effector-triggered susceptibility (NETS) underlies the barley-Pyrenophora teres f. teres interaction specific to chromosome 6H. Mol Plant Pathol. 2015 Feb;16(2):188–200.

24. Lally D, Ingmire P, Tong HY, He ZH. Antisense expression of a cell wall-associated protein kinase, WAK4, inhibits cell elongation and alters morphology. Plant Cell. 2001 Jun;13(6):1317–1331.

25. Ye Y, Ding Y, Jiang Q, Wang F, Sun J, Zhu C. The role of receptor-like protein kinases (RLKs) in abiotic stress response in plants. Plant Cell Rep. 2017 Feb;36(2):235–242.

26. Kacperska A. Sensor types in signal transduction pathways in plant cells responding to abiotic stressors: do they depend on stress intensity? Physiol Plant. 2004 Oct;122(2):159–168.

27. Huang T-L, Nguyen QTT, Fu S-F, Lin C-Y, Chen Y-C, Huang H-J. Transcriptomic changes and signalling pathways induced by arsenic stress in rice roots. Plant Mol Biol. 2012 Dec;80(6):587–608.

28. Kohorn BD, Kobayashi M, Johansen S, Friedman HP, Fischer A, Byers N. Wall-associated kinase 1 (WAK1) is crosslinked in endomembranes, and transport to the cell surface requires correct cell-wall synthesis. J Cell Sci. 2006 Jun 1;119(Pt 11):2282–2290.

29. Brutus A, Sicilia F, Macone A, Cervone F, De Lorenzo G. A domain swap approach reveals a role of the plant wall-associated kinase 1 (WAK1) as a receptor of oligogalacturonides. Proc Natl Acad Sci USA. 2010 May 18;107(20):9452–9457.

30. Asai T, Tena G, Plotnikova J, Willmann MR, Chiu W-L, Gomez-Gomez L, et al. MAP kinase signalling cascade in Arabidopsis innate immunity. Nature. 2002 Feb 28;415(6875):977–983.

31. Huffaker A, Pearce G, Ryan CA. An endogenous peptide signal in Arabidopsis activates components of the innate immune response. Proc Natl Acad Sci USA. 2006 Jun 27;103(26):10098–10103.

32. Flor HH. Current status of the gene-for-gene concept. Annu Rev Phytopathol. 1971 Sep;9(1):275–296.

33. Zuo W, Chao Q, Zhang N, Ye J, Tan G, Li B, et al. A maize wall-associated kinase confers quantitative resistance to head smut. Nat Genet. 2015 Feb;47(2):151–157.

34. Zhang N, Zhang B, Zuo W, Xing Y, Konlasuk S, Tan G, et al. Cytological and Molecular Characterization of ZmWAK-Mediated Head-Smut Resistance in Maize. Mol Plant Microbe Interact. 2017 Apr 27;30(6):455–465.

35. Hurni S, Scheuermann D, Krattinger SG, Kessel B, Wicker T, Herren G, et al. The maize disease resistance gene Htn1 against northern corn leaf blight encodes a wall-associated receptor-like kinase. Proc Natl Acad Sci USA. 2015 Jul 14;112(28):8780–8785.

36. Saintenac C, Lee W-S, Cambon F, Rudd JJ, King RC, Marande W, et al. Wheat receptor-kinase-like protein Stb6 controls gene-for-gene resistance to fungal pathogen Zymoseptoria tritici. Nat Genet. 2018 Mar;50(3):368–374.

37. Shi G, Zhang Z, Friesen TL, Raats D, Fahima T, Brueggeman RS, et al. The hijacking of a receptor kinase-driven pathway by a wheat fungal pathogen leads to disease. Sci Adv. 2016 Oct 26;2(10):e1600822.

38. Fetch TG, Steffenson BJ. Rating Scales for Assessing Infection Responses of Barley Infected with*Cochliobolus sativus*. Plant Dis. 1999 Mar;83(3):213–217.

39. Drader T, Johnson K, Brueggeman R, Kudrna D, Kleinhofs A. Genetic and physical mapping of a high recombination region on chromosome 7H(1) in barley. Theor Appl Genet. 2009 Feb;118(4):811–820.

40. Yu Y, Tomkins JP, Waugh R, Frisch DA, Kudrna D, Kleinhofs A, et al. A bacterial artificial chromosome library for barley (Hordeum vulgare L.) and the identification of clones containing putative resistance genes. TAG Theoretical and Applied Genetics. 2000 Nov 10;101(7):1093–1099.

41. Mascher M, Gundlach H, Himmelbach A, Beier S, Twardziok SO, Wicker T, et al. A chromosome conformation capture ordered sequence of the barley genome. Nature. 2017 Apr 26;544(7651):427–433.

42. Holzberg S, Brosio P, Gross C, Pogue GP. Barley stripe mosaic virus-induced gene silencing in a monocot plant. Plant J. 2002 May;30(3):315–327.

43. Choi Y, Chan AP. PROVEAN web server: a tool to predict the functional effect of amino acid substitutions and indels. Bioinformatics. 2015 Aug 15;31(16):2745–2747.

44. Kohorn BD, Johansen S, Shishido A, Todorova T, Martinez R, Defeo E, et al. Pectin activation of MAP kinase and gene expression is WAK2 dependent. Plant J. 2009 Dec;60(6):974–982.

45. Glazebrook J. Contrasting mechanisms of defense against biotrophic and necrotrophic pathogens. Annu Rev Phytopathol. 2005;43:205–227.

46. Thomas PD, Campbell MJ, Kejariwal A, Mi H, Karlak B, Daverman R, et al. PANTHER: a library of protein families and subfamilies indexed by function. Genome Res. 2003 Sep;13(9):2129–2141.

47. Wang X, Jiang N, Liu J, Liu W, Wang G-L. The role of effectors and host immunity in plant-necrotrophic fungal interactions. Virulence. 2014;5(7):722–732.

48. Gao Z, Johansen E, Eyers S, Thomas CL, Noel Ellis TH, Maule AJ. The potyvirus recessive resistance gene, sbm1, identifies a novel role for translation initiation factor eIF4E in cell-to-cell trafficking. Plant J. 2004 Nov;40(3):376–385.

49. Iyer-Pascuzzi AS, McCouch SR. Recessive resistance genes and the Oryza sativa-Xanthomonas oryzae pv. oryzae pathosystem. Mol Plant Microbe Interact. 2007 Jul;20(7):731–739.

50. Büschges R, Hollricher K, Panstruga R, Simons G, Wolter M, Frijters A, et al. The barley *Mlo* gene: a novel control element of plant pathogen resistance. Cell. 1997 Mar 7;88(5):695–705.

51. Consonni C, Humphry ME, Hartmann HA, Livaja M, Durner J, Westphal L, et al. Conserved requirement for a plant host cell protein in powdery mildew pathogenesis. Nat Genet. 2006 Jun;38(6):716–720.

52. Yuan M, Chu Z, Li X, Xu C, Wang S. Pathogen-induced expressional loss of function is the key factor in race-specific bacterial resistance conferred by a recessive R gene xa13 in rice. Plant Cell Physiol. 2009 May;50(5):947–955.

53. Condon BJ, Leng Y, Wu D, Bushley KE, Ohm RA, Otillar R, et al. Comparative genome structure, secondary metabolite, and effector coding capacity across Cochliobolus pathogens. PLoS Genet. 2013 Jan 24;9(1):e1003233.

54. Leng Y, Zhong S. Sfp-type 4'-phosphopantetheinyl transferase is required for lysine synthesis, tolerance to oxidative stress and virulence in the plant pathogenic fungus Cochliobolus sativus. Mol Plant Pathol. 2012 May;13(4):375–387.

55. Kohorn BD, Hoon D, Minkoff BB, Sussman MR, Kohorn SL. Rapid oligo-galacturonide induced changes in protein phosphorylation in Arabidopsis. Mol Cell Proteomics. 2016 Apr;15(4):1351–1359.

56. Galletti R, Ferrari S, De Lorenzo G. Arabidopsis MPK3 and MPK6 play different roles in basal and oligogalacturonide- or flagellin-induced resistance against Botrytis cinerea. Plant Physiol. 2011 Oct;157(2):804–814.

57. Gramegna G, Modesti V, Savatin DV, Sicilia F, Cervone F, De Lorenzo G. GRP-3 and KAPP, encoding interactors of WAK1, negatively affect defense responses induced by oligogalacturonides and local response to wounding. J Exp Bot. 2016 Mar;67(6):1715–1729.

58. Harkenrider M, Sharma R, De Vleesschauwer D, Tsao L, Zhang X, Chern M, et al. Overexpression of Rice Wall-Associated Kinase 25 (OsWAK25) Alters Resistance to Bacterial and Fungal Pathogens. PLoS One. 2016 Jan 21;11(1):e0147310.

59. Wolf S, van der Does D, Ladwig F, Sticht C, Kolbeck A, Schürholz A-K, et al. A receptor-like protein mediates the response to pectin modification by activating brassinosteroid signaling. Proc Natl Acad Sci USA. 2014 Oct 21;111(42):15261–15266.

60. Foley RC, Kidd BN, Hane JK, Anderson JP, Singh KB. Reactive Oxygen Species Play a Role in the Infection of the Necrotrophic Fungi, Rhizoctonia solani in Wheat. PLoS One. 2016 Mar 31;11(3):e0152548.

61. Survila M, Davidsson PR, Pennanen V, Kariola T, Broberg M, Sipari N, et al. Peroxidase-Generated Apoplastic ROS Impair Cuticle Integrity and Contribute to DAMP-Elicited Defenses. Front Plant Sci. 2016 Dec 23;7:1945.

62. Daudi A, Cheng Z, O'Brien JA, Mammarella N, Khan S, Ausubel FM, et al. The apoplastic oxidative burst peroxidase in Arabidopsis is a major component of pattern-triggered immunity. Plant Cell. 2012 Jan 13;24(1):275–287.

63. Levine A, Tenhaken R, Dixon R, Lamb C. H2O2 from the oxidative burst orchestrates the plant hypersensitive disease resistance response. Cell. 1994 Nov 18;79(4):583–593.

64. Pham J, Desikan R. Modulation of ROS production and hormone levels by AHK5 during abiotic and biotic stress signaling. Plant Signal Behav. 2012 Aug;7(8):893–897.

65. Choi J, Huh SU, Kojima M, Sakakibara H, Paek K-H, Hwang I. The cytokinin-activated transcription factor ARR2 promotes plant immunity via TGA3/NPR1-dependent salicylic acid signaling in Arabidopsis. Dev Cell. 2010 Aug 17;19(2):284–295.

66. Lim G-H, Shine MB, de Lorenzo L, Yu K, Cui W, Navarre D, et al. Plasmodesmata Localizing Proteins Regulate Transport and Signaling during Systemic Acquired Immunity in Plants. Cell Host Microbe. 2016 Apr 13;19(4):541–549.

67. Jung HW, Tschaplinski TJ, Wang L, Glazebrook J, Greenberg JT. Priming in systemic plant immunity. Science. 2009 Apr 3;324(5923):89–91.

68. Maldonado AM, Doerner P, Dixon RA, Lamb CJ, Cameron RK. A putative lipid transfer protein involved in systemic resistance signalling in Arabidopsis. Nature. 2002 Sep 26;419(6905):399–403.

69. van Damme M, Zeilmaker T, Elberse J, Andel A, de Sain-van der Velden M, van den Ackerveken G. Downy mildew resistance in Arabidopsis by mutation of HOMOSERINE KINASE. Plant Cell. 2009 Jul 21;21(7):2179–2189.

70. Brewer HC, Hawkins ND, Hammond-Kosack KE. Mutations in the Arabidopsis homoserine kinase gene DMR1 confer enhanced resistance to Fusarium culmorum and F. graminearum. BMC Plant Biol. 2014 Nov 29;14:317.

71. Shah K, Russinova E, Gadella TWJ, Willemse J, De Vries SC. The Arabidopsis kinase-associated protein phosphatase controls internalization of the somatic embryogenesis receptor kinase 1. Genes Dev. 2002 Jul 1;16(13):1707–1720.

72. Tsilo TJ, Jin Y, Anderson JA. Identification of flanking markers for the stem rust resistance gene Sr6 in wheat. Crop Sci. 2010;50(5):1967–1970.

73. Szklarczyk D, Franceschini A, Wyder S, Forslund K, Heller D, Huerta-Cepas J, et al. STRING v10: protein-protein interaction networks, integrated over the tree of life. Nucleic Acids Res. 2015 Jan;43(Database issue):D447–52.

74. Ameen G, Vogiatzis C, Solanki S, Brueggeman R. Gazala-Ameen/PPIN: Dependencies and run requirements or PPIN. 2018 Dec 4;

75. Hagberg A, Swart P, Chult DS. Exploring network structure, dynamics, and function using NetworkX. Exploring network structure, dynamics, and function using NetworkX [Internet]. 2008 [cited 2018 Feb 20]; Available from: http://permalink.lanl.gov/object/tr?what=info:lanl-repo/lareport/LA-UR-08-05495

76. Solanki S. Dissecting the Mystery behind Rpg5 Mediated Puccinia graminis Resistance in Barley Using Genetics, Molecular and Bioinformatics Approaches. 2017;

CHAPTER 3: THE *NEC3* GENE IS A PUTATIVE NEGATIVE REGULATOR OF PATHOGEN INDUCED PROGRAMMED CELL DEATH IN BARLEY

Abstract

Differential Programmed Cell Death (PCD) has important roles in plant immunity responses, which determines the outcome with biotrophic and necrotrophic pathogens, and symbiotic microbes. However, the immunity mechanisms including components that suppress or enhance PCD resulting in differential amplitude and/or timing of disease resistance responses are relatively unknown, thus, characterizing mutants in these pathways can fill important knowledge gaps. The *nec3* mutants of barley predominantly show a distinct PCD phenotype, large cream to orange necrotic lesions that were previously described as spontaneous lesion mimic mutants (LMMs). We determined that *nec3* is not a LMM, as seedlings grown under sterile conditions did not express the phenotype but were only observed after infection with specific pathogens, showing that the phenotype is induced by host-pathogen interactions. A newly identified gamma-irradiation induced necrotic mutant, *nec3*-g1, was confirmed as *nec3* by allelism tests with four previously characterized mutants. The F_2 progeny of a cross of *nec3*-g1 (cultivar (cv) Bowman) x cv Quest segregated as a single recessive gene post inoculation with *Bipolaris sorokiniana,* fitting the expected 3 wildtype:1 mutant ratio (χ^2=0.32). The homozygous F_2 mutant progeny were genotyped with 4 SSR and 25 SNP markers spanning the centromeric region of barley chromosome 6H where *nec3* was previously mapped at low resolution. The mapping delimited *nec3* to ~ 6.0 cM flanked by four cosegregating SNP markers (11_20052, 12_30665, SCRI_RS_171247 and 12_30665) distally and six cosegregating markers (SCRI_RS_239962, 12_30133, SCRI_RS_140158, SCRI_RS_239889, SCRI_RS_169829 and GBM1423) proximally. The positions of the 29 markers were in perfect linear order with the newly released

barley genome sequence and the barley POPSEQ positions, delimiting the *nec3* region to ~ 0.14 cM correlating to a physical region spanning ~ 16.96 Mb containing 143 high confidence annotated genes. Robust exome sequencing of three independent *nec3* mutants, *nec3*-g1, *nec3.l,* and *nec3.m,* failed to identify the candidate gene suggesting that the mutations may occur in the promoter region which is not targeted by the exome capture array or the gene is not present in the exome capture probe set. However, RNAseq analysis identified two of the delimited genes with > 3 fold down regulation in the *nec3*-g1 mutant, representing candidate *nec3* genes.

Introduction

Programmed cell death (PCD) is a highly evolved and tightly regulated physiological response of plant and animal cells that adapted to function in development, cell differentiation, cell number homeostasis, and immunity (1). In plants, PCD is activated by environmental cues including biotic stress induced by pathogens, representing the major physiological response and mechanism of defense against invading microbes or feeding invertebrates. Pathogens evolve virulence effectors to facilitate entry and host cellular machinery manipulation to induce inappropriate physiological responses that promote access to nutrients and life cycle completion in the host, thus becoming adapted pathogens (2). However, plant innate immune systems counter evolved to recognize these pathogen virulence mechanisms by direct recognition of effectors (3–6) or more commonly the manipulation of the targeted host susceptibility proteins (7). This direct or indirect recognition of non-self typically induces effector triggered immunity (ETI) which is characterized by a strong PCD response known as the hypersensitive response (HR), which functions to sequester and inhibit further pathogen colonization. Although the scientific community is beginning to elucidate these mechanisms in plants, major gaps exist in

our understanding of how overlapping and complex PCD responses function in important immunity and developmental pathways.

The plant innate immune system has evolved to detect invading pathogens by several means, yet, dichotomously has been separated into layers with the first line of defense known as pathogen associated molecular patterns (PAMP) triggered immunity (PTI). These "nonhost" resistance mechanisms are triggered at the cell surface by the detection of extracellular pathogen molecules, inducing resistance responses that include callose deposition at the point of ingress, pathogen related (PR) gene expression, a quick transient reactive oxygen species (ROS) burst, and in some PTI responses, a PCD response at the site of attempted entry or colonization (8). PTI responses are induced through transmembrane cell surface receptors known to reside in heterologous complexes of pattern recognition receptors (PRRs; (9)) that activate underlying cytosolic signaling protein kinase cascades including the mitogen activated protein kinase (MAPK) pathways (10). The PRRs contain diverse extracellular receptor domains but are typically grouped into two classes, those that contain an intracellular kinase signaling domain known as receptor-like kinases (RLKs) or those that are missing the kinase domain and are known as receptor-like proteins (RLPs) (8).

The PRRs typically identify PAMPs, which are highly conserved molecules of microbial origin conserved across genera or species that are indispensable for fitness. Important bacterial PAMPS known to date include elongation factor EF-Tu (11), lipopolysacharides (12) and flagellin, the subunit of bacterial flagella required for motility of many gram-negative bacteria (13). Known fungal PAMPs are chitin, a major component of fungal cell walls (14), B-glucan (15) and ergosterol (16). PTI responses can also be elicited by damage associated molecular patterns (DAMPs), which are host extracellular matrix subunits such as oligogalacturonide

residues (OGs) released from plant cell walls upon partial degradation by pathogens. The detection of OGs by wall associated kinase PRRs sounds the alarm of compromised cell integrity indicating pathogen ingress or challenge also eliciting PTI-like defense responses (17).

Host specific pathogens counter evolved virulence effectors to evade these PTI responses by blocking the cytosolic signaling pathways via secreted effectors as is seen with *P. syringae* effectors that inhibit FLS2 PRR-mediated signaling following flg22 perception (18). However, as postulated in the zig-zag model that simplistically describes the host-parasite molecular arms race (19), plants counter-evolved cytoplasmically localized immunity receptors, typically with nucleotide binding site-leucine rich repeat (NLR) protein domain architecture, to recognize the presence of these effectors and elicit the hallmark higher amplitude PCD immunity response referred to as the hypersensitive response (HR).

Once an effector is recognized by a cognate NLR immunity receptor then it becomes an avirulence protein. For biotrophic pathogens that require living host cells to feed, these effectors no longer facilitate colonization but rather alert the host to their presence eliciting PCD, which kills the cells they are feeding from effectively stopping the colonization process. Thus, HR is critical to plant innate immunity against biotrophic plant pathogens including viruses, bacteria, fungi, oomycetes, and invertebrates (20). However, the necrotrophic pathogens such as *Parastagonospora nodorum* (21) and *Pyrenophora teres* (22) have evolved to hijack these gene-for-gene immunity mechanisms by evolving necrotrophic effectors (NEs) to purposely alert the host immune system through immunity receptor recognition. These inverse-gene-for-gene interactions initiate PCD responses, which the necrotrophic pathogens utilize to facilitate disease formation because they acquire nutrient from the dying and dead tissue. Thus, they complete their lifecycle on the host facilitating further disease development through necrotrophic effector

triggered susceptibility (NETS; (22)). Both biotrophic and necrotrophic pathogens elicit PCD immunity responses in plants with different outcomes, incompatible –vs- compatible, respectively, determined by the lifestyle of the pathogen and the timing of the responses. Thus, understanding PCD pathways is important to manage both classes of pathogens in crop plants.

Following pathogen recognition via PTI or ETI receptors, reactive oxygen species (ROS), reactive nitrogen species (RNS) and the phytohormone salicylic acid (SA) are produced (23). The HR, higher amplitude PCD, is generally associated with ETI and some PTI responses and begins with an efflux of hydroxide and potassium into the apoplastic spaces and an influx of calcium and hydrogen ions into the cytoplasm (23,24). This is followed by the production of ROS, which results in an oxidative burst in the cells undergoing the HR that includes super oxide anions, hydrogen peroxide, and hydroxyl radicals (25). The species and amount of ROS molecules present and their compartmentalization have been implicated in HR signaling (26,27). Although the production of these molecules is common to both PTI and ETI responses and ROS bursts occur for both, they are different in their timing and duration (26). The PTI induced burst is rapid and transiently induced within minutes of PAMP recognition, however, the higher amplitude ETI burst is sustained over several hours after pathogen attacks and is hypothesized to play an important role in regulating HR (28). PTI can also induce a HR-like PCD, although, some PAMPs induce PCD and others do not (29,30). Interestingly, it has been shown that different PAMPs can induce different pathways (31) and that the duration of phosphorylation of the MAPK pathway may determine the outcome of non-HR or HR PTI and/or ETI HR elicitation (32,33). Phenolics, phytoalexins, and other compounds are also synthesized in the cells surrounding the HR lesions (34). There is also a buildup of callose, lignin, and HGRP whose

deposition probably function to sequester the pathogen in the HR lesion but may also play a role in sequestering the HR responses as well (35).

The LMM mutants in diverse plant species are a genetic resource that once characterized may begin to answer the questions of which PCD pathways are common or unique and how they are differentially regulated. Although induced mutants in crops have been available for close to 100 years (36), we have only just begun to characterize the LMMs and their loss of suppression, which results in spontaneous PCD, considered an inappropriate induction of PCD or physiological disorder (37–40). The mutant collections and LMMs discovered in them by forward genetics approaches are starting to provide valuable information for the identification of genes that are important in abiotic and biotic stresses as well as different developmental PCD processes (38). However, the LMMs are still an underutilized tool for elucidating the function of these genes, and the pathways in which they play a role.

In barley, although several LMMs have been described (38), only two LMM genes have been cloned, *Hvnec1* and *mlo*. The *Hvnec1* gene encodes a cyclic-gated ion channel protein (41,42) with sequence homology to the *Arabidopsis thaliana HLM1* gene, which was previously cloned and characterized (43). The *HLM1* gene is similar to *Hvnec1* in that it has increased pathogen-related (PR) protein expression and produces spontaneous necrotic lesions and leaf tip necrosis with increased susceptibility to certain pathogens (44,45). The *mlo* gene confers increased resistance to the ascomycete fungal pathogen *Erysiphe graminis* f. sp. *hordei,* the cause of powdery mildew, and has been deployed in Northern Europe as a source of durable powdery mildew resistance in barley for 37 years (46). However, in the absence of the disease it confers an ~4% yield penalty on varieties due to its LMM phenotype which results in loss of photosynthetic potential, thus is only economically effective under high disease pressure (47).

The *Mlo* gene encodes a ROP like G-protein that appears to be a suppressor of PCD and is conserved and found in other species including pea, *Arabidopsis* and tomato (48).

In barley, both chemical and irradiation mutagenesis have been utilized to induce a large collection of LMMs (49). One interesting LMM mutant designated as *nec3* was shown to produce distinct cream to orange necrotic lesions (Fig. 1) and was further characterized and mapped to the centromeric region of barley chromosome 6HS ~29.2 cM distal of the *rob1* (orange lemma 1) locus (49–51) and about 16.7 cM distal of the msg36 (male sterile genetic 36) locus (50) utilizing morphological markers (51). The *nec3* gene was more precisely positioned using SNP markers with *nec3.d* shown to be associated with SNP markers 1_00616 to 1_0882 (position 70.15 cM) in 6H bin 05 of the Bowman backcross-derived line BW629 (39) and *nec3.e* was shown to be associated with SNP markers 1_0427 to 1_0494 (positions 56.64 to 70.15 cM) in 6H bin 05 of the Bowman backcross-derived line BW630 (39).

Utilizing the Affymetrix Barley1 GeneChip assay, an attempt was previously made to identify the gene underlying the mutant phenotype, however the results of the study were unsuccessful in identifying *nec3* (52). Despite the gene not being found it was observed that the *nec3.l* and *nec3.m* mutants (Fig. 1) had differential regulation of abiotic stress responsive genes involved in cold and drought stress as compared to the wild type. The highest fold change differences in biotic stress related genes were identified as lipid transfer, pathogen defense and cell wall modifying enzymes (52).

Here we report on delimiting the *nec3* gene to a small genetic interval of ~0.14 cM using the barley POPSEQ positions which represents ~ 16.96 Mb of physical sequence containing 143 high confidence annotated barley genes. The exome capture DNAseq and RNAseq analysis on the nec3 mutants did not definitively identify the nec3 gene but has provided strong candidate

genes. We also show that the *nec3* phenotype is not a spontaneous LMM response but is rather induced by several species of *Ascomycete* pathogenic fungi, both necrotrophs and a biotroph, and the bacterial pathogen *Xanthomonas translucens,* representing pathogens that penetrate the host cells directly by disrupting the cell wall and plasma membrane. We speculated that the pathogen induced PCD responses may be elicited by DAMP or PAMP-like immunity pathway that are regulated by *Nec3,* thus the *Nec3* gene may play a role in suppressing PCD response once set into motion. The genetic analyses and tools developed here will facilitate the identification of the *nec3* gene and allow for the further testing of this hypothesis.

Materials and Methods

Plant Material

Approximately 0.25 kg of cv Bowman seed was irradiated using 20 kRADs of gamma radiation at the Washington State University nuclear reactor in Pullman, WA USA. The M_1 seed was allowed to self and M_2 seed were harvested. The M_2 generation of irradiated cv Bowman seed was bulked and screened for *Bipolaris sorokiniana* isolate ND90Pr resistance following inoculations as described in Fetch and Steffenson (1999) (53). The *nec3*-g1 mutant described here was originally identified from this g-irradiated M_2 seed in an attempt to identify barley mutants resistant to *B. sorokiniana* isolate ND90Pr (54). Following inoculation, infection type rating of individual seedlings were performed using the 1-10 rating scale (53). The two cvs Villa and Proctor were irradiated using x-ray mutagenesis and cv Steptoe was irradiated by fast neutron mutagenesis to generate the *nec3* mutants utilized in allelism tests (52). The *nec3.d* (GSHO 1330) mutant was generated in cv Proctor (PI 280420) (51). The *nec3.e* (GSHO 2423) mutant was generated in cv Villa (PI 399506) (49). The *nec3.l* (FN362, GSHO 3605) and *nec3.m* (FN363, GSHO 3606) mutants were generated in cv Steptoe (CIho 15229) (52). The *nec3.1* and

nec3.m mutant lines used in this study were kindly provided by Dr Andris Kleinhofs, Washington State University. The *nec3.d* and *nec3.e* mutants used in this study were provided by Dr. Jerry Franckowiak and were *nec3.d* in Bowman*6 (BW629) and *nec3.e* in Bowman*6 (BW630).

Allelism Crosses

The *nec3*-g1 mutant identified in this study was crossed with *nec3.1*, *nec3.m*, *nec3*.d and *nec3*.e. The resulting F_1 seed were planted in the field with wildtype parental lines Steptoe and Bowman and phenotyped from seedling to adult plant stages. The F_2 progeny were planted in the greenhouse and inoculated with the *B. sorokiniana* isolate ND85F and disease was rated on the secondary leaves of the seedlings. The phenotyping was performed in the field and greenhouse to take advantage of the entire year. This was made possible due to the consistency of the elicitation of the *nec3* phenotype when grown adjacent to susceptible spreader rows in a disease nursery inoculated with the *B. sorokiniana* isolate ND85F in the field and when inoculated in the greenhouse with *B. sorokiniana* isolate ND85F. In addition, barley heads from the *nec3* allelic crosses were observed and documented in the field.

Elicitation of *nec3* Phenotype and Pathogen Isolates

An isolation box experiment was performed over the course of a month to observe the *nec3* phenotype independent of pathogen challenge. The experiments were conducted using a plexiglass box with the dimensions of 60x30x30 cm (H/W/L) with two holes on opposite sides with a diameter of 7.5 cm to allow for airflow. The ventilation holes were packed with cheesecloth to protect plants from pathogen spores or insects. The wildtype Bowman and *nec3*-g1 seeds were planted and observed for 1 month. Two pots of each genotype with two seedlings per container were planted inside the isolation box in the greenhouse and two pots of the controls

were planted outside the isolation box inside the greenhouse. The plants were watered as needed using distilled autoclaved water. Growth conditions in the greenhouse under sterile conditions inside the isolation box were 16 hour photoperiod at ~ 26C +/- 3C due to greenhouse effect of the plexiglass chamber and the normal greenhouse conditions outside of the isolation box were 16 hour photoperiod at ~22C +/- 3C. The control plants outside the box were either non-inoculated or inoculation with *B. sorokiniana* isolate ND85F using the procedure described below.

Following observation of the *nec3* phenotype on *nec3*-g1 plants in the greenhouse, leaves were documented to determine if an identifiable pathogen, mainly *Blumeria graminis*, was present at the lesion sites. Following photographic documentation, the leaves containing lesions were removed, surface sterilized using 10% bleach for one minute, rinsed and plated on water agar plates and grown under light for 16 hrs/day for 3-5 days.

nec3 Phenotypic Observations

To determine which pathogens were capable of inducing the *nec3* phenotype, inoculations of the mutant line *nec3*-g1 and wildtype lines were performed using diverse pathogens including *B. sorokiniana*, *Pyrenophora teres* f. *teres*, *Pyrenophora teres* f. *maculata*, *Pyrenophora tritici-repentis*, *Parastagonospora nodorum*, *Cercospora beticola*, *Xanthomonas translucens* pv *undulosa*, and virulent and avirulent races of *Puccinia graminis* f. sp. *tritici*.

B. sorokiniana isolate ND85F (Spot Blotch) infections were conducted by growing ten Bowman plants and ten *nec3*-g1 plants in a growth chamber with settings of a 14 hr photoperiod at 22.5C and 10 hr dark period at 19C. When the secondary leaves were fully expanded, approximately ten day old seedlings, inoculations were performed with an atomizer (model) having a 25mL volume using 7psi of pressure. Once inoculated, the seedlings were placed in a

dark mist chamber with misting every 12 minutes for 30s for 16 hours. Following inoculation the plants were placed in the growth chamber and observed every day for symptom development for 10 days (Fig 3.2).

The inoculum was produced by placing a PDA plug with *B. sorokiniana* isolate ND85F derived from infected leaves on a V8- potato dextrose agar (V8-PDA) plate followed by incubation at room temperature for ten days under constant light. The spores were resuspended in sterile H_20 using a sterile loop and adjusted to a concentration of ~7,000 spores/mL with 10ul of Tween20 in order to reduce spore clustering.

Two forms of the net blotch pathogen, *Pyrenopthora teres* f. *teres* and f. *maculata,* the causal agents of spot form and net form net blotch, respectively, were inoculated on the *nec3*-g1 and Bowman wt seedlings. The inoculum production and inoculation procedure used for *Pyrenopthora teres* f. *teres* were performed as described in Shjerve et al., 2014 (55). The inoculum production and inoculation procedure used for *Pyrenopthora teres* f. *maculata* were performed as described in Neupane et al., 2015 (56).

The *Blumeria graminis* inoculations were performed by gently dropping spores from infected leafs on the experimental varieties. Snce *B. graminis* is an obligate biotroph, previously infected barley leaves were used as inoculum source. Following spore application, the plants were left in the greenhouse (16 hour photoperiod at 24C, dark 60C) until symptoms developed.

Pyrenophora tritici-repentis was cultured on V8-PDA media by incubation in the dark followed by 24 hour incubation under light at room temperature and then 24 hours in the dark at 15 C (57). The conidia were then harvested in sterilized distilled water (about 30 ml) by gently scratching the surface of the culture with a sterilized inoculation loop. Final spore concentration

was adjusted to ~3000 spores/mL with 2 drops of Tween 20 per 100 mL of inoculum and Friesen and Faris (2004) was followed for the inoculation conditions and disease evaluation (58).

Parastagonospora nodorum was grown on V8-PDA by spreading 300ul of pycnidial spores and incubated for 7 days under light at room temperature (64). The spores were harvested by washing the plates with distilled water and adjusted to 10^6 spores/mL with 2 drops of tween 20 per mL of inoculum (64). Liu et al. (2004b) was followed for inoculation conditions and disease evaluation. *Cercospora beticola* was grown on V8-PDA media at 13C and 24 hours of cool white light. The conidial suspensions were harvested in distilled water and adjusted to ~1.2 X 10^4 spores/ mL with two drops of tween 20 (Nielsen et al., 1993) and inoculated following Kleinwanzleber, 1970 (59). Inoculations with *Puccinia graminis* f. *tritici* races HKHJ (avirulent on cv Bowman containing *Rpg1*) and QCCJ (virulent on Bowman) were performed after the primary leaves were fully expanded, approximately 10 day old seedlings. The inoculations were performed with *P. graminis* f. *tritici* races HKHJ and QCCJ according to previously established methods (60). Infection types were assessed 12 to 14 days post-inoculation using a 0-4 scale modified from the one developed for wheat by Stakman et al. 1962 (61). The plants were also observed for the typical *nec3* phenotype from 1-14 days post inoculation.

Xanthomonas translucens pv *undulosa* strain BLS-LB10, originally cultured from a wheat plant in Lisbon, ND was grown on WBA plates for 3 days at 28C and resuspended in sterile, distilled water at 0.2 OD (62,63). Three seedlings of *nec3*-g1 and three Bowman wt were infiltrated with the inoculum using a syringe without a needle on the secondary leaves as described in Faris et al., 2010. Inoculated seedlings were then placed in a growth chamber under a 14 hr light at 22C and 10 hr dark at 19C. The symptoms were observed and documented seven days post-infiltration.

Infiltrations

Culture filtrate infiltrations were performed by growing *B. sorokiniana* isolate ND85F on V8-PDA plates at room temperature for one week under 18 hours of light per day from infected plant plugs. 6mL of dH20 was added to the plate and spores were gently resuspended using a rubber policeman. 1mL of the suspension (10-20k spores) was taken from the plate and added to 75-100mL of Fries media (64). The flasks with Fries and *B. sorokiniana* were incubated at 26C in the dark for three days with shaking at 100rpm then placed in the dark at room temperature with continued shaking for an additional four days. Following the 7 days of growth, the exudates were filtered with Miracloth and concentrated using a 15mL Microsep Advance Centrifugal Device with a 3kD cut off to concentrated the exudates ~8x. A syringe without a needle was used to administer four infiltration treatments on the secondary leaves of Bowman, Steptoe, *nec3*-g1, Quest, FN362, FN363, *nec3*.d and *nec3*.e. The four treatments consisted of 1) Concentrated exudates + Fries Media 2) Concentrated exudates + MOPs buffer 3) Concentrated exudates + MOPs + Pronase (Sigma) and 4) Fries Media + MOPS + Pronase. All treatments were at 1:1 ratio with specifications performed according to Liu 2004. Leaves were scored 4 and 7 days after infiltration. Pronase treatments were originally performed at 1mg/mL with subsequent experiments increasing the concentration and time of treatment from 4 hours to overnight.

Due to the results of the last experiment, infiltrations were also performed with trigalacturonic acid and FLG22. Steptoe, Bowman, FN362 and *nec3*-g1 were infiltrated with trigalacturonic acid, a DAMP at 10mg/mL, 1mg/mL and 0.1mg/mL. The same plants were infiltrated with FLG22, a MAMP at 1mg/mL. All infiltrations were performed at the two leaf stage. Following infiltration, plants were kept in a growth chamber with a 14 hour photoperiod at

22.5C and 10 hour of dark at 19.1C. Plants were observed every day and pictures were taken seven days after infiltration.

DAB Staining

To observe ROS at the site of infection, we collected five 3 cm leaf samples from secondary leaves at 0, 8, 12, 24 and 36 hpi from Bowman wild type and nec3-g1 mutant inoculated with *B. sorokiniana* isolate ND85F and immediately transferred in 10 ml freshly prepared 1mg/ml DAB (Sigma Aldrich, MO) solution (pH 3.6) in 15 ml tubes. Samples were DAB stained for 6 hours on an orbital shaker (VWR) at room temperature at 120 rpm shaking. Later DAB solution was removed and samples were washed twice with anhydrous Farmer's fixative (3-ethanol:1- glacial acetic acid) and transferred into 50 ml tubes for clearing and fixing in the 50 ml Farmers' fixative (FF) for 12 hours. Cleared samples were stored in fresh 45 ml FF solution in the 50 ml tube in dark until visualized under microscope. To visualize the germination and growth of *B. sorokiniana* conidial spores and their association with DAB staining, we followed protocol of Solanki et al., 2017 (65).

Electron Microscopy

After visualization of the striking difference of leaves collected from Bowman wild type and *nec3*-γ1 mutant at 12 hpi with *B. sorokiniana* isolate ND85F, we carried out electron microscopy at the same time point during infection. The leaves of both cvs were collected at 12 hpi with *B. sorokiniana* isolate ND85F and cut into squares with a new razor blade, then fixed in 2.5% glutaraldehyde in sodium phosphate buffer (Tousimis, Rockville, Maryland USA) and stored at 4C overnight. They were rinsed in buffer and water and then dehydrated using a graded alcohol series from 30% to 100% ethanol. The leaf samples were critical-point dried using an Autosamdri-810 critical point drier (Tousimis, Rockville, Maryland USA) with liquid carbon

dioxide as the transitional fluid. Dried tissue was attached to aluminum mounts with silver paint (SPI Supplies, West Chester, Pennsylvania USA) and sputter coated with gold (Cressington sputter coater 108auto, Ted Pella Inc., Redding, California USA). Images were obtained using a JEOL JSM-6490LV scanning electron microscope operating at an accelerating voltage of 15 kV.

Nec3 Map Development

The original *nec3*-g1 M_2 plant was utilized as the female parent in a cross with the six-rowed cvQuest that was originally developed for malting and released by the University of Minnesota (66). Two hundred *nec3*-g1 x Quest F_2 individuals were screened in the greenhouse for the *nec3* phenotype after inoculation with *B. sorokiniana* isolate ND85F as previously described and a chi square test was used to determine the goodness of fit. The *B. sorokiniana* isolate ND85F was utilized as it was shown to induce the *nec3* phenotype on M_2 *nec3*-g1 plants similar to the *B. sorokiniana* isolate 90Pr which was used to originally identify *nec3*-g1. Allelism tests determined that *nec3*-g1 was a *nec3* mutant, thus, to genetically position the *nec3* gene more precisely several markers from the centromeric region of barley chromosome 6HS were used to genotype the homozygous *nec3* mutant F_2 individuals, as determined by expression of the *nec3* phenotype.

Genomic DNA was extracted from *nec3*-g1, Quest and 33 homozygous *nec3*-g1 F_2 progeny representing 66 recombinant gametes. DNA extraction of tertiary leaves was performed by homogenizing a 4 cm leaf section in 400ul of extraction buffer (200 mM Tris-HCl pH 7.5, 250 mM NaCl, 25 mM EDTA, 0.5% SDS). After homogenization with a disposable tissue grinder, 200ul of chloroform was added followed by vortexing for 10s and centrifugation at 16.1 rcf for 10 minutes. The supernatant (300ul) was tranfered to a new tube and 200ul of chilled isopropanol was added. The tubes were placed in 4C for 10 minutes followed by centrifugation

at 16.1 rcf for 10 minutes. The supernatant was poured off and the DNA pellet rinsed with 75% EtOH. After rinsing and removal of excess EtOH, the DNA was air dried for 15 minutes and resuspended in 50ul sterile water.

Four microsatellite markers designated Bmag0807, GBM1053, GBM1212, and GBM1423 were PCR amplified using oligonucleotide primers designed from the publicly available probe sequences mined from GrainGenes (67). The standard parameters for the PCR reactions were: 94C for 5 minutes, followed by 35 cycles of 94C for 30 seconds, 62C for 30 seconds, and 72C for 60 seconds, with a final extension at 72C for 7 minutes. The PCR reactions consisted of 1.25 units of NEB Standard Taq polymerase, forward and reverse primers (1.2 μM), NEB Standard Taq buffer (1x), dNTPs (200 μM), in 25 μL reactions. PCR products were visualized on a 1% agarose gel containing GelRed (Biotium, CA), bands excised and subsequently purified using E.Z.N.A. Cycle Pure Kit (Omega Bio-Tek, Norcross, GA) following the manufacturers standard protocol. The amplicons purified from the gel excised bands were directly sequenced using each amplicon specific forward primer (Genscript). The SSR repeat number polymorphisms and single nucleotide polymorphisms (SNPs) were identified by alignment using Vector NTI software (Invitrogen). The Bowman and Quest PCR amplicons for the SSR marker Bmag0807 had a nucleotide difference large enough to be separated and visualized on a 1.5% agarose gel while the GBM1212 amplicons had small enough differences that they were separated on a 12.5% polyacrylamide gel (Amresco) for genotype scoring. The sequencing of the GBM1053 and GBM1423 alleles identified SNPs between cvs Bowman and Quest that were utilized to develop CAPS markers (Table x) using the restriction enzymes BsiHKAI and StyI (New England Biolabs), respectively. The CAPS marker fragments were visualized and scored from 1% agarose gels stained with GelRed (Biotium, CA).

PCR-GBS Library Preparation, Ion Torrent Sequencing and SNP Calling

A PCR genotyping-by-sequencing (PCR-GBS) panel was developed using SNP source file sequences mined from the T3 database (68) as previously described (69). The POPSEQ positions were utilized from the IPK Barley BLAST Server (70) to identify 43 SNP markers that mapped to the *nec3* locus between the SSR markers GBM1053 and GBM1423. The parental lines *nec3*-g1 (cv Bowman) and cv Quest plus the 33 F_2 recombinants were assayed. The PCR-GBS library preparation, Ion Torrent sequencing and SNP calling were performed as described in Richards et al., 2016 (69), however, due to the low number of lines and markers the library was sequenced on a 314 chip. The genetic map was generated and the POPSEQ positions of each marker mined from the IPK genome browser.

Physical Map Development and Candidate Gene Identification

The 43 SNP markers were anchored to the barley physical map, which uses whole genome shotgun (WGS) sequences and bacterial artificial chromosome (BAC) sequences to create a minimum tiling path (MTP) of the genome of barley cv Morex. The flanking markers GBM1053 and GBM1423 were used to determine the physical region of *Nec3* and all the high confidence annotated genes in the region were considered as candidate genes.

Exome Capture and Analysis

DNA was extracted from excised embryos of 5 water-soaked seeds of Bowman, Steptoe and the nec3-g1, FN362, FN363 mutants. DNA extraction was performed on mechanically lysed samples using the PowerPlant Pro DNA isolation kit (MoBIO Laboratories Inc., QIAGEN Carlsbad CA), following Solanki et al., 2019 (71). The quality of extracted DNA was checked by running an aliquot of 1 μL of gDNA on a 1% agarose gel supplemented with GelRED (Biotium) fluorescent nucleic acid dye. The DNA with good integrity showing a high molecular weight

band ~15-20 kb with minimal low molecular weight without smearing indicative of DNA degradation was quantified by the Qubit Broad Range DNA Quantification kit (Thermo Scientific). Enzymatic DNA shearing was optimized to generate desired fragment sizes of 250-450 bp with digestion reactions consisting of 1.5 µg of gDNA in a 20 µl reaction with NEB dsDNA Fragmentase enzyme, 1x Fragmentase reaction buffer and 10mM MgCl2 (New England Biolabs, Ipswich MA). The digested DNA was analyzed on the Agilent 2100 Bioanalyzer (Agilent Technologies) using a DNA 1000 kit (Agilent Technologies) following the manufacturer protocol for chip loading and data analysis for size distribution. The 25-minute enzymatic digestion was found to produce the optimal fragment size distribution ranging between 250-450 base pairs and was used to produce fragmented DNA libraries of Bowman and Steptoe wildtypes, as well as the nec3-g1, FN362, FN363 mutants.

Fragmented gDNA samples were used for exome capture using the Roche NimbleGen SeqCap EZ Developer probe pool barley exome design 120426_Barley_BEC_D04 with a total capture design size of 88.6 Mb. After exome capture, the KAPA HTP gDNA library preparation kit was used for Illumina sequencing library preparation. The standard manufacturer protocol was followed for library preparation using the KAPA HTP kit, except for size selection being performed on a Pippin Prep gel purification system (Sage Science) with a 250-450 bp targeted size selection. The gDNA used to prepare the barcoded barley whole exome capture multiplexed library was developed according to seqCAP EZ Library SR user guide 4.1 protocol. Quality and size distribution of the final capture library was determined using a bioanalyzer following manufacturer's guidelines. A Qubit fluorometer was used to quantify the library for final dilution and subsequent sequencing on an Illumina NextSeq flow cell generating 150 base pair, single end reads.

The mutant *nec3*-g1, FN362 and FN363 along with the wildtype Bowman and Steptoe sequencing reads were parsed by their specific barcodes and quality scores of the raw reads were determined by FQC dashboard (72). The Illumina reads were imported into CLC Genomics Workbench v8.0 in FASTQ format and trimmed for the presence of adapter sequences. Mutant and wildtype reads were aligned to the barley reference genome (73) using the BWA 'mem' algorithm with default settings (74). The alignments were used to identify deleted region utilizing two separate data analysis pipelines, where small deletions (less than 100 bp) were identified using SAMtools 'mpileup' with default settings (75). The identified variants were filtered for a minimum read depth of 3 and a minimum individual genotype quality of 10 using VCFtools (76). As fast neutron mutagenesis may induce large chromosomal deletions, sequencing coverage was calculated across all exome capture targets using BEDTools 'genomecov' to identify full gene deletions (71,77).

RNAseq

Bowman wild type (BWT) and *nec3*-g1 seedlings were grown for ~14 days until the secondary leaves were fully expanded in a growth chamber set at 14 hr light at 22C and 10 hr dark at 19C. The seedlings were inoculated with *B. sorokiniana* isolate ND85F following the procedure described earlier and the control seedlings were inoculated with water mixed with two drops tween 20. Secondary leaf tissue was collected from three biological replicates (one individual seedling is considered one biological replicate) from non-inoculated and inoculated seedlings at 72 hours post inoculation (hpi) and total RNA was extracted using the RNeasy Mini kit (Qiagen, CA) The RNAseq library was constructed using TruSeq RNA library prep kit v2 (illumine) and sequenced on the Illumina NextSeq 500. The read length were 151bp and total reads obtained were analyzed for quality using FastQC v0.11.5 (78). The quality trimmed reads

were then imported into CLC Genome Workbench 8.0.3 for differential gene expression analysis (QIAGEN Bioinformatics, CA). The reads of the 12 samples (the three biological replicates of Bowman wild type and nec3-g1 non-inoculated and 72 hpi) were aligned using barley concatenated reference high confidence and low confidence gene list provided from the barley IBSC IPK 2016 database (73). Alignment was performed using mismatch cost 2, insertion and deletion cost 3, length, similarity fraction 0.9. The reads were aligned for both strand specificity and maximum number of hits for a read was set at 10. Expression was calculated by normalization of reads for read depth and gene length using the RPKM (reads per kilobase million). Empirical analysis of DGE (EDGE) was performed to run "Exact test" for two group comparison (79). FDR corrected $P< 0.05$ and EDGE ≥3-fold regulation values were used to get the differentially regulated genes between the non-inoculated and inoculated samples for both genotypes to create the final list of differentially regulated candidate genes. The final list was then produced by using the candidate genes in the mapped *Nec3* physical region with differential expression between the Bowman wild type and *nec3*-g1 mutant DEGs during pathogen interaction.

Functional Validation of *CRS2-associated factor 2* Candidate Gene

The post-transcriptional gene silencing was carried out utilizing *Barley Stripe Mosaic Virus*-Virus Induced Gene Silencing (*BSMV*-VIGS) following the methodology as described by (80). To design gene specific *BSMV*-VIGS constructs for the candidate gene, a 238 bp fragment was identified from the predicted mRNA transcript that had a single hit in the BLAST search against the barley genome. The amplicons were generated by PCR, using primers CRS2_KO_F1 (AGTTTAATTAACGGAAGTTGTAAGACTAGATTGCTC), CRS2_KO_R1 (AGTGCGGCCGCAATACAATGAGCAGAAACAGAGTCC) and CRS2_KOR_F1

(AGTGCGGCCGCCGGAAGTTGTAAGACTAGATTGCTC), CRS2_KOR_R1 (AGTTTAATTAAAATACAATGAGCAGAAACAGAGTCC) for *HvCrs2* with Not1 and Pac1 sites in sense and anti-sense directions, from the cultivar Bowman cDNA. The amplicons were then sequenced for confirmation. Once confirmed, these cDNA fragments were cloned into the *BSMV* gamma genome-based vector (pSL38.1) using NotI and PacI in both sense and anti-sense directions. RNA was synthesized using the mMessage mMachine T7 transcription kit (Ambion, MA), according to the manufacturer's guidelines for the alpha, beta and gamma genome of *BSMV* and the gamma genome construct containing the candidate gene fragment. RNA of *BSMV* sense and antisense fragments were rub-inoculated onto 10-day-old seedlings of Bowman (20 replicates for each) with a carrier, FES (0.1M Glycine, 0.06M K_2HPO_4, 1% Bentonite w/v, 1% Celite w/v). After inoculation, plants were kept in humidity chambers with 100% humidity for 24 h and later transferred to the growth chambers with 21°C temperature with 16/8 h light/dark photoperiod. After 14 days, when *BSMV* symptoms were systemic in the entire plant, *B. sorokiniana* isolate ND85F was inoculated as described above. After 6 and 10 dpi, the plants were evaluated as a double-blind test for disease reaction on the 0-9 scale (53).

Tissue samples were collected from three biological replicates of each control *BSMV* and *BSMV*: *HvCrs2* at 72 hpi with *B. sorokiniana* for total RNA extraction using RNeasy plant Mini kit (Qiagen) and cDNA was synthesized using GoScript reverse transcription kit (Promega) and diluted 1:5 folds. The RT-PCR was conducted using primers CRS2_KO2_F1 (ACAAATTATTCTCTGGAGAGGGAAG) and CRS2_KO2_R1 (TAGTAGTTTACAGGCACTTGCATCA) which produced a 98 bp fragment. For quantification of the transcripts post inoculation BSMV-VIGS, a 20 µl qPCR reaction was prepared using 0.8 µl of 100 nM of each gene specific forward and reverse primer, 4 µl of 1:5 diluted cDNA

template, 10 µl Sso Advanced supermix, and 4.4 µl qPCR grade ultrapure water (Ambion) in a hard-shell 96 well plate (BioRad) and sealed with Microseal 'B' PCR plate seal (BioRad). The qPCR protocol was denaturation for 30 sec at 95°C, followed by 45 cycles of denaturation at 95°C for 15 sec and annealing at 60 °C for 60 sec. Then, a melt-curve was generated for temperatures from 65°C to 95°C with 0.5°C increment (2-5 sec per step). All the samples were normalized with the reference *SnoR14* transcript using primers HvuSnoR14 -F1 and HvuSnoR14 -R1at the same qPCR conditions as described above.

Results

nec3 Phenotypic Observations

The noninoculated plants outside the chamber also produced symptoms but were challenged primarily by *Blumeria graminis* spores as this pathogen is endemic in the NDSU greenhouse during the spring and summer months and was shown to induce the *nec3* phenotype under our normal greenhouse conditions. However, the isolation box experiment allowed us to answer the question of whether the *nec3* mutant was in fact an LMM as previously described (52) or if the phenotype was only observed upon the introduction of a pathogen or culture filtrates. The *nec3* mutation is only observable under the conditions mentioned in the latter (Fig 3.1). The observed phenotype is hypothesized to be the plant eliciting PCD via a resistance response elicited by several pathogens that are regulated by the *Nec3* gene, yet the *nec3* mutation causes misregulation of genes involved in the pathway allowing PCD to proceed in cells unhindered. These data demonstrate the *nec3* mutation is not a LMM but rather a pathogen induced runaway PCD (PIRP) mutant (Fig 3.2). A single Bowman mutant seedling was identified with a phenotype that was consistent with the *nec3* phenotype as all but one of the *nec3* mutants are characterized by very distinctive tan to orange lesions (43,52).

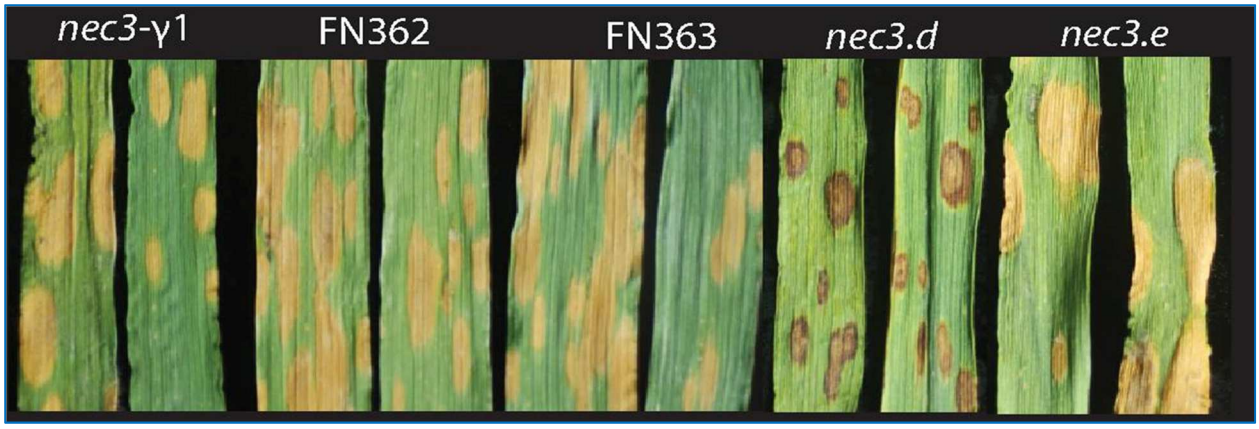

Figure 3.1. The *nec3* mutants are shown from left to right (*nec3*-g1, FN362, FN363, *nec3*.d and *nec3*.e) after infection with *Bipolaris sorokiniana* isolate ND85F.

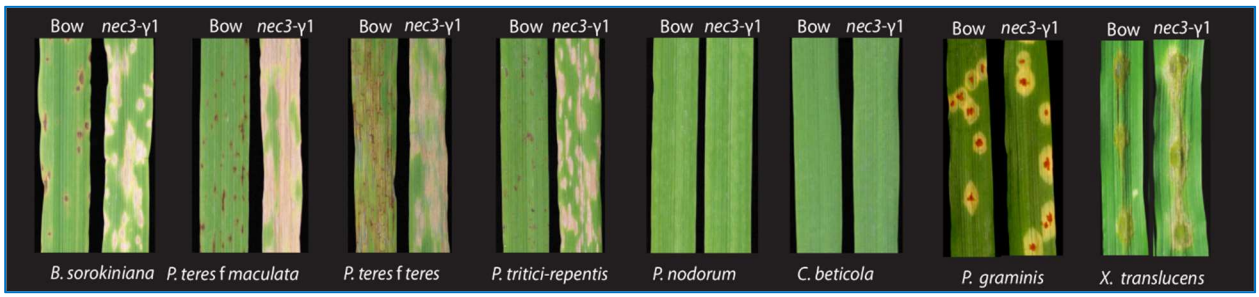

Figure 3.2. The nec3 phenotype was induced by *Bipolaris sorokiniana*, *Pyrenophora teres* f. sp. *teres* and *maculata*, *P. tritici repentis*, and *Xanthomonas translucens* pv *undulosa* and no phenotype was observed when inoculated with *Puccinia graminis*, *Cercospora beticola* and *Parastagonospora nodorum.*

Allelism Crosses

Allelism crosses were completed in the field to determine if the four confirmed *nec3* mutants, FN362, FN363, *nec3*.d and *nec3*.e, are allelic to *nec3*_γ1, the newly identified mutant (Fig 3.3). Crosses between *nec3*-γ1 and the other four mutants were attempted; all were successful with the exception of FN363 which had previously been shown to be allelic to FN362. Due to head sterility, very few F_1 individuals were planted from each cross (2-5 seeds). However, 100% of the F_1 plants displayed a *nec3* phenotype following *B. sorokiniana* inoculation in the greenhouse. This indeed was true for the F_2 seed, which were planted in the field. Fortunately, there was a spot blotch nursery adjacent to the field plot containing the

mutants and F_2 progeny providing prime inoculum for phenotyping. These data demonstrate *nec3*-γ1 to be a fifth *nec3* mutant. Thus, forward genetics approaches have resulted in the identification of the five *nec3* mutants designated as *nec3*-γ1, FN362, FN363, *nec3*.d and *nec3*.e.

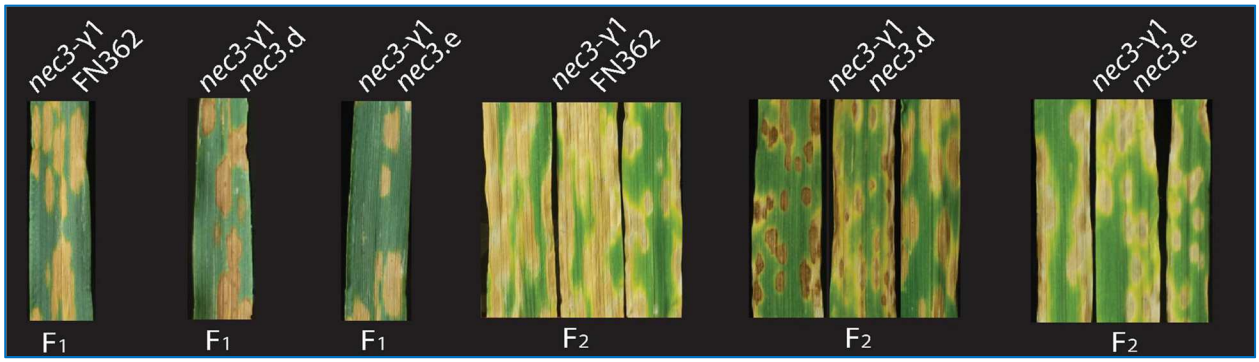

Figure 3.3. The phenotype of F_1 progeny of the *nec3* mutants from allelic test crosses after infection with *Bipolaris sorokiniana* isolate ND85F. The plants were advanced to F_2 and were assessed for the *nec3* phenotype post *B. sorokiniana* inoculation.

Infiltrations

Infiltrations performed on wild type Bowman and the mutants showed differential reactions after *B. sorokiniana* exudates from filtrates were injected on the secondary leaves (Fig 3.4). The reaction visible on the mutant varieties showed the typical runaway PCD as described previously with a lack of defined margins around lesions with a bleached out appearance. However, the wildtype displayed a dark margin with a black necrotic center, typical of phenolic production. In order to determine if the inducer of the *nec3* pathway is a protein, Pronase treatments were performed resulting in no observable phenotypic change compared to filtrates with no Pronase treatment, indicating a non-proteinaceous elicitor produced by the pathogen *B. sorokiniana* (Fig 3.4).

In addition, Trigalacturonic acid infiltrations of Bowman, *nec3*_γ1, Steptoe and FN362 at three concentrations, 10mg/mL, 1mg/mL and 0.1mg/mL resulted in no observable reaction one week after infiltration (data not provided). FLG22 infiltrations were conducted on the same cvs

at a concentration of 1mg/mL. The results reflected the trigalacturonic acid treatment as no observable change occurred one week after infiltration.

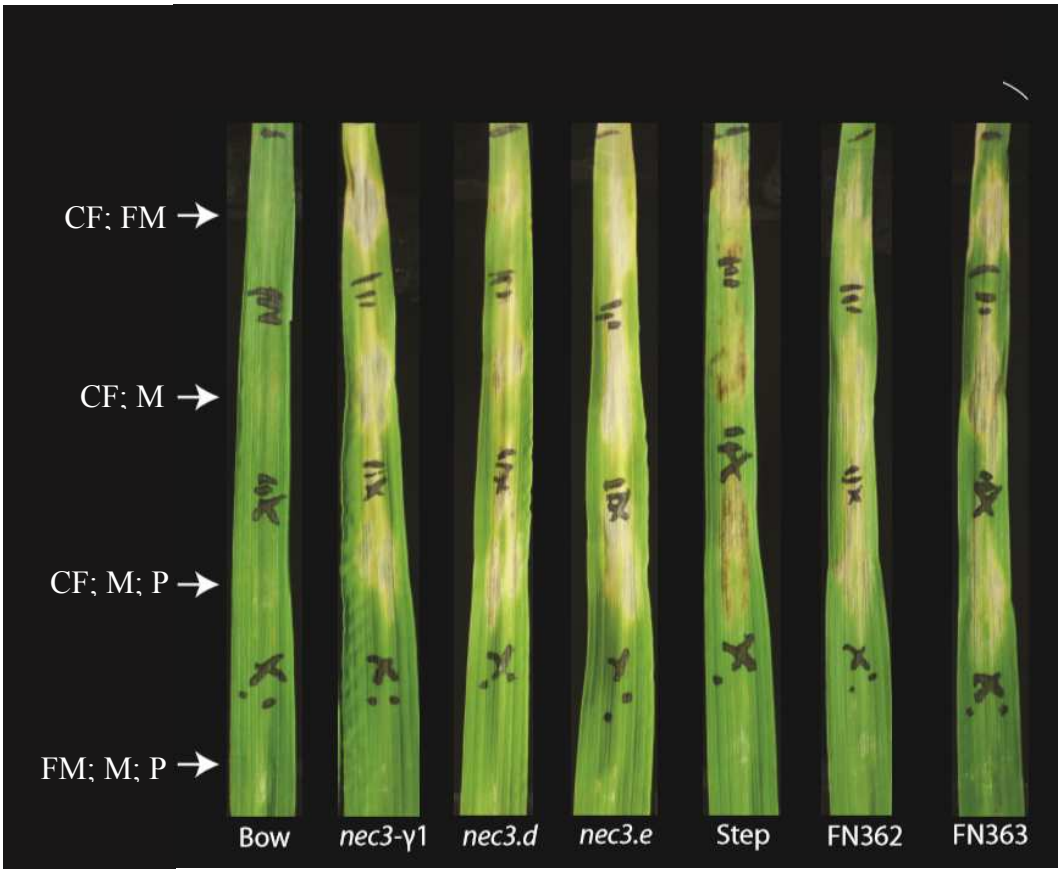

Figure 3.4. Infiltrations of secondary leaves of barley with *Bipolaris sorokiniana* culture filtrates (CF). The treatments were Culture filtrates (CF) with Fries Media (FM); CF with MOPS Buffer (M); CF with M and Pronase (P); and FM with M and P. Infiltrations were performed at the two leaf stage with the third just emerging were rated and documented 4 and 7 days after infiltration.

DAB Staining and Electron Microscopy

As indicative of the runaway PCD phenotype we suspected differential ROS production by the *nec3*_γ1 mutants. We observed *B. sorokiniana* inoculated leaves at 0, 8, 12, 24, and 36 hpi on the resistant wildtype Bowman and the susceptible mutant *nec3*-g1 and found that in the mutant *nec3*-g1, there was early DAB staining associated with most of the *B. sorokiniana* penetration sites as early as 12 hpi. The DAB staining was observed in the resistant wildtype bowman only after 24hpi. The Bowman wildtype has normal *B. sorokiniana* isolate ND85F

growth, however, the *nec3*-g1 mutant had interaction with the pathogen which influenced multiple branching of germ tubes, localized HR, and specific interaction with the cuticle/of the barley leaves at 12 hpi (Fig 3.5). During the later time-points (24-36 hpi) the DAB staining associated with *B. sorokiniana* penetration and colonization in the susceptible *nec3*-g1, rapidly increased in the neighboring host cells, including the underlying mesophyll cells. However, in the resistant wildtype bowman, the DAB staining was not observed until 24 hpi but appeared to have a higher intensity that remained limited to a few cells adjacent to the penetration site and did not expand at the later time-points during the infection process.

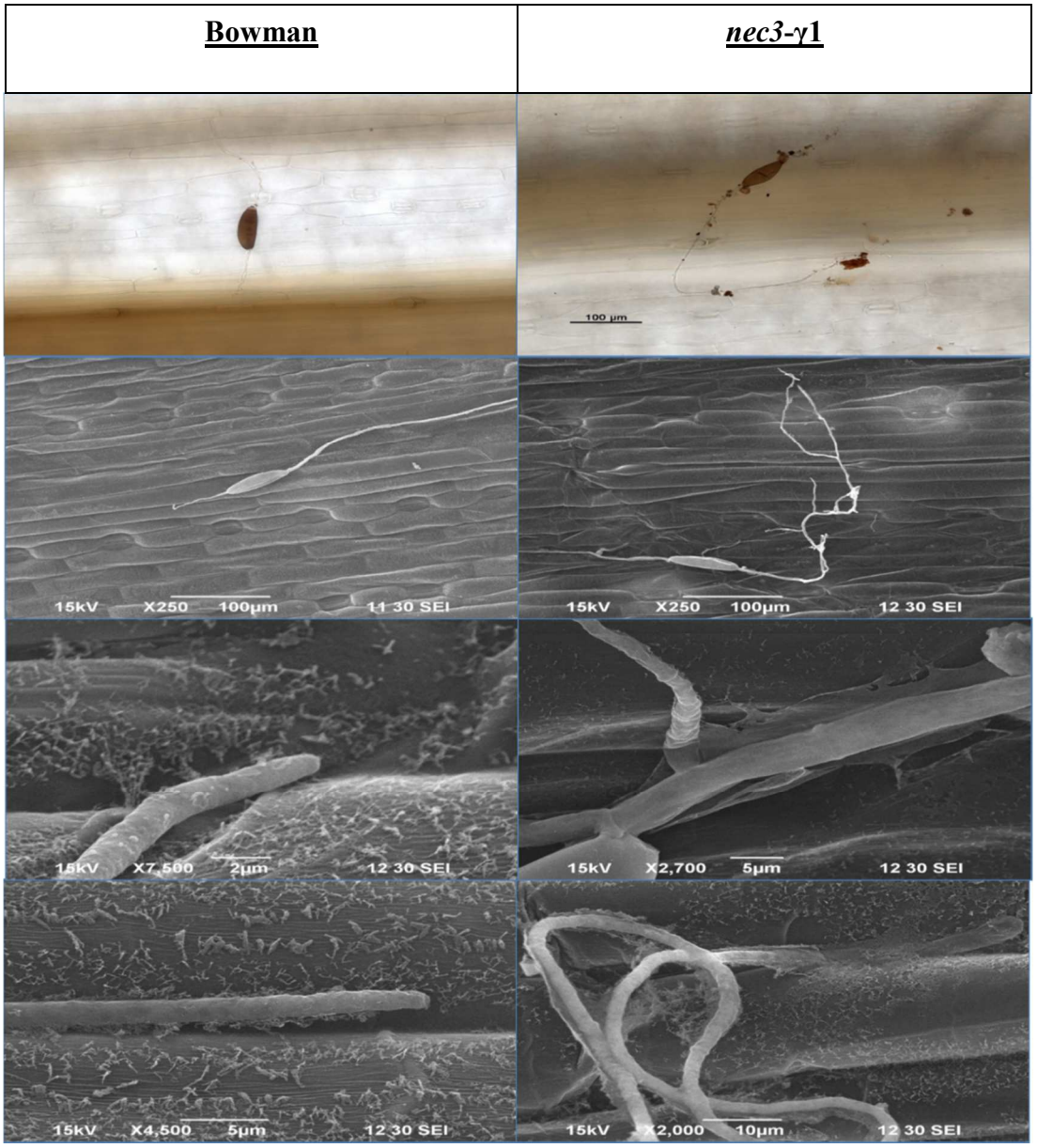

Figure 3.5. Microscopic visualization of the *nec3*-g1 mutant and Bowman wildtype for ROS production and pathogen growth on the leaf surface during infection process. On the left is the Bowman wildtype no HR and normal *Bipolaris sorokiniana* isolate ND85F growth and on the right multiple branching of germ tubes, localized HR, and mutant specific interaction with the cuticle/of the barley leaves at 12 hours post inoculation.

nec3 Map Development

Using homozygous F_2 mutant progeny from the cross between *nec3*_γ1 and Quest, a genetic map was developed. Due to the recessive nature of the genotype/phenotype, a 3:1 wild

type: mutant ratio was expected. Unfortunately, due to a background mutation, out of the 200 plants grown, 54 died as a result of a lethal chlorophyll mutation which also segregated in a recessive 3:1 single gene manner ($\chi^2 = 0.32$). This mutation was not linked to the *nec3* mutation which gave the expected 3:1 ratio after 34 of the 146 surviving plants developed the *nec3* phenotype ($\chi^2=0.17$) indicating a single gene segregating in a recessive manner.

The co-segregating marker for *nec3*, GBM1212, is found at approximately 49.07cM on chromosome 6 with the proximal flanking marker, GBM1423, positioned at 49.22cM according to the cv Morex contig sequences on IPK. GBM1423 was positioned 1.4cM from GBM1212 with the other flanking marker GBM1053 positioned 4.4cM distal of GBM1212 (Fig 3.3). Synteny analysis was difficult in this region as only one of the markers with sequences matching either Arabidopsis or Brachypodium was the proximal non-flanking marker SNP10539, which was similar enough to the Brachypodium contig Bradi3g03270.1. This lack of synteny is likely due to translocations and expansion of the genome following divergence from the common progenitor species (81). The 29 SNP markers were anchored to the barley physical map, which contains the WGS and BAC sequences comprising the MTP of barley cv Morex to identify the *Nec3* physical location. The positions of the 29 markers were in perfect linear ordered with the newly released barley genome sequence and the barley POPSEQ positions. The physical *nec3* region was flanked by SCRI_RS_171247 distally at pseudomolecule position 40.9 Mb and marker SCRI_RS_239962 proximally at 57.8 Mb, delimiting the region to ~ 0.14 cM correlating to a physical region spanning ~ 16.96 Mb containing 143 high confidence annotated genes (Fig 3.6).

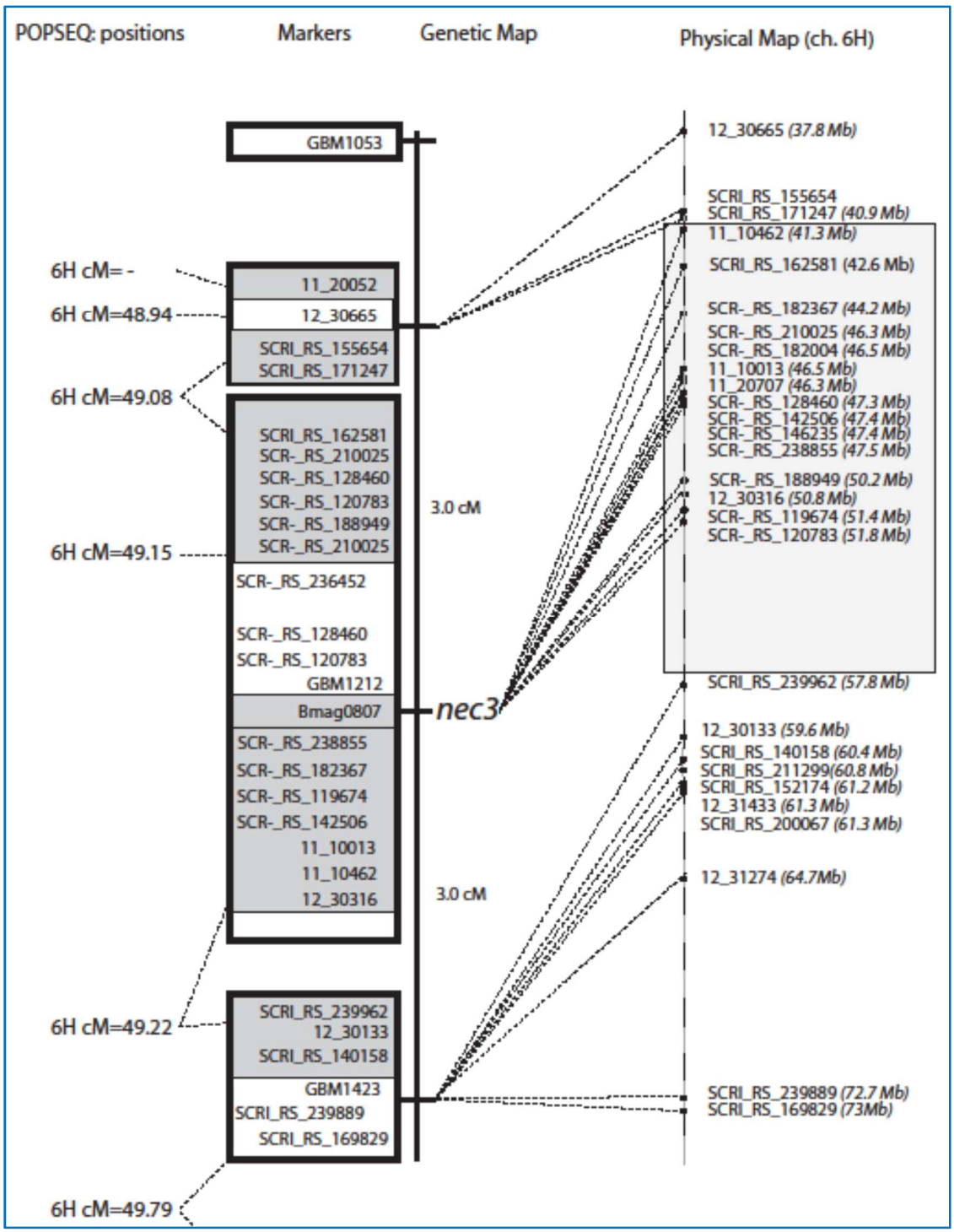

Figure 3.6. Genetic and physical map of the *nec3* region. On the left is the genetic map developed from 33 homozygous mutant F_2 individuals (representing 66 recombinant gametes) from the cross between *nec3*-g1 and Quest. The genetic distance, based on recombination frequency is shown with the boxes indicating cosegregating markers based on the F_2 map and white or gray shading indicating cosegregating markers based on POPSEQ consensus positions, which are given on the far left. The relative physical location of the markers is shown on the right which were derived from the new released whole genome assembly from the IPK database.

Exome Capture for Identification of Candidate Genes

Sequences obtained from the barley exome capture array 120426_Barley_BEC_D04, which has a total capture design size of 88.6 Mb, were analyzed to identify potential deletions within the 143 candidate genes in the *nec3* region. A total of 14 genes from the *nec3* region were not represented in the exome capture probe set, as shown in Supplementary File 14. The rest of the 129 annotated high confidence genes in the *Nec3* region were analyzed in cv Bowman, Steptoe and the allelic mutants *nec3*-g1, FN362 and FN363. No deletions were observed in the exons of the 129 genes common in the three mutants.

RNAseq and Candidate Gene Identification

The RNAseq analysis at 72 hpi identified a total of 3,981 differentially expressed genes **(**DEGs) with greater than a threefold change (2130 upregulated and 1,851 downregulated) in the *nec3*-g1 mutant comparison with non-inoculated (Supp File 15). In the resistant wildtype Bowman, 1,532 DEGs (923 upregulated and 609 downregulated) were identified in comparison to the non-inoculated control (Supp File 15). A comparison of the DEGs during spot blotch disease in the *nec3*-g1 and Bowman is shown as a heat map (Fig 3.7).

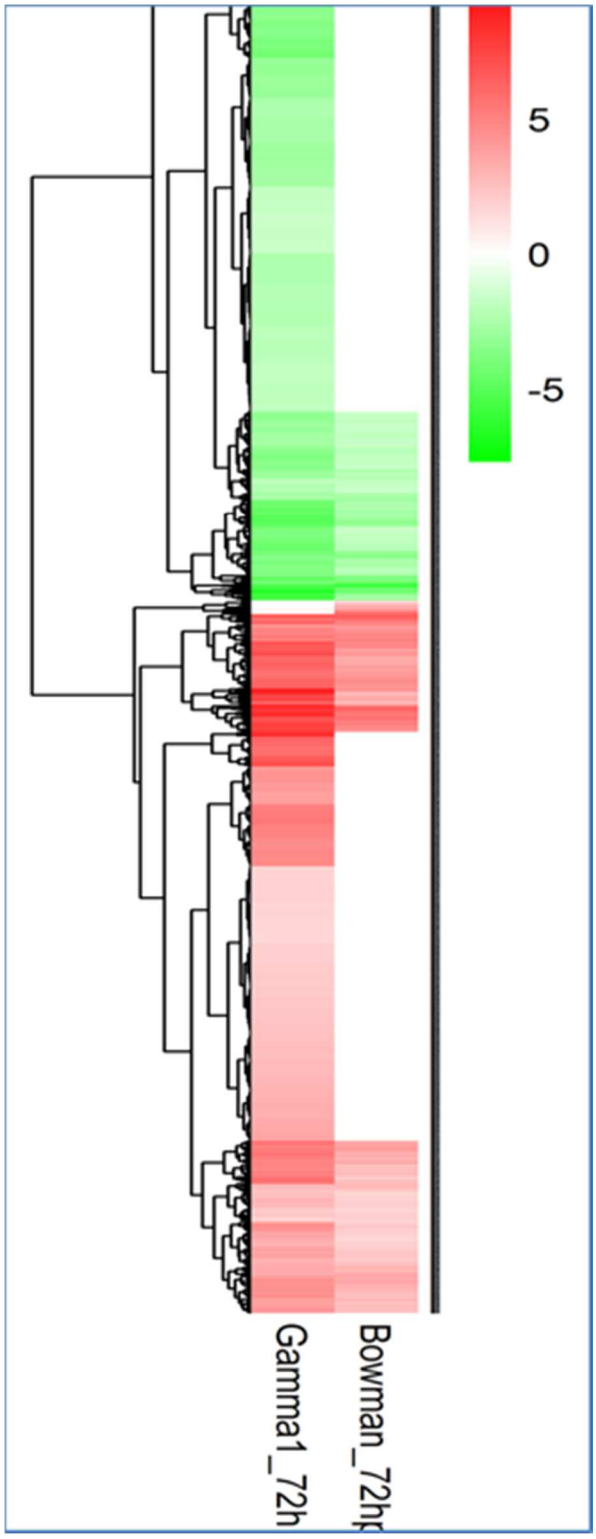

Figure 3.7. Heatmap of the log transformed fold changes of the total differentially expressed genes from RNAseq conducted on the *nec3*-g1 mutant and the wildtype Bowman inoculated with *Bipolaris sorokiniana* isolate ND85F compared with their respective non-inoculated control.

In the *Nec3* region of 16.96 Mb with the 143 High confidence annotated genes, we found two candidate genes HORVU6Hr1G018830 and HORVU6Hr1G020050 that were constitutively expressed in non-inoculated wildtype Bowman and the mutant *nec3*-g1. However, during pathogen infection, HORVU6Hr1G020050 remained constitutively expressed at the same level in wildtype bowman but was downregulated in the mutant *nec3*-g1. The other candidate gene, HORVU6Hr1G018830, was downregulated during pathogen infection three fold and 14 fold in wildtype bowman and *nec3*-g1, respectively (Table 3.1)

Table 3.1. The differentially expressed genes underlying the *nec3* region (~16.96 Mb) identified by the RNAseq conducted on the *nec3*-g1 and wildtype Bowman non-inoculated and inoculated with *Bipolaris sorokiniana* isolate ND85F at 72 hours post-inoculation.

Feature ID	Function	Fold Changes			
		Bowman 0hpi vs nec3-g1 0hpi	**Bowman 72hpi vs Bowman 0hpi**	**nec3-g1 72hpi vs Bowman 72hpi**	**nec3-g1 72hpi vs nec3-g1 0hpi**
HORVU6Hr1G018830	50S ribosomal protein L3	ns	-3.3	-4.4	-14.3
HORVU6Hr1G020050	CRS2-associated factor 2, mitochondrial	ns	ns	-3.7	-5.8

Functional Validation of *CRS2-associated factor 2* Candidate Gene

The *Barley Stripe Mosaic Virus*-virus induced gene silencing (BSMV-VIGS) system was utilized for post-transcriptional gene silencing of the candidate gene *HvCrs2* in the resistant cv Bowman wildtype. The controls inoculated with only empty BSMV constructs and the treatment were inoculated with the candidate gene specific BSMV silencing constructs. The silencing of the candidate gene in the resistant cv Bowman did not alter the spot blotch disease phenotype when compared with the BSMV only control. The seedlings remained resistant across all the 20 replicates of the control BSMV empty virus and the silenced BSMV:*HvCrs2* treatments with

average infection types were not significantly different with a mean disease score of 3 on the 1-9 scale (Fig 3.8).

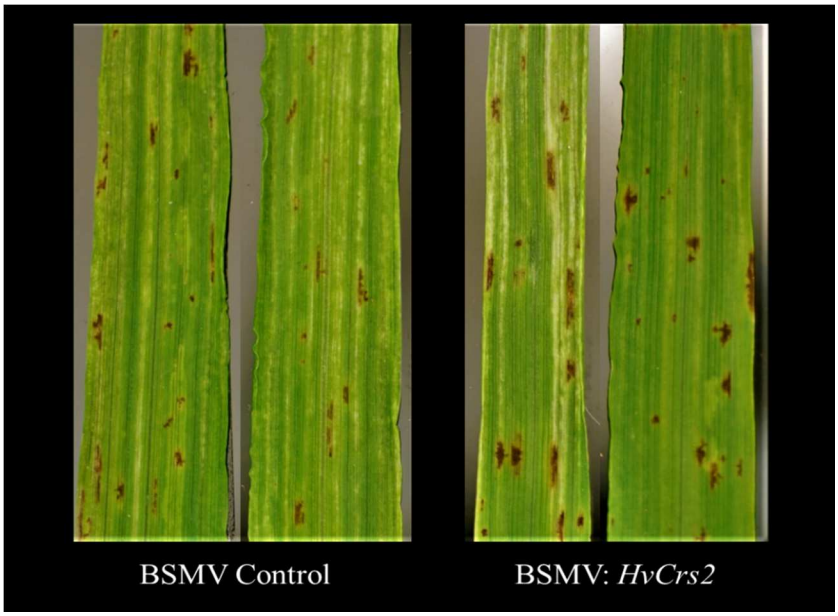

Figure 3.8. Utilization of BSMV-VIGS for the validation of the *HvCrs2*, as *Nec3*. For the functional validation of *HvCrs2* as the negative regulator of PCD, resistant barley cultivar (cv) Bowman was analyzed after BSMV-VIGS-mediated post transcriptional gene silencing of the *HvCrs2* and the empty BSMV-VIGS control (pSL38.1). Pictures show typical reactions for each construct.

The gene expression of *HvCrs2* was analyzed in three biological replicates and normalized by transcripts of *HvSnoR14* for normalized gene expression. The three replicates had 70 to 76 % less transcripts of *HvCrs2* in the silenced plants as compared to the BSMV only controls (Fig 3.9).

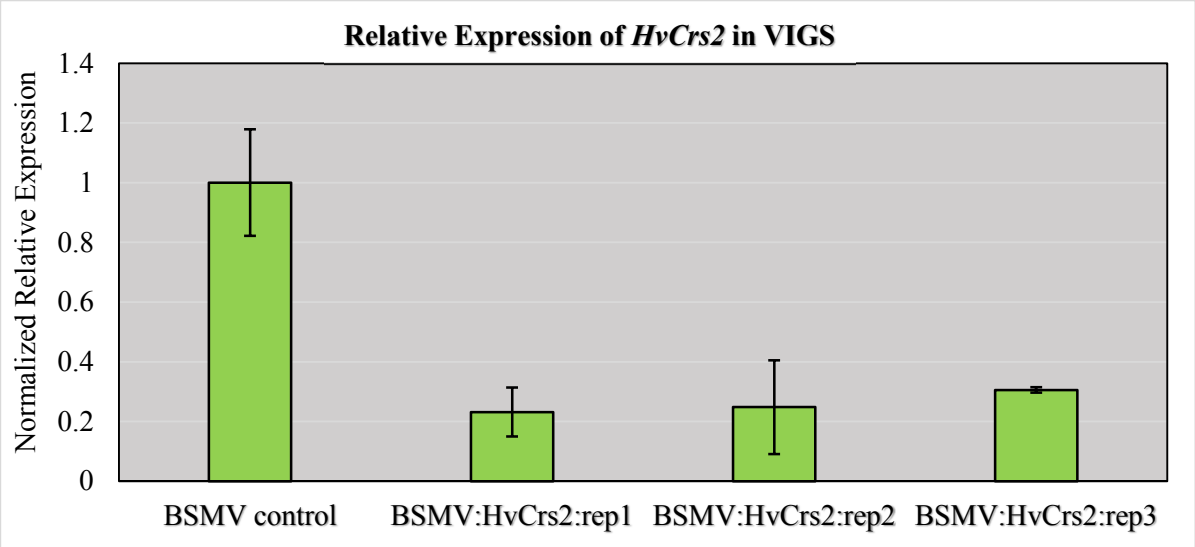

Figure 3.9. Transcript analysis of *HvCrs2* was analyzed at 72 hours post inoculation of *Bipolaris sorokiniana* in the BSMV control and BSMV:*HvCrs2* silenced plants of cultivar Bowman (n=3). The reference gene *HvSnoR14* expression in each sample was used to normalize the transcripts (X-axis). Error bars depict SEM±1(n=3). BSMV-VIGS control was used as control sample for relative expression analysis (Y-axis).

Discussion

The ubiquity of HR in plant defense and its shared features with mammalian apoptosis suggests that it is under highly conserved endogenous control and it is accepted that every plant cell has been preprogrammed to undergo cell death (82). This is necessary in the absence of a circulating and adaptive immune system so the innate immune system of plants enables every cell with the capability to respond to a diversity of pathogens or environmental stimuli to undergo PCD and protect the rest of the plant. Due to the complex nature of distinct genes or crosstalk between pathways involved in developmental and immunity mediated PCD, it has been challenging to delineate these specific mechanisms into different classes and responses (83). We speculate that distinct genes or pathways may negatively regulate the responses once set into motion by different classes of immunity receptors suggesting that PTI and ETI PCD pathways could be distinct at some level but still have overlapping pathways (39,40,84,85). ETI PCD pathways and some PTI pathways may be more loosely regulated as compared to the majority of

PTI responses, thus the levels of ROS and duration of signaling may send the cell down a terminal HR pathway or a less aggressive defense pathway that doesn't lead to PCD. We posit that regardless of the pathway, there is reliance on PCD suppressors (86) because if left unchecked after sequestering the pathogen, there would be a severe effect on the plants fitness. Effective immunity requires a tight regulation on PCD amplitude such that there is successful arrest of the colonizing pathogen by death of the cells that its feeding structures are engaged with, yet is regulated so the terminal cells can be partitioned from healthy cells to maintain photosynthetic capacity and normal plant growth.

Previous work described the *nec3* mutants as a spontaneous induced lesion mimic mutants (52) because the phenotype appears when the mutants were grown in the greenhouse and in the field. However, when the mutant was reportedly grown in the growth chamber for transcriptome analysis, the phenotype was not observed in the seedlings (52). In our search for a mutant of the dominant susceptibility to the *B. sorokiniana* isolate ND90Pr, we identified a mutant, *nec3*_γ1, that showed a phenotype that was consistent with *nec3* phenotype upon induction with the pathogen leading us to speculate that the phenotype is induced upon pathogen challenge. Thus, we report *nec3* as not a lesion mimic mutant but a Pathogen Induced Runaway PCD (PIRP) mutant.

Recent research has shown an overlap in P/DAMP triggered PCD and ETI HR (24) changing the long held belief that there is a distinction between PTI and ETI PCD responses. However, here we pose that there may be a distinction in the proteins that suppress these possibly different amplitude PCD responses. The PCD pathways in plants are relatively unknown, but those observed in the *nec3* mutants after challenge by different pathogens trigger an early response PCD. Pathogen challenge may provide a PCD suppressor specific to early low

amplitude PCD responses to begin probing the plants ability to suppress these responses once elicited by the immunity receptors. Maybe *Nec3* could be used as a biological probe that differentiates low amplitude PCD reactions to a minor threat being the non-host pathogens at the door step compared to the higher amplitude PCD unleashed against a major threat posed by a specialist pathogen that has infiltrated the plants initial defense responses and is set up to colonize the host.

With emerging technologies, the genetic and functional analysis of disease resistance/susceptibility mechanisms in plants are being elucidated at a much accelerated pace. However, a major knowledge gap still exists concerning the elicitation and mechanisms involved in PCD pathways that lead to resistance against biotrophic pathogens and susceptibility to the necrotrophs. It is important to further our understanding of PCD pathways and how they play a role in the outcome of plant immune responses. This knowledge could be used to protect a wide variety of crops from a wide range of pathogens making these pathways all the more important to understand.

The *nec3*_γ1 mutant described here was originally identified from this g-irradiated M_2 seed in an attempt to identify barley mutants resistant to *B. sorokiniana* isolate ND90Pr (Spot Blotch). From the limited pathogens tested, the necrotrophic ascomycete fungal pathogens *B. sorokiniana*, *P. teres* f. *teres*, and *P. teres* f. *maculata*, as well as the biotrophic ascomycete *Blumeria graminis* elicited the *nec3* phenotype. The phenotype was also induced by the bacterial pathogen *X. translucens* pv *undulosa*. These fungal pathogens are known to initiate colonization through direct penetration of the host cell wall and plasma membrane and this bacterial pathogen utilizes the type three secretion system to deliver virulence effectors directly through the host cell wall and plasma membrane. The phenotype was not elicited by either virulent or avirulent races

of the basidiomycete biotrophic pathogen *P. graminis* f. sp. *tritici,* whose strategy is to invade the host "incognito" without eliciting immunity responses and colonizes the host via entering host through natural openings, the stomata. The Bowman background contains the stem rust resistance gene *Rpg1* which is known to elicit a higher amplitude race specific effector triggered immunity response yet did not elicit the *nec3* runaway PCD phenotype. These data led to the hypothesis that pathogens inducing cellular damage may be detected by Damage Associated Molecular Pattern (DAMP) cell surface receptors that possibly activate an early DAMP triggered immunity-like PCD response that is negatively regulated by the wildtype *Nec3* gene. Alternatively, these pathogens possibly carry different pathogen associated molecular patterns (PAMPs) that activate PAMP triggered immunity (PTI) PCD responses that are suppressed by *Nec3*. The NEC3 protein or regulatory molecule is hypothesized to be involved in the negative regulation of a distinct signaling pathway that leads to PCD. The functional NEC3 protein is possibly involved in the early, tightly regulated PTI elicited PCD, but may not play a role in the regulation of the higher amplitude PCD known as the hypersensitive response as the result of ETI. A runaway PCD response occurs following infection from various ascomycete pathogens including *B. sorokiniana, P. teres* f. *teres, P teres* f. *maculata* and *B. graminis,* as well as the bacterial pathogen *X. translucens,* which infect the host cells directly and cause cellular damage that may elicit an early DAMP or PAMP triggered immunity response. Interestingly, both compatible and incompatible Basidiomycete pathogens of *P. graminis* did not elicit the runaway PCD phenotype. This could be due to the entry of pathogen through stomata, without damaging cell wall and remain concealed from the plant defenses until it establishes itself in the host cells by forming haustoria. The latest literature has reported that barley host defends stem rust pathogen by non-HR based resistance and thus supports our hypothesis that NEC3 is involved in

the cell-wall disruption-initiated HR based PCD. Because culture filtrates elicit the runaway necrotic response, it can be said that the mutant variety does not have increased susceptibility to the pathogen, rather the infiltrations elicit cell-wall damage and plant defense initiates uncontrolled PCD providing additional nutrients to the pathogen leaving the host more susceptible to infection.

The *nec3* mutants of barley show a distinct phenotype consisting of large cream to orange necrotic lesions, lacking the dark pigmentation indicative of the accumulation of phenolic compounds and were originally described as spontaneous lesion mimic mutants (LMMs). Originally the *nec3* mutants were classified as LMMs (51), but this research has provided evidence that the *nec3* phenotype is elicited by a diverse taxonomy of pathogens, possibly through the elicitor recognition during disruption of cell-wall for entry into the host. The LMMs share many characteristics with the *nec3* mutants (38,44) however due to the lack of phenotype in the absence of pathogen challenge we propose the *nec3* mutants are not LMMs, but rather Pathogen Induced Runaway PCD (PIRP) mutants. It is likely *nec3* and LMMs share similar pathways, however, we hypothesize that a broad range of pathogens with a necrotrophic lifestyle making entry into host via directly penetrating the cell-wall elicit an early PCD pathway that is inhibited or controlled by the *nec3* gene or pathway. Thus, the *nec3* mutants result in a runaway PCD phenotype at the point of pathogen challenge or following infiltrations using certain culture filtrates.

The pathogens tested to date which induce the *nec3* phenotype, *B. sorokiniana*, *P. teres*, and *B. graminis* cause damage to cell, usually in the form of appresoria and a penetration peg that punctures the cell wall and plasma membrane in order to initiate infection (87–89). These structures are also accompanied by a variety of other proteins and signaling molecules used to

cause infection that could be the *nec3* inducer. This highly disruptive form of infection sets off many immune response alarms in the cell known as PTI or DTI resulting in a signaling cascade. The PTI/DTI signaling responses activate transcription factors that induce a succinct and tightly regulated PCD response that is limited to the infected cell and a few surround cells at the point of pathogen introgression. This signaling cascade induces the production of PR proteins which rapidly arrest pathogen infection processes and induces systemic acquired resistance (SAR) (90).The *Xanthamonas translucens*, the bacteria that induces the *nec3* phenotype, also causes damage through the use of the type three secretion system which punctures the host cell and introduces effectors into the mesophyll of the plant cell. These bacteria enter the plant through stomatal openings or damaged cells. During colony increase an extracellular polysaccharide (EPS) exudate is released to facilitate communication between bacteria and increase chances of a successful infection. The EPS also transports enzymes and other such molecules that increase the permeability of the cell wall. This leakiness allows nutrients to be acquired by the bacteria and increase in population.

However even though a pathogen is able to cause infection on barley it does not mean it will lead to the nec3 phenotype as seen following infection from compatible and incompatible *P. graminis* rust races QCCJ and MCCF respectively. The infection phenotype was the same for gamma1/nec3 plants and *Rpg1* containing Bowman wild type. Histology data with several races on Rpg1 containing barley lines similar to Bowman show no post haustorial HR response suggesting that the mode of entry of the pathogen through damaging cell-wall is critical to induce the *nec3* phenotype. We demonstrated that the *nec3*-g1 mutant was producing ROS when infected by a necrotrophic pathogen *B. sorokiniana* as early as 12 hpi as compared to the resistant bowman wildtype showing ROS at 24hpi. The ROS production in the *nec3*-g1 mutant

was also accompanied by an abnormal interaction of the pathogen infection hyphae with the host cuticle, making it to branch profusely and possible cuticle residues along the germ tubes. The increased transcripts of cell wall related genes were also reported in the transcriptomic study of the nec3 mutant FN362 and FN363 by Keisa, 2010.

Because of the rapid *nec3* phenotypic response upon infection it was hypothesized the *nec3* gene is constitutively expressed. RNAseq was performed to test this hypothesis on plant tissue not exposed to a pathogen and compared with the plant leaves infected with the pathogen. The results identified two candidate genes, Ribosomal protein L3 and mitochondrial CRS2 associated factor 2, underlying the delimited *Nec3* region which were consecutively expressed and were downregulated upon pathogen infection in *nec3*-g1 mutant. The ribosomal protein L3 binds directly near the 3' end of the 23S rRNA, where it nucleates assembly of the 50S subunit of the ribosomes (91). Silencing of ribosomal protein L3 homolog in *Nicotiana tabacum* strongly altered the physiology of the plant and had severe reduced plant height, flower and leaves (92), however the *nec3*-g1 doesn't produce any phenotype alterations.

The mitochondrial CRS2- associated factor 2 (CAF2) is a nuclear encoded protein which directly interacts with plant organelle RNA recognition protein What's This Factor (WTF1) (93). The WTF interacts with the HSP60s in the mitochondria (94). The HSP60s are molecular chaperons that assist in protein folding and disruption in WTF or HSP60 results in absence of cytochrome oxidase (94). Important events in PCD orchestrated by the mitochondria involves release of cytochrome c into the cytosol, which drives the assembly of the apoptosome and activates caspases (95). The absence of cytochrome oxidases would incur no release of cytochrome c and thus would negatively regulate PCD (96). Thus, making the CAF2 as the best candidate gene underlying the *Nec3* region.

We used BSMV induced gene silencing of CAF2 in the bowman wildtype and achieved about 76 percent silencing of the target. However, the *nec3* phenotype was not produced, which does not support our hypothesis. This leads us to think, either the gene was not transcriptionally reduced enough to produce the nec3 phenotype or it is not the *Nec3* gene at all. Looking back to our exome capture analysis underlying the *Nec3* region, we did find 14 annotated high confidence genes missing in the exome capture probe. However, none of the 14 genes were differentially expressed at the non-inoculated and 72 hpi in both wildtype Bowman and *nec3*-g1 mutant. So, either the missing gene in not annotated or is expressed at very low level in the Bowman wiltype.

Based on the data gathered during the experiment, a new working hypothesis has been developed that will lead to the identification of the *Nec3* gene. Following infection from a pathogen that produces DAMPs or PAMPs due to cellular disruption, the PTI pathways are induced resulting in the tightly regulated PCD observed to rapidly stop the pathogen at the point of infection. But due to the uncontrolled PCD in the *nec3* mutants, we hypothesize the *nec3* gene is a negative regulator within this pathway. The lack of this protein or transcription factor leads to unhindered PCD and eventual death of the entire leaf originally infected. It could be that the *nec3* gene is a conserved, non-specific gene downstream of pathogen recognition as the phenotype is observed following infection from a variety of pathogens. All biological pathways and systems need to be kept in check in order to maintain proper cellular and organismal health (97). The lack of control of PCD in the *nec3* mutant appears to lead to 10-50% seed loss demonstrating the importance of control points within cellular pathways. This seed loss also indicates the use of *Nec3* is not limited to leaf tissue but is utilized during production of

reproductive structures. The *nec3* roots were not tested in this study but it would be interesting to see how root rot caused by *B. sorokiniana* would affect the roots.

Because we saw the *nec3* phenotype following infiltrations the hypothesis seems to agree that the *nec3* gene is involved in DAMP recognition and response. DAMPs include cell wall components, eATP, eDNA and other endogenous molecules disrupted during the infection process. This particular recognition of disrupted self is seen across all multicellular life including algae, fungi, fish, insects, mammals and plants (98). Since we are not privy to the proteins and other molecules produced and released during fungal growth and reproduction in Fries Media it is unclear what is eliciting the PCD pathway, however data from this study has demonstrated the elicitor is not proteinaceous and are not affected by Pronase treatments. Because of this the *nec3* elicitor may be a secondary metabolite, a non-proteinacious toxin or a tightly folded small protein produced by the pathogen that may lead to DAMP release and eventual recognition by the plant leading to unhindered PCD.

These data provide evidence that the *Nec3* gene could also play a role as a virulence target of necrotrophic effectors. This is clearly demonstrated by the fact that PCD, especially uncontrolled, would benefit the pathogen greatly as it provides a quicker supply of nutrients with less energy output by the pathogen to acquire it. The *Nec3* gene and pathway could also prove to be a valuable gene to study when differentiating between PTI and ETI elicited pathways. The main goal of this research was to clone the *Nec3* gene, however a finer map needs to be developed in order to fully take advantage of data gathered from the RNAseq induction assay following infection by *B. sorokiniana*. Further characterization of the mutant gene should include screening with a wider range of pathogens across Kingdom and Phyla with varying lifestyles as well as screening the roots for various pathogens and other P/DAMPs.

Here we show that the *nec3* phenotype is not a spontaneous LMM response but is rather induced by several species of *Ascomycete* pathogenic fungi, both necrotrophs and a biotroph, and the bacterial pathogen *X. translucens.* All these *nec3* inducing pathogens enter the cell or secrete elicitors by direct penetration through the cell wall and plasma membrane. However, the *nec3* phenotype was not induced by either virulent or avirulent races of the biotrophic Basidiomycete pathogen, *Puccinia graminis* f. sp. *tritici,* which enters the plant through the stomata. *P. graminis* f. sp. *tritici* pathogens attempt to enter and colonize the host "incognito" without alerting the host to their presence and the races that carry avirulence proteins are known to elicit a non-HR based resistance in host plants that carry the cognate *R*-genes. The ROS is elicited in *nec3*-g1 mutant as early as 12 hpi by the pathogen, which was observed later at 24 hpi in cv bowman, the background cultivar of the *nec3* mutant. Thus, we hypothesize that the pathogens inducing the *Nec3* regulated PCD responses may be eliciting a DAMP associated PCD immunity pathway and that the *Nec3* gene plays a role in the tight regulation of this lower amplitude PCD immunity response. Thus, the *nec3* mutants are unable to regulate this class of PCD, which results in expanding necrotic lesions that are elicited by pathogens that induce these early DAMP induced PCD pathways.

Literature Cited

1. Van Hautegem T, Waters AJ, Goodrich J, Nowack MK. Only in dying, life: programmed cell death during plant development. Trends Plant Sci. 2015 Feb;20(2):102–113.
2. Lo Presti L, Lanver D, Schweizer G, Tanaka S, Liang L, Tollot M, et al. Fungal effectors and plant susceptibility. Annu Rev Plant Biol. 2015;66:513–545.
3. Dodds PN, Lawrence GJ, Catanzariti A-M, Teh T, Wang C-IA, Ayliffe MA, et al. Direct protein interaction underlies gene-for-gene specificity and coevolution of the flax

resistance genes and flax rust avirulence genes. Proc Natl Acad Sci USA. 2006 Jun 6;103(23):8888–8893.

4. Jia Y, McAdams SA, Bryan GT, Hershey HP, Valent B. Direct interaction of resistance gene and avirulence gene products confers rice blast resistance. EMBO J. 2000 Aug 1;19(15):4004–4014.
5. Deslandes L, Olivier J, Peeters N, Feng DX, Khounlotham M, Boucher C, et al. Physical interaction between RRS1-R, a protein conferring resistance to bacterial wilt, and PopP2, a type III effector targeted to the plant nucleus. Proc Natl Acad Sci USA. 2003 Jun 24;100(13):8024–8029.
6. Krasileva KV, Dahlbeck D, Staskawicz BJ. Activation of an Arabidopsis resistance protein is specified by the in planta association of its leucine-rich repeat domain with the cognate oomycete effector. Plant Cell. 2010 Jul 2;22(7):2444–2458.
7. van der Biezen EA, Jones JD. The NB-ARC domain: a novel signalling motif shared by plant resistance gene products and regulators of cell death in animals. Curr Biol. 1998 Mar 26;8(7):R226–7.
8. Zipfel C. Pattern-recognition receptors in plant innate immunity. Curr Opin Immunol. 2008 Feb;20(1):10–16.
9. Monaghan J, Zipfel C. Plant pattern recognition receptor complexes at the plasma membrane. Curr Opin Plant Biol. 2012 Aug;15(4):349–357.
10. Macho AP, Zipfel C. Plant PRRs and the activation of innate immune signaling. Mol Cell. 2014 Apr 24;54(2):263–272.

11. Kunze G, Zipfel C, Robatzek S, Niehaus K, Boller T, Felix G. The N terminus of bacterial elongation factor Tu elicits innate immunity in *Arabidopsis* plants. Plant Cell. 2004 Dec;16(12):3496–3507.

12. Silipo A, Molinaro A, Sturiale L, Dow JM, Erbs G, Lanzetta R, et al. The elicitation of plant innate immunity by lipooligosaccharide of Xanthomonas campestris. J Biol Chem. 2005 Sep 30;280(39):33660–33668.

13. Felix G, Duran JD, Volko S, Boller T. Plants have a sensitive perception system for the most conserved domain of bacterial flagellin. Plant J. 1999 May;18(3):265–276.

14. Kaku H, Nishizawa Y, Ishii-Minami N, Akimoto-Tomiyama C, Dohmae N, Takio K, et al. Plant cells recognize chitin fragments for defense signaling through a plasma membrane receptor. Proc Natl Acad Sci USA. 2006 Jul 18;103(29):11086–11091.

15. Klarzynski O, Plesse B, Joubert J, Yvin J, Kopp M, Kloareg B, et al. Linear ß-1,3 glucans are elicitors of defense responses in tobacco. Plant Physiol. 2000 Nov 1;124(3):1027–1038.

16. Laquitaine L, Gomès E, François J, Marchive C, Pascal S, Hamdi S, et al. Molecular basis of ergosterol-induced protection of grape against botrytis cinerea: induction of type I LTP promoter activity, WRKY, and stilbene synthase gene expression. Mol Plant Microbe Interact. 2006 Oct;19(10):1103–1112.

17. Ferrari S, Savatin DV, Sicilia F, Gramegna G, Cervone F, Lorenzo GD. Oligogalacturonides: plant damage-associated molecular patterns and regulators of growth and development. Front Plant Sci. 2013 Mar 13;4:49.

18. Hauck P, Thilmony R, He SY. A Pseudomonas syringae type III effector suppresses cell wall-based extracellular defense in susceptible Arabidopsis plants. Proc Natl Acad Sci USA. 2003 Jul 8;100(14):8577–8582.

19. Jones JDG, Dangl JL. The plant immune system. Nature. 2006 Nov 16;444(7117):323–329.

20. Glazebrook J. Contrasting mechanisms of defense against biotrophic and necrotrophic pathogens. Annu Rev Phytopathol. 2005;43:205–227.

21. Shi G, Zhang Z, Friesen TL, Raats D, Fahima T, Brueggeman RS, et al. The hijacking of a receptor kinase-driven pathway by a wheat fungal pathogen leads to disease. Sci Adv. 2016 Oct 26;2(10):e1600822.

22. Liu Z, Holmes DJ, Faris JD, Chao S, Brueggeman RS, Edwards MC, et al. Necrotrophic effector-triggered susceptibility (NETS) underlies the barley-Pyrenophora teres f. teres interaction specific to chromosome 6H. Mol Plant Pathol. 2015 Feb;16(2):188–200.

23. Tsuda K, Katagiri F. Comparing signaling mechanisms engaged in pattern-triggered and effector-triggered immunity. Curr Opin Plant Biol. 2010 Aug;13(4):459–465.

24. Thomma BPHJ, Nürnberger T, Joosten MHAJ. Of PAMPs and effectors: the blurred PTI-ETI dichotomy. Plant Cell. 2011 Jan;23(1):4–15.

25. Baker CJ, Orlandi EW, Mock NM. Harpin, An Elicitor of the Hypersensitive Response in Tobacco Caused by Erwinia amylovora, Elicits Active Oxygen Production in Suspension Cells. Plant Physiol. 1993 Aug;102(4):1341–1344.

26. Torres MA. ROS in biotic interactions. Physiol Plant. 2010 Apr;138(4):414–429.

27. Zurbriggen MD, Carrillo N, Hajirezaei M-R. ROS signaling in the hypersensitive response: when, where and what for? Plant Signal Behav. 2010 Apr 26;5(4):393–396.

28. Mur LAJ, Laarhoven LJJ, Harren FJM, Hall MA, Smith AR. Nitric oxide interacts with salicylate to regulate biphasic ethylene production during the hypersensitive response. Plant Physiol. 2008 Nov;148(3):1537–1546.

29. Ron M, Avni A. The receptor for the fungal elicitor ethylene-inducing xylanase is a member of a resistance-like gene family in tomato. Plant Cell. 2004 Jun;16(6):1604–1615.

30. Couto D, Zipfel C. Regulation of pattern recognition receptor signalling in plants. Nat Rev Immunol. 2016 Aug 1;16(9):537–552.

31. Bigeard J, Colcombet J, Hirt H. Signaling mechanisms in pattern-triggered immunity (PTI). Mol Plant. 2015 Apr;8(4):521–539.

32. Tsuda K, Mine A, Bethke G, Igarashi D, Botanga CJ, Tsuda Y, et al. Dual regulation of gene expression mediated by extended MAPK activation and salicylic acid contributes to robust innate immunity in Arabidopsis thaliana. PLoS Genet. 2013 Dec 12;9(12):e1004015.

33. Ranf S, Eschen-Lippold L, Pecher P, Lee J, Scheel D. Interplay between calcium signalling and early signalling elements during defence responses to microbe- or damage-associated molecular patterns. Plant J. 2011 Oct;68(1):100–113.

34. Chong J, Baltz R, Schmitt C, Beffa R, Fritig B, Saindrenan P. Downregulation of a pathogen-responsive tobacco UDP-Glc:phenylpropanoid glucosyltransferase reduces scopoletin glucoside accumulation, enhances oxidative stress, and weakens virus resistance. Plant Cell. 2002 May;14(5):1093–1107.

35. Voigt CA. Callose-mediated resistance to pathogenic intruders in plant defense-related papillae. Front Plant Sci. 2014 Apr 28;5:168.

36. Stadler LJ. Mutations in barley induced by x-rays and radium. Science. 1928 Aug 24;68(1756):186–187.

37. Penmetsa RV, Cook DR. Production and characterization of diverse developmental mutants of Medicago truncatula. Plant Physiol. 2000 Aug;123(4):1387–1398.

38. Lorrain S, Vailleau F, Balagué C, Roby D. Lesion mimic mutants: keys for deciphering cell death and defense pathways in plants? Trends Plant Sci. 2003 Jun;8(6):263–271.

39. Druka A, Franckowiak J, Lundqvist U, Bonar N, Alexander J, Houston K, et al. Genetic dissection of barley morphology and development. Plant Physiol. 2011 Feb;155(2):617–627.

40. Greenberg JT, Ausubel FM. Arabidopsis mutants compromised for the control of cellular damage during pathogenesis and aging. Plant J. 1993 Aug;4(2):327–341.

41. Rostoks N, Schmierer D, Kudrna D, Kleinhofs A. Barley putative hypersensitive induced reaction genes: genetic mapping, sequence analyses and differential expression in disease lesion mimic mutants. Theor Appl Genet. 2003 Oct;107(6):1094–1101.

42. Rostoks N, Schmierer D, Mudie S, Drader T, Brueggeman R, Caldwell DG, et al. Barley necrotic locus nec1 encodes the cyclic nucleotide-gated ion channel 4 homologous to the Arabidopsis HLM1. Mol Genet Genomics. 2006 Feb;275(2):159–168.

43. Lundqvist U, Franckowiak JD, Konishi T. New and revised descriptions of barley genes. Barley genetics newsletter. 1997;

44. Balagué C, Lin B, Alcon C, Flottes G, Malmström S, Köhler C, et al. HLM1, an essential signaling component in the hypersensitive response, is a member of the cyclic nucleotide-gated channel ion channel family. Plant Cell. 2003 Feb;15(2):365–379.

45. Stintzi A, Heitz T, Prasad V, Wiedemann-Merdinoglu S, Kauffmann S, Geoffroy P, et al. Plant “pathogenesis-related” proteins and their role in defense against pathogens. Biochimie. 1993;75(8):687–706.

46. Lyngkjær MF, Carver TL. Conditioning of cellular defence responses to powdery mildew in cereal leaves by prior attack. Mol Plant Pathol. 2000 Jan 1;1(1):41–49.

47. Kjaer B, Jensen HP, Jensen J, Jorgensen JH. Associations between three ml-o powdery mildew resistance genes and agronomic traits in barley. Euphytica. 1990 Apr;46(3):185–193.

48. Wolter M, Hollricher K, Salamini F, Schulze-Lefert P. The mlo resistance alleles to powdery mildew infection in barley trigger a developmentally controlled defence mimic phenotype. Mol Gen Genet. 1993 May;239(1-2):122–128.

49. Fischbeck G, Hauser H. Cytogenetic studies of some induced barley mutants. Barley Genetics Newsletter. 1978. p. 36–37.

50. Falk DE, Swartz MJ, Kasha KJ. Linkage data with genes near the centromere of barley chromosome 6. Barley Genetics Newsletter. 1980;

51. Fischbeck G, Hauser H. Research Notes. Barley Genetic Newsletter. (2) ed. 1976.

52. Keisa A, Brueggeman R, Drader T, Kleinhofs A, Rostoks N. Transcriptome analysis of the barley nec3 mutant reveals a potential link with abiotic stress response related signaling pathways. Environ Exp Bot. 2010;8:1–16.

53. Fetch TG, Steffenson BJ. Rating Scales for Assessing Infection Responses of Barley Infected with*Cochliobolus sativus*. Plant Dis. 1999 Mar;83(3):213–217.

54. Zhong S, Steffenson BJ. Identification and characterization of DNA markers associated with a locus conferring virulence on barley in the plant pathogenic fungus Cochliobolus sativus. Theor Appl Genet. 2002 May;104(6-7):1049–1054.

55. Shjerve RA, Faris JD, Brueggeman RS, Yan C, Zhu Y, Koladia V, et al. Evaluation of a Pyrenophora teres f. teres mapping population reveals multiple independent interactions with a region of barley chromosome 6H. Fungal Genet Biol. 2014 Sep;70:104–112.

56. Neupane A, Tamang P, Brueggeman RS, Friesen TL. Evaluation of a barley core collection for spot form net blotch reaction reveals distinct genotype-specific pathogen virulence and host susceptibility. Phytopathology. 2015 Apr;105(4):509–517.

57. Lamari L, Bernier CC. Virulence of isolates of *Pyrenophora tritici-repentis* on 11 wheat cultivars and cytology of the differential host reactions. Canadian Journal of Plant Pathology. 1989 Sep;11(3):284–290.

58. Friesen TL, Faris JD. Molecular mapping of resistance to Pyrenophora tritici-repentis race 5 and sensitivity to Ptr ToxB in wheat. Theor Appl Genet. 2004 Aug;109(3):464–471.

59. Einbeck KS. Cercospora. Kleinwanzlebener Saatzucht Ag Einbeck Rabbethge and Geisecke. 1970;

60. Steffenson BJ, Jin Y, Brueggeman RS, Kleinhofs A, Sun Y. Resistance to stem rust race TTKSK maps to the rpg4/Rpg5 complex of chromosome 5H of barley. Phytopathology. 2009 Oct;99(10):1135–1141.

61. Stackman EC, Stewart DM, Loegering WQ. Identification of physiologic races of Puccinia graminis var. tritici. USDA. Agricultural Research Service E. 1962;617.

62. Duveiller E. The Bacterial Diseases of Wheat: Concepts and Methods of Disease Management. Duveiller E, editor. CIMMYT; 1997.

63. Adhikari TB, Gurung S, Hansen JM, Jackson EW, Bonman JM. Association mapping of quantitative trait loci in spring wheat landraces conferring resistance to bacterial leaf streak and spot blotch. The Plant Genome Journal. 2012;5(1):1.

64. Liu ZH, Friesen TL, Rasmussen JB, Ali S, Meinhardt SW, Faris JD. Quantitative Trait Loci Analysis and Mapping of Seedling Resistance to Stagonospora nodorum Leaf Blotch in Wheat. Phytopathology. 2004 Oct;94(10):1061–1067.

65. Solanki S. Dissecting the Mystery behind Rpg5 Mediated Puccinia graminis Resistance in Barley Using Genetics, Molecular and Bioinformatics Approaches. 2017;

66. Smith KP, Budde A, Dill-Macky R, Rasmusson DC, Schiefelbein E, Steffenson B, et al. Registration of "Quest" Spring Malting Barley with Improved Resistance to Fusarium Head Blight. J Plant Regist. 2013;7(2):125.

67. GrainGenes | A Database for Triticeae and Avena [Internet]. [cited 2019 Jun 27]. Available from: https://wheat.pw.usda.gov/GG3/

68. T3/Barley [Internet]. [cited 2019 Jun 27]. Available from: https://triticeaetoolbox.org/barley/

69. Richards J, Chao S, Friesen T, Brueggeman R. Fine mapping of the barley chromosome 6H net form net blotch susceptibility locus. G3 (Bethesda). 2016 Jul 7;6(7):1809–1818.

70. IPK Barley BLAST Server Home Page [Internet]. [cited 2019 Jun 27]. Available from: https://webblast.ipk-gatersleben.de/barley_ibsc/

71. Solanki S, Richards J, Ameen G, Wang X, Khan A, Ali H, et al. Characterization of genes required for both Rpg1 and rpg4-mediated wheat stem rust resistance in barley. BMC Genomics. 2019 Jun 14;20(1):495.

72. Brown J, Pirrung M, McCue LA. FQC Dashboard: integrates FastQC results into a web-based, interactive, and extensible FASTQ quality control tool. Bioinformatics. 2017 Jun 9;

73. International Barley Genome Sequencing Consortium, Mayer KFX, Waugh R, Brown JWS, Schulman A, Langridge P, et al. A physical, genetic and functional sequence assembly of the barley genome. Nature. 2012 Nov 29;491(7426):711–716.

74. Li H, Durbin R. Fast and accurate long-read alignment with Burrows-Wheeler transform. Bioinformatics. 2010 Mar 1;26(5):589–595.

75. Li H, Handsaker B, Wysoker A, Fennell T, Ruan J, Homer N, et al. The Sequence Alignment/Map format and SAMtools. Bioinformatics. 2009 Aug 15;25(16):2078–2079.

76. Danecek P, Auton A, Abecasis G, Albers CA, Banks E, DePristo MA, et al. The variant call format and VCFtools. Bioinformatics. 2011 Aug 1;27(15):2156–2158.

77. Quinlan AR, Hall IM. BEDTools: a flexible suite of utilities for comparing genomic features. Bioinformatics. 2010 Mar 15;26(6):841–842.

78. Andrews S. FastQC: a quality control tool for high throughput sequence data. 2010;

79. Marioni JC, Mason CE, Mane SM, Stephens M, Gilad Y. RNA-seq: an assessment of technical reproducibility and comparison with gene expression arrays. Genome Res. 2008 Sep;18(9):1509–1517.

80. Holzberg S, Brosio P, Gross C, Pogue GP. Barley stripe mosaic virus-induced gene silencing in a monocot plant. Plant J. 2002 May;30(3):315–327.

81. Thiel T, Graner A, Waugh R, Grosse I, Close TJ, Stein N. Evidence and evolutionary analysis of ancient whole-genome duplication in barley predating the divergence from rice. BMC Evol Biol. 2009 Aug 22;9:209.

82. Bacete L, Mélida H, Miedes E, Molina A. Plant cell wall-mediated immunity: cell wall changes trigger disease resistance responses. Plant J. 2018 Feb 2;93(4):614–636.

83. Dickman MB, de Figueiredo P. Death be not proud--cell death control in plant fungal interactions. PLoS Pathog. 2013 Sep 12;9(9):e1003542.

84. Foyer CH, Noctor G. Redox homeostasis and antioxidant signaling: a metabolic interface between stress perception and physiological responses. Plant Cell. 2005 Jul;17(7):1866–1875.

85. Nakagami H, Pitzschke A, Hirt H. Emerging MAP kinase pathways in plant stress signalling. Trends Plant Sci. 2005 Jul;10(7):339–346.

86. Torres MA, Jones JDG, Dangl JL. Reactive oxygen species signaling in response to pathogens. Plant Physiol. 2006 Jun;141(2):373–378.

87. Acharya, Dutta K, Pradhan AK, Prakash. Bipolaris sorokiniana ' (Sacc.) Shoem.: The most destructive wheat fungal pathogen in the warmer areas. Australian Journal of Crop Science. 2011;

88. O'Connell RJ, Panstruga R. Tête à tête inside a plant cell: establishing compatibility between plants and biotrophic fungi and oomycetes. New Phytol. 2006;171(4):699–718.

89. Schmidt SM, Kuhn H, Micali C, Liller C, Kwaaitaal M, Panstruga R. Interaction of a Blumeria graminis f. sp. hordei effector candidate with a barley ARF-GAP suggests that host vesicle trafficking is a fungal pathogenicity target. Mol Plant Pathol. 2014 Aug;15(6):535–549.

90. Sels J, Mathys J, De Coninck BMA, Cammue BPA, De Bolle MFC. Plant pathogenesis-related (PR) proteins: a focus on PR peptides. Plant Physiol Biochem. 2008 Nov;46(11):941–950.

91. Petrov A, Meskauskas A, Dinman JD. Ribosomal protein L3: influence on ribosome structure and function. RNA Biol. 2004 May 1;1(1):59–65.

92. Popescu SC, Tumer NE. Silencing of ribosomal protein L3 genes in N. tabacum reveals coordinate expression and significant alterations in plant growth, development and ribosome biogenesis. Plant J. 2004 Jul;39(1):29–44.

93. Kroeger TS, Watkins KP, Friso G, van Wijk KJ, Barkan A. A plant-specific RNA-binding domain revealed through analysis of chloroplast group II intron splicing. Proc Natl Acad Sci USA. 2009 Mar 17;106(11):4537–4542.

94. Hsu Y-W, Juan C-T, Wang C-M, Jauh G-Y. Mitochondrial Heat Shock Protein 60s Interact with What's This Factor 9 to Regulate RNA Splicing of ccmFC and rpl2. Plant Cell Physiol. 2019 Jan 1;60(1):116–125.

95. Skulachev VP. Mitochondria in the programmed death phenomena; a principle of biology: "it is better to die than to be wrong". IUBMB Life. 2000 May;49(5):365–373.

96. Ludovico P, Rodrigues F, Almeida A, Silva MT, Barrientos A, Côrte-Real M. Cytochrome c release and mitochondria involvement in programmed cell death induced by acetic acid in Saccharomyces cerevisiae. Mol Biol Cell. 2002 Aug;13(8):2598–2606.

97. Danial NN, Korsmeyer SJ. Cell Death. Cell. 2004 Jan;116(2):205–219.

98. Heil M, Land WG. Danger signals - damaged-self recognition across the tree of life. Front Plant Sci. 2014 Oct 31;5:578.

CHAPTER 4. SUMMARY

The host susceptibility factors are targeted by a necrotrophic pathogen elicitor directly or indirectly to hijacks the host defense and may result in Programmed Cell Death, which facilitates disease. Yet, very few such susceptibility factors and their functional mechanism is known in plant immunity. *Rcs5* mediated recessive resistance or more accurately dominant susceptibility against *Bipolaris sorokiniana* requires two WAKs at this locus, *Sbs1* and *Sbs2*. The barley WAKs, *Sbs1* and *Sbs2,* is specifically induced by the pathogen elicitor for susceptibility to *B. sorokiniana*, the spot blotch pathogen. This dissertation work presents the identification, characterization and cloning of the Sbs susceptibility factors. Due to the complex nature of distinct genes or crosstalk between pathways involved in developmental and immunity mediated PCD, it has been challenging to distinguish the distinct classes of genes involved in different forms of PCD. Regardless of the pathways, plants rely on PCD suppressors to keep it under check after sequestering the pathogen in regard to the plants fitness. Thus, effective immunity requires a tight regulation on PCD. The efforts to identify such key factors that associate in plant immunity related PCD will improve our understanding of this complex, conserved and tightly regulated trait. The research in this dissertation addresses a genetic characterization and mapping of a PCD suppressor in barley, namely *Nec3*. The absence of *Nec3* results in uncontrolled necrosis at the infection site of adapted biotrophic or necrotrophic pathogens that infect via direct penetration to cell wall. In addition, the onset of PCD is early during the infection process, interacts with the cuticle of host and influences the growth of the pathogen.